



Regional Climate
Change Initiative
Republic of
Cyprus



THE CYPRUS
INSTITUTE
RESEARCH • TECHNOLOGY • INNOVATION

Report of the Task Force on

The Physical Basis of Climate Change



Eastern Mediterranean and Middle East
Climate Change Initiative

Copyright © 2022 by The Cyprus Institute

Special edition for the June 7th, 2022 Ministerial Meeting in Lemesos, Cyprus.
Published by The Cyprus Institute, www.cyi.ac.cy.

No part of this work may be copied, reproduced, digitalized, distributed, translated or modified in any way without written permission from the copyright owners.

Eastern Mediterranean and Middle East Climate Change Initiative, Report of the Task Force on The Physical Basis of Climate Change. Received: January 2021.

Disclaimer: The information contained in the present publication represents the views and opinions of the authors; it does not necessarily represent the views or opinions of The Cyprus Institute nor those of the Government of the Republic of Cyprus.

<https://emme-cci.org/>



Regional Climate
Change Initiative
Republic of
Cyprus



THE CYPRUS
INSTITUTE

RESEARCH • TECHNOLOGY • INNOVATION

Report of the Task Force on

Physical Basis of Climate Change

Eastern Mediterranean and Middle East
Climate Change Initiative

Task Force Coordination

Jos Lelieveld, Climate and Atmosphere Research Center (CARE-C), The Cyprus Institute, Nicosia, Cyprus & Max Planck Institute for Chemistry, Mainz, Germany

Jean Sciare, Climate and Atmosphere Research Center (CARE-C), The Cyprus Institute, Nicosia, Cyprus

Cyprus Institute Liaison Scientist

George Zittis, Climate and Atmosphere Research Center (CARE-C), The Cyprus Institute, Nicosia, Cyprus

Task Force Members

Mansour Almazroui: Center of Excellence for Climate Change Research, Department of Meteorology, King Abdulaziz University, Jeddah, Saudi Arabia

Pinhas Alpert: Department of Geophysics, Tel Aviv University, Tel Aviv, Israel

Philippe Ciais: Laboratoire des Sciences du Climat et de l'Environnement (LSCE), Institut Pierre Simon Laplace, Paris, France & Climate and Atmosphere Research Center (CARE-C), The Cyprus Institute, Nicosia, Cyprus

Wolfgang Cramer: IMBE, Aix Marseille University, CNRS, IRD, Avignon University, Aix-en-Provence, France

Yara Dahdal: Nature Palestine Society, Palestine

Diana Francis: Environmental and Geophysical Sciences (ENGEOS) Lab, Khalifa University of Science and Technology, Abu Dhabi, UAE

Panos Hadjinicolaou: Climate and Atmosphere Research Center (CARE-C), The Cyprus Institute, Nicosia, Cyprus

Fares Howari: College of Natural and Health Sciences (CNHS), Zayed University, Abu Dhabi, UAE

Amna Jrrar: Computational E-Research Unit, Advanced Research Centre, Royal Scientific Society, Amman, Jordan

Dimitris G. Kaskaoutis: Institute for Environmental Research and Sustainable Development, National Observatory of Athens, Athens, Greece & Environmental Chemical Processes Laboratory, Department of Chemistry, University of Crete, Crete, Greece

Markku Kulmala: Institute for Atmospheric and Earth System Research (INAR/Physics), University of Helsinki, Helsinki, Finland

Xin Lin: Laboratoire des Sciences du Climat et de l'Environnement (LSCE), Institut Pierre Simon Laplace, Paris, France

Nikos Mihalopoulos: Institute for Environmental Research and Sustainable Development,
National Observatory of Athens, Athens, Greece & Environmental Chemical
Processes Laboratory, Department of Chemistry, University of Crete, Crete, Greece

Yinon Rudich: Department of Earth and Planetary Sciences, Weizmann Institute of
Science, Rehovot, Israel

Georgiy Stenchikov: King Abdullah University of Science and Technology, Thuwal, Saudi
Arabia

Elena Xoplaki: Department of Geography, Justus Liebig University Giessen, Giessen,
Germany & Center for international Development and Environmental Research,
Justus Liebig University Giessen, Giessen, Germany

Contents

Abbreviations	vii
Abstract	viii
Executive summary	x
1 Introduction and scope	1
2 Historical greenhouse gas emissions and pollution	4
2.1 Global and regional greenhouse gas emissions	4
2.2 Regional pollution and dust	8
3 Past and present state of the climate	11
3.1 Variability over the past 2000 years	11
3.2 Recent changes	16
4 Future climate	20
4.1 Temperature – averages and extremes	20
4.2 Precipitation – averages and extremes	28
4.3 Other meteorological parameters	33
4.4 Changes in climate regimes	36
4.5 Regional sea-level rise	39
5 Special topics	42
5.1 The interplay between atmospheric composition and climate	42
5.2 Land-use change and climate	44

6. Challenges and recommendations	48
6.1 Critical sectors and impacts	48
6.2 Data limitations, uncertainties and needs	53
6.3 Research recommendations and outlook for regional co-operation	55
References	60

Figures

1 Historical total emissions in the EMME region by gas and share of total world emissions	4
2 Historical emissions of greenhouse gases across selected countries and regions.	5
3 Historical emissions by gas	6
4 Historical emissions by sector	7
5 Historical emissions of CO ₂ and CH ₄ by country.	8
6 Natural and documentary proxies covering the past 2 000 years in the EMME region	12
7 Regional hydroclimate proxy records of the past 2 000 years	13
8 EMME vs. global and regional time series of temperature anomalies since 1901 . . .	15
9 Projections of mean annual temperature anomalies in EMME	20
10 Projected changes of mean annual temperature	21
11 Probability density curves of annual temperature anomalies, averaged across the region	23
12 Monthly temperature and precipitation climatologies for Nicosia and Riyadh	25
13 Projections of EMME annual precipitation anomalies.	28
14 Projected changes in annual precipitation	29
15 Application of the Köppen-Geiger climate classification system	37

16	Annual mean distributions of PM _{2.5} over the EMME, derived from satellite observations	38
17	Annual mean tropospheric NO ₂ column concentrations in the EMME, observed by the TROPOMI satellite instrument	46

Tables

1	Simulated annual temperature and projected changes, averaged for 17 EMME countries	24
2	Simulated annual precipitation and projected changes, averaged for 17 EMME countries	30

Abbreviations

AOD	aerosol optical depth
CH ₄	methane
CMIP	Climate Model Intercomparison Project
CO ₂	carbon dioxide
CORDEX	Coordinated Regional Downscaling Experiment
CORE	Coordinated Output for Regional Evaluations
CRU	Climate Research Unit of University of East Anglia
CTL	control reference period (1986-2005)
EMME	Eastern Mediterranean and Middle East
END	end of the 21st century (2081-2100)
ESCWA	Economic and Social Commission for Western Asia
EU	European Union
GHG	greenhouse gas
GtCO ₂ eq/yr	gigatonnes of carbon dioxide equivalent per year
IPCC	Intergovernmental Panel on Climate Change
ITCZ	Inter-Tropical Convergence Zone
MCA	Medieval Climate Anomaly period
MedECC	Mediterranean Experts on Climate and Environmental Change
MENA	Middle East and North Africa
MHWs	marine heatwaves
MID	mid-21st century (2041-60)
NO ₂	nitrogen dioxide
PAHs	polycyclic aromatic hydrocarbons
PM	particulate matter
RCP	Representative Concentration Pathway
SLR	sea-level rise
UHI	urban heat island

Abstract

Many observation-based and modelling studies have identified the Eastern Mediterranean and Middle East (EMME) region as a prominent environmental and climate change hot-spot. Over the past half century and especially the most recent decades, the region has warmed faster than the global mean. At the same time, changes in the hydrological cycle (mainly through decreasing precipitation) have become more evident. The observed temperature trend, characterised by an increase of about 0.45°C per decade, is projected to continue throughout the 21st century, depending on greenhouse gas emission scenarios. While several initiatives have addressed the impacts of climate change on parts of the EMME or at the national level, here we present an updated assessment, covering a wide range of timescales, phenomena and future pathways. Our assessment is based on an updated analysis of recent observations and regional climate projections and an extensive review of the recent scientific literature on the causes and effects of climate change in the EMME region. In addition to projected changes in mean climate conditions, we call attention to extreme events that could have major societal impacts, across the region as a whole and within its 17 countries. These include the increased severity and duration of summer heatwaves, high night-time temperatures, droughts and dust storms, as well as torrential rain events that can trigger flash floods. Our assessment is complemented by a discussion of atmospheric pollution and land-use change in the region, including urbanisation and forest fires. Finally, we identify critical sectors, knowledge gaps and scientific challenges and formulate recommendations for regional co-operation towards improved understanding and greater resilience of the EMME to climate change.

Executive summary

The Eastern Mediterranean and Middle East (EMME) region is warming almost two times faster than the global average and more rapidly than most other inhabited parts of the world, especially during summer.

Over the past hundred years, precipitation variability in the region was high, with pronounced fluctuations between drier and wetter periods. In recent decades, there are indications of a general decrease in precipitation and a transition to a drier climate.

Greenhouse gas emissions in the EMME increased fivefold over the past several decades. Today, regional emissions are comparable to those of the European Union + United Kingdom and India, and a strong upward trend suggests that the region will shortly become one of the world's dominant emitters.

For the rest of the 21st century, climate projections indicate an overall warming of up to 5°C, strongest in the summer. Precipitation will likely decrease by up to 20-30% in many regions, particularly in the eastern Mediterranean.

Business-as-usual pathways for the future imply a northward expansion of arid climate zones at the expense of more temperate Mediterranean zones. Mountainous climate zones with snow will likely diminish by the end of the century.

A strong increase in both the intensity and duration of heatwaves is expected. This is a robust outcome of all climate models and emission scenarios. Depending on the scenario, heat extremes have the potential to disrupt society.

The combination of precipitation decreases and strong warming will likely contribute to severe meteorological and hydrological droughts. In combination with a rapid growth in water demand, significant water shortages may be expected.

The frequency, duration and severity of dust storms, which are common natural hazards across the region, are expected to increase under a warmer climate, which may affect atmospheric circulation, ecosystems, agriculture and human health.

The regional mean sea level is projected to rise at a pace similar to global estimates with a possible outcome of more than 1 metre above the present level by the end of the 21st century (under high-end scenarios). This would imply severe challenges for coastal infrastructure and agriculture, and lead to the salinisation of coastal aquifers in the EMME region.

Virtually all socio-economic sectors will be critically affected by the projected changes. Human health and well-being will be directly affected, especially among underprivileged people, the elderly, children and pregnant women.

The magnitude of climate change and its impacts during the second half of the 21st century and beyond strongly depend on greenhouse gas emission scenarios.

Many countries in the EMME rely on climate data and analyses in countries outside the region. The EMME will need to strengthen its research capacity, enhanced by regional networking, to conduct independent climate mitigation and adaptation assessments and verify policies.

Immediate and effective climate change mitigation measures are required, while local communities in urban, rural and coastal areas of the EMME will need to adapt to the increasingly challenging environmental conditions, especially heat extremes, prolonged droughts and sea-level rise.

1. Introduction and scope

The human influence on the Earth's climate is unequivocal (IPCC, 2013). Since the industrial revolution, a continuous increase in the volume of greenhouse gases (GHGs) being emitted into the atmosphere, in addition to land-use changes (e.g. extensive deforestation and urbanisation), have caused a significant increase in the global surface temperature, as well as changes in other meteorological parameters such as rainfall. The regional responses to climate forcing due to anthropogenic GHG emissions are not linear or uniformly distributed. Because climate feedback mechanisms are geographically specific, some regions warm more rapidly than the global mean. One such climate change hotspot is the Eastern Mediterranean and Middle East (EMME) region (Giorgi, 2006; Zittis and Hadjinicolaou, 2017; Cramer et al., 2018; Zittis et al., 2019).

The observed temperature trends are projected to continue and intensify throughout the 21st century, depending on future trajectories of GHG concentrations that, in turn, are subject to societal and technological developments (Lelieveld et al., 2012; Zittis et al., 2019). Besides the mean climate conditions, relatively large changes are expected in the temporal variability of the EMME's meteorological features, adding support to the characterisation of the region as a global climate change hotspot (Giorgi, 2006; Diffenbaugh and Giorgi, 2012; Lionello and Scarascia, 2018; Zittis et al., 2019). The temperature is projected to mostly increase in summer, which, along with the mean warming, will lead to an enhancement of extreme weather events (Giorgi and Lionello, 2008). Parts of the region have already been affected by some of the most severe record-breaking weather events of recent decades (Coumou and Rahmstorf, 2012). Examples include the exceptional summer of 2007, which was, at the time, the hottest on record in Greece since 1891, and was associated with devastating wildfires throughout the country (Founda and Giannakopoulos, 2009). In the same year, the strongest tropical cyclone over the Arabian Sea since 1970 was observed. In terms of economic damage and fatalities, this storm caused the biggest natural disaster in the history of Oman (Fritz et al., 2010). Future high-impact events may include unprecedented extreme heatwaves (Lelieveld et al., 2016; Zittis et al., 2021a), more prolonged and severe droughts (Spinoni et al., 2020), extreme precipitation (Zittis et al., 2021b), storms as well as combinations of events with great societal impact (Hochman et al., 2021). Unless substantial mitigation efforts are undertaken by the international community, such events are projected to occur with greater frequency, duration and magnitude.

Such considerable changes in environmental and climate conditions could imply severe impacts on a variety of sectors and socio-economic activities including the management

of water resources and agriculture, human health, energy demand and production, transportation, ecosystems, biodiversity, forest fires and many more (Lelieveld et al., 2012; Waha et al., 2017; Cramer et al., 2018). These impacts will likely be exacerbated by additional factors, such as rapid regional population growth and urbanisation, which will inevitably increase the demand and competition for natural resources. The EMME region is also prone to pronounced social inequalities, and the poor are expected to suffer the most from climate change impacts, for example, from heat extremes and shortage of water resources (Waha et al., 2017).

The EMME region includes a variety of climatic zones ranging from deserts and semi-arid to sub-tropical and temperate climates (Lelieveld et al., 2012, 2016; Belda et al., 2014). With warm to hot, dry summers, occasional droughts and mild, relatively wet winters, the climate of the northern EMME is mostly temperate (Lionello et al., 2006). The southern EMME encompasses large, arid and hot desert regions with sparse vegetation (Issar and Zohar, 2007). Precipitation is among the highest in Europe in some regions, for example, up to 2 000 millimetres (mm)/year or more over the Dinaric Alps, Taurus, Caucasus and Alborz mountains, while several degrees latitude further south it is near zero. The region is located at an atmospheric crossroads, directly influenced by a variety of atmospheric circulation patterns and meteorological processes on different continents. For example, winter precipitation, critical for replenishing water resources, is largely related to the southward movement of the polar front jet, that drives cyclonic disturbances across the region (Krichak et al., 2000). The steep orography, the complex coastlines and the effect of large water bodies (e.g. the Mediterranean, Red and Black seas) add important feedbacks that influence the regional peculiarities of global warming. To adequately assess the regional and local-scale impacts, climate information of high spatial resolution and quality is required. Comprehensive regionalised information has only recently become available, mainly through international collaboration, such as the Coordinated Regional Downscaling Experiment, or CORDEX (Giorgi and Gutowski, 2016).

Similar assessments of climate change and its impacts have been made for the region as a whole or for parts of it. The CIMME¹ project (Lelieveld et al., 2012), supported by the Cyprus Institute,² was one of the first of such initiatives to make use of high-resolution regional climate projections. The Regional Initiative for the Assessment of Climate Change Impacts on Water Resources and Socio-Economic Vulnerability in the Arab Region³ is a more recent initiative, supported by the United Nations Economic and Social Commission

1. Climate Change and Impacts in the Eastern Mediterranean and the Middle East.

2. <https://www.cyi.ac.cy/>.

3. <https://www.unescwa.org/climate-change-water-resources-arab-region-riccar>.

for Western Asia (ESCWA et al., 2017). The First Mediterranean Assessment Report prepared by the independent network of Mediterranean Experts on Climate and Environmental Change⁴ was released recently (MedECC, 2020). Its main objective is to communicate the latest scientific results to policy makers and stakeholders in the Mediterranean area to support improved policies on mitigation and adaptation. In addition, several national initiatives and assessments have been conducted.

The present study complements and updates these previous regional and national initiatives using extended observational records, improved information on climate models with more geographical coverage and a greater variety of future scenarios modelled at relatively high resolution. Our main objectives are to 1) assess the regional manifestations of global warming in the EMME region by using state-of-the-art climate information from up-to-date observational records and regional climate models, 2) provide an extensive literature review of the causes and regional effects of climate change and 3) identify knowledge gaps and scientific challenges and formulate recommendations for regional co-operation towards improved understanding of and resilience to climate change. The 17 countries included in our analysis are Bahrain, Cyprus, Egypt, Greece, Iran, Iraq, Israel, Jordan, Kuwait, Lebanon, Oman, Palestine, Qatar, Saudi Arabia, Syria, Turkey and the United Arab Emirates.

This report is organised as follows. In Chapter 2 we discuss recent observations and trends of regional GHG emissions, air pollution and dust. These are identified as key drivers of both global and regional climate change. In Chapter 3 we present information on the regional climate, from palaeoclimatic evidence to very recent observations. Then, in Chapter 4 we forecast key meteorological variables. In Chapter 5 we discuss additional important drivers of regional environmental change. Finally, in Chapter 6 we identify knowledge gaps, assess the challenges and propose research recommendations.

4. <https://www.medecc.org/>.

2. Historical greenhouse gas emissions and pollution

2.1. Global and regional greenhouse gas emissions

Anthropogenic greenhouse gas (GHG) emissions in the EMME region have increased substantially after the 1950s (Figure 1), with emission rates rising almost fivefold, from 0.7 ± 0.2 gigatonnes of carbon dioxide equivalent per year ($\text{GtCO}_2\text{eq/yr}$) during the 1960s to $3.4 \pm 0.2 \text{ GtCO}_2\text{eq/yr}$ during the 2010s based on the PRIMAP dataset (Gütschow et al., 2016). Given the disproportionate rate with respect to global GHG emissions (which saw a 2.5-fold increase), the share contributed by the EMME region doubled from $3.5 \pm 0.5\%$ in the 1960s to $7.3 \pm 0.3\%$ in the 2010s (Figure 1). In the 2010s, emission rates in the EMME region ($3.4 \pm 0.2 \text{ GtCO}_2\text{eq/yr}$) were larger than those of India ($2.6 \pm 0.3 \text{ GtCO}_2\text{eq/yr}$)

FIGURE 1. Historical total emissions in the EMME region by gas (solid lines) and share (%) of total world emissions (dashed lines)

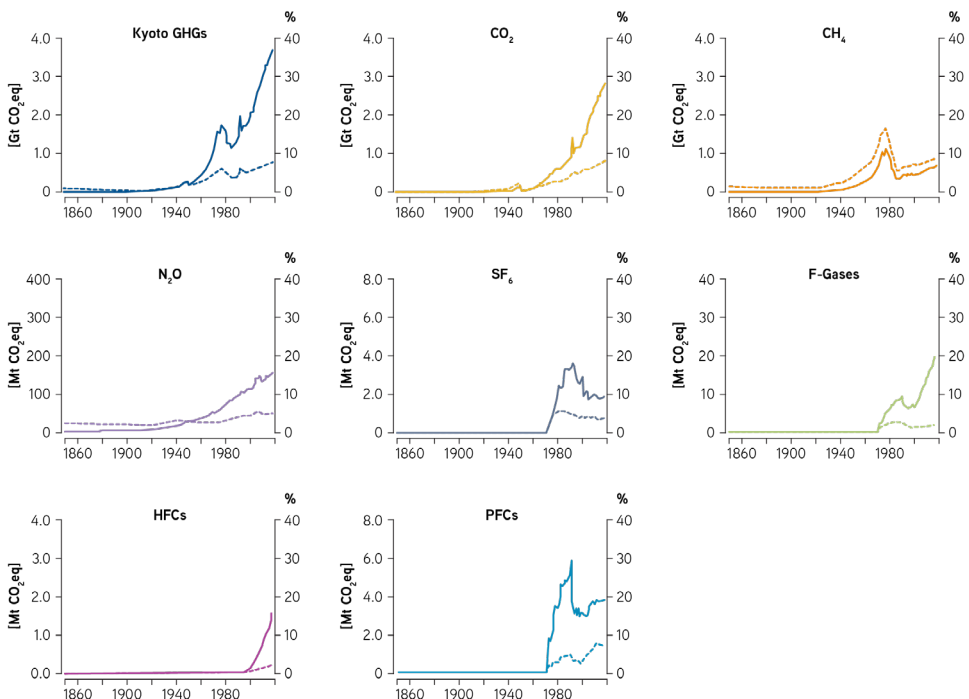
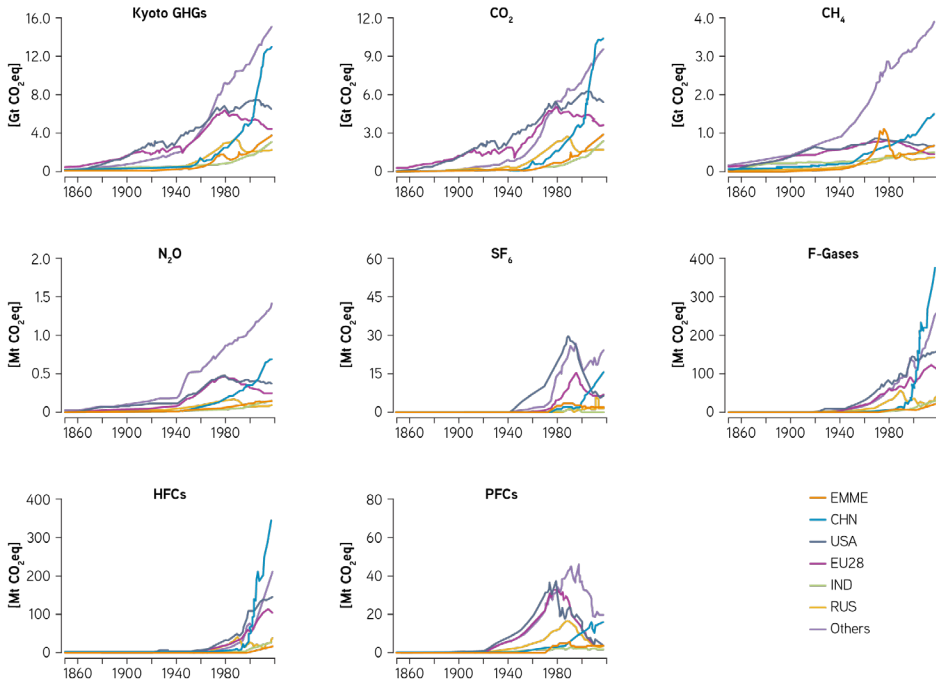


FIGURE 2. Historical emissions of greenhouse gases across selected countries and regions



Note: EMME = Eastern Mediterranean and Middle East; CHN = China; USA = United States of America; EU28 = European Union and United Kingdom; IND = India; RUS = Russia; OTHERS = other countries.

and close to the EU28⁵ (Figure 2), and were characterised by a steeper long-term increase than India's (0.054GtCO₂eq/yr vs. 0.042GtCO₂eq/yr, respectively, between the 1960s and the 2010s). While annual total regional emissions are now similar to those of the EU28, considering Europe's strong decarbonisation trends and ambitious targets, EMME emissions will likely exceed those of the European Union in the coming years.

e emission trends in the EMME region have not been constant over the past 50 years (Figure 1). Steep growth of 0.081GtCO₂eq/yr between the early 1960s and the early 1970s was followed by a sharp decline of 34% during the years 1976-84, associated with the first oil crisis. After that, emissions surged again at a rate of 0.076 GtCO₂eq/yr, except for an abnormal spike of 37% during the Gulf War. Regional emissions increased from 1.4GtCO₂eq/yr in 1990 to 2.0GtCO₂eq/yr in 1991 and declined to 1.6GtCO₂eq/yr in 1992.

5. EU27 and United Kingdom.

Breaking down the emissions by different gases and sectors shows that, historically, emissions of methane (CH₄), followed by nitrous oxide (N₂O), dominated total GHG emissions in the EMME region (Figure 3), with major contributions from the agricultural sector (including industrial livestock activities) until the late 1910s and early 1920s (Figure 4). Socio-economic growth and increasing global energy demand, notably after World War II, have promoted fossil fuel exploitation and use in many EMME countries, where energy production has gradually become the sector with the greatest emissions (Figure 4). Accordingly, increasing emissions of CO₂ and CH₄ from the energy sector have driven the evolution of GHG emissions in the EMME region (Figures 3 and 4). Based on the PRIMAP dataset (Gütschow et al., 2016), CO₂ and CH₄ together account for 92-96% of the total anthropogenic GHG emissions over the past five decades, of which the vast majority, or 88-94%, are emitted from the energy sector. The two gases also contributed 95% of the emissions increase between the 1960s and the 2010s. The relative share of CO₂ and CH₄ in total GHG emissions has shifted over time. The contribution from CO₂ has generally

FIGURE 3. Historical emissions by gas (absolute emissions are indicated by solid lines, share (%) of the total GHG emissions in the EMME region are indicated by dashed lines)

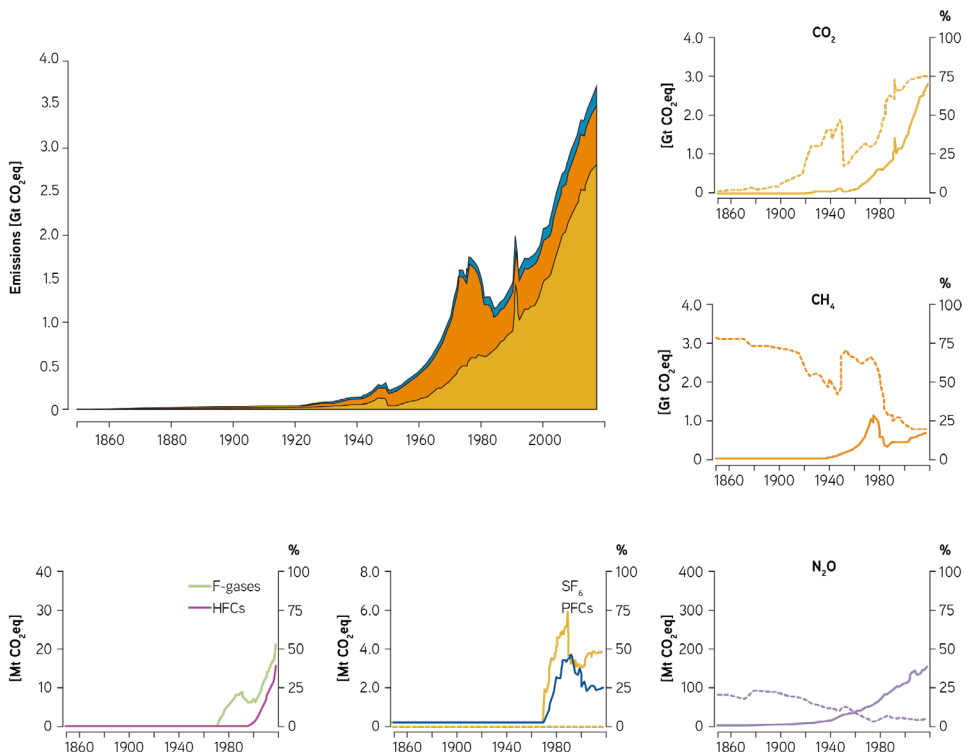
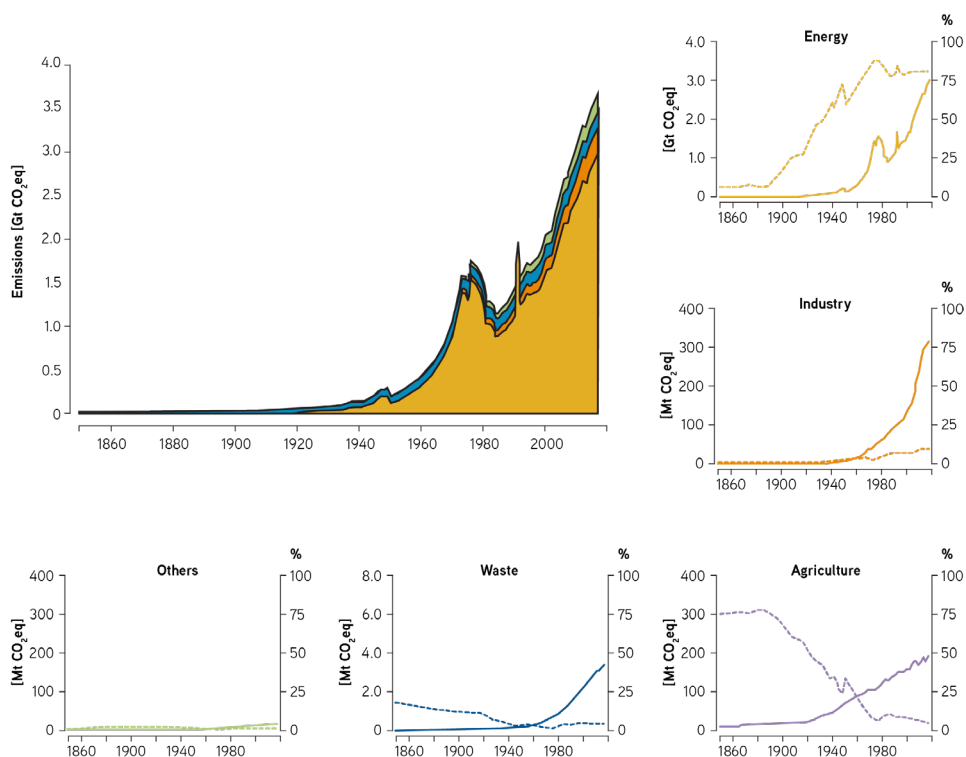


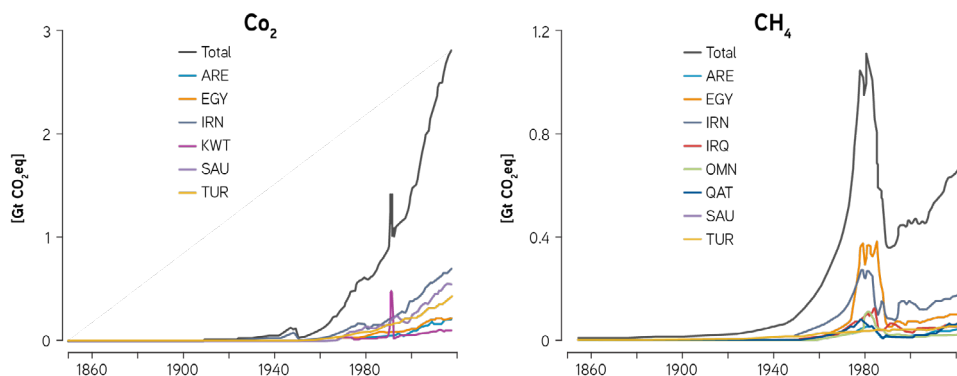
FIGURE 4. Historical emissions by sector (absolute emissions are indicated by solid lines, share (%) of the total GHG emissions in the EMME region are indicated by dashed lines)



increased to become dominant since the 1980s (Figure 3). This is accompanied by an overall decrease in the contribution of (mainly fugitive) CH₄ emissions that peaked between the 1950s and the 1970s. The historical spike in emissions during the Gulf War is due to an unusually large share of CO₂ emissions, whereas increased gas extraction explains the rapid growth of CH₄ emissions since the 1960s, followed by the implementation of advanced technologies to reduce leaks after the first oil shock of 1976-84 (Figures 1 and 3). This peak and decline of CH₄ in EMME countries is reconstructed by inventories and was not verified by atmospheric observations, although independent global methane measurements from ice cores suggest that fossil sources of methane peaked during the 1960s-70s and decreased sharply afterwards (Aydin et al., 2011).

The major CO₂ emitting countries in the region are Iran, Saudi Arabia, Turkey, Egypt and the United Arab Emirates (Figure 5). These five countries alone account for 74% of the total emissions during the 2010s, and 75% of the increase in emissions over the past five

FIGURE 5. Historical emissions of CO₂ and CH₄ by country



ARE = United Arab Emirates; EGY = Egypt; IRN = Iran; IRQ = Iraq; OMN = Oman; QAT = Qatar; KWT = Kuwait; SAU = Saudi Arabia; TUR = Turkey.

decades. Kuwait, ranked as the eighth-largest CO₂ emitting country in the EMMR region, was also the driver of the anomalous emissions spike in 1991, related to the ignition of oil wells which were difficult to extinguish (Figure 5). Iran and Saudi Arabia are the two largest emitters of CH₄ in the EMMR region (Figure 5), contributing 43% of the regional total during the 2010s. These two countries, together with Iraq, Qatar and Oman, were also responsible for the exceptionally high CH₄ emissions in the early 1970s and the drastic decline afterwards (Figure 5).

2.2. Regional pollution and dust

The Middle East is a major contributor to global dust emissions (15-20% of the total), affecting the regional climate, human health and the marine environments of the eastern Mediterranean and the Arabian Sea. Several active deserts are located in the region such as the Egyptian and Nubian deserts in the northeastern Sahara; the Rub-Al Khali, An Nafud and Al Dahna deserts in the Arabian Peninsula; the Negev desert in Israel; the Syrian-Iraqi desert; the alluvial flood plains in Mesopotamia; the Dasht-e Kavir and Dasht-e Lut deserts in Iran as well as the desiccated, ephemeral or dried-up lakes like Urmia, Jazmurian and Hamouns in Iran (Ginoux et al., 2012; Cao et al., 2015; Kaskaoutis et al., 2016). The dust activity over the region is highly sensitive to weather conditions (Nabavi et al., 2016; Bodeneheimer et al., 2018; Hermida et al., 2018; Shaheen et al., 2021) and climate perturbations such as temperature increase and precipitation decrease (Hemming et al., 2010; Hoerling et al., 2012). Dust storms originating in the Middle East strongly affect the regional atmospheric radiation budget, cyclogenesis, monsoon circulation and air quality (Solmon et al., 2015; Jin et al., 2016; Soleimani et al., 2020; Francis et al., 2020; Behrooz et al.,

2021). Desert dust dominates; other aerosol types include sea salt, soot from fossil-fuel combustion and burning biomass, and mixed particulates (Kaskaoutis et al., 2007; Basart et al., 2009; Hamill et al., 2016; Ali et al., 2020; Shaheen et al., 2020; Ukhov et al., 2020; Xu et al., 2020; Sabetghadam et al., 2021). Dust activity exhibits a distinct seasonality with a spring/summer maximum and a winter minimum, driven by specific synoptic circulation patterns that trigger persistent or seasonal winds like the Shamal and Levar (Hamidi et al., 2013; Yu et al., 2016; Bou Karam Francis et al., 2017; Rashki et al., 2019). Furthermore, the interrelation of large-scale atmospheric dynamics and teleconnection patterns like the El-Nino, the Siberian High, changes in sea surface temperature over the Indian Ocean and the eastern Mediterranean and displacements of the Inter-Tropical Convergence Zone (ITCZ) affect the intra-seasonal and inter-annual variations of dust activity (Yu et al., 2015; Labban et al., 2021; Huang et al., 2021). Dust also severely affects the regional seas, the Red Sea and the Arabian Gulf (Osipov and Stenchikov, 2018). The mean dust shortwave radiative forcing over the southern Red Sea is the largest in the world, reaching 60 watts per square metre (W/m^2).

Several studies report a general increase in dust aerosols, and in the frequency and intensity of dust storms over the Iraqi Plains and the Arabian Peninsula over the past two decades, with notable changes depending on the region and period (Ganor et al., 2010; De Meij and Lelieveld, 2011; De Meij et al., 2012; Hsu et al., 2012; Pozzer et al., 2015; Klingmüller et al., 2016). Over eastern Iran a decrease in dust aerosol optical depth (AOD) was observed after 2003 (Rashki et al., 2014; Miri et al., 2021). More specifically, climatological AOD trends (1980–2018) over the EMME region based on the MERRA-2⁶ re-analysis reveal a declining trend over southeastern Europe and the marine environment and an increase in AOD over the desert areas in the Middle East (Shaheen et al., 2020). Reversed decadal AOD tendencies are also observed in specific periods (e.g. after 2010), while MODIS⁷ satellite data confirm increasing AOD over desert areas in the past two decades (Shaheen et al., 2020). Dust emissions increased by 15% per year over the EMME region from 2001 to 2012 (Yu et al., 2018). A shift in 2006–07 from an inactive to an active dust period in the Fertile Crescent has been attributed to synergistic interrelations between the El Niño Southern Oscillation (ENSO) and the Pacific Decadal Oscillation (PDO) (Notaro et al., 2015). The combination of these large-scale atmospheric circulation patterns enhanced prolonged dryness over the region that increased dust activity during 2008–12. Stronger Shamal winds in recent years, with a higher probability of dust activity, were observed in central Iraq and the eastern and southern parts of the Arabian Peninsula (Yu et al., 2016). Moreover, the AOD variability over desert areas in the Middle East is directly related to soil

6. Modern Era Retrospective-Analysis for Research and Applications, Version 2.

7. MODerate resolution Imaging Spectroradiometer.

moisture, precipitation and surface winds (Klingmüller et al., 2016). The increasing AOD trend is associated with declining precipitation, soil moisture and relative humidity, and an increase in temperature during the past decade, indicating the sensitivity of dust emissions to climate change.

On the other hand, several studies note a decreasing AOD trend over the eastern Mediterranean in the past two to three decades, attributed to decreasing anthropogenic aerosol emissions and sulphate levels following fuel desulfurisation policies (Nabat et al., 2013, 2014). Particulate matter with a diameter of 10 micrometres or less (PM₁₀) decreased over the past decade in Cyprus (Pikridas et al., 2018), while a positive PM₁₀ trend was observed in the Gaza Strip during 2001-14 (Shaheen et al., 2017). Statistically significant decreasing trends in MODIS-AOD were found over Egypt and the eastern Mediterranean, and increasing trends over the Middle East (Georgoulas et al., 2016). Likewise, the long-term dust variability over the past 10-15 years across the eastern Mediterranean indicates a decrease (-4% per year) in dust AOD during 2007-15 (Marinou et al., 2017). These results are in accordance with those of other studies (De Meij et al., 2012; Hsu et al., 2012; Yoon et al., 2014; Pozzer et al., 2015; Shaheen et al., 2021) based on data from several satellite sensors. Other regional studies report increasing trends in dust frequency over Israel in 1958-2006 (Ganor et al., 2010) and 2001-15 (Krasnov et al., 2016), while in Cyprus a statistically significant decreasing tendency was detected in the frequency of dust events (-6.9 dust events per year) during 2006-17 (Achilleos et al., 2020). A negative trend in nitrogen dioxide (NO₂) was recorded over major cities in the Middle East during 2010-15 due to declining anthropogenic emissions from fossil fuel combustion, related to regional conflict and migration (Lelieveld et al., 2015). Apart from the declining trend in anthropogenic AOD over the eastern Mediterranean due to environmental policies in Europe (Nabat et al., 2013; Floutsi et al., 2016), the significant decrease in AOD is also attributed to a weakened dust contribution, consistent with a decrease in dust activity over the Sahara Desert (Hsu et al., 2012). The debate about which factors (anthropogenic or natural) drive AOD decreases over the Mediterranean continues, with most studies agreeing that dust variations are mostly responsible for the AOD trends in the southern parts of the area (Gkikas et al., 2013; Floutsi et al., 2016; Marinou et al., 2017), while a decrease in anthropogenic emissions triggered the AOD decline over the European part of the Mediterranean and around major urban centres. In accord with the observed increasing AOD, model predictions suggest an increase in the intensity of dust events over the region in the 21st century, likely due to climate change (Lelieveld et al., 2014).

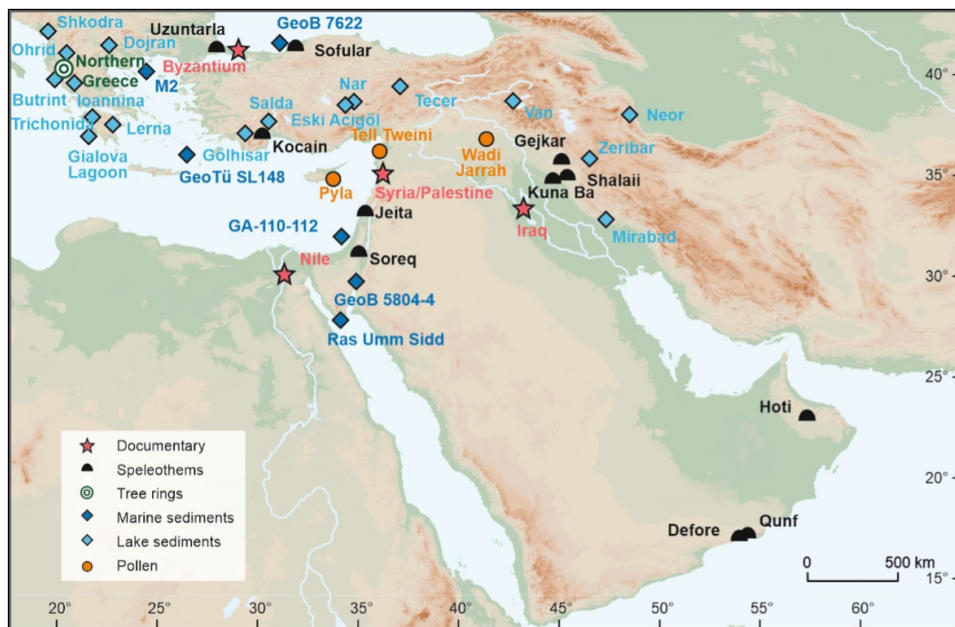
3. Past and present state of the climate

3.1. Variability over the past 2 000 years

Palaeoclimate proxy information provides the basis for reconstructing climates before the instrumental period (e.g. Bradley, 2015). Past climate information for the Mediterranean is preserved in natural archives, such as marine and lacustrine sediments, corals, tree rings, loess and cave deposits (speleothems). Although calibration against instrumental data is a necessary step to determine how well proxies reflect climate, proxy records are not to be compared with rain gauges or thermometers, yet they provide a measure of prevailing climatic conditions at a particular point in time. The temporal resolution of records ranges from annual (e.g. corals, tree rings, some speleothems) to decadal (sediments), the latter characterised by dating uncertainties and changing sampling resolution over time. Natural proxies are also influenced by variables other than the target climate variable or they are sensitive to multiple and interacting climate signals (e.g. precipitation, soil moisture, air or sea surface temperature, sea-level changes, water circulation and pH), and the length of their records vary. Apart from natural proxies, there is a wealth of textual evidence from the Mediterranean covering the past centuries (Luterbacher et al., 2012, 2021; Haldon et al., 2014; Izdebski et al., 2016b, 2016a; Xoplaki et al., 2016, 2018, 2021; Labuhn et al., 2019) that supports the reconstruction of historical weather and climate conditions, including extreme events and their potential link to impacts. The EMME region offers a relatively dense network of natural archives and documentary evidence covering the past 1000 to 2000 years with a strong bias towards hydrological changes. There is hardly any palaeoclimatic evidence available that resolve temperature conditions.

Luterbacher et al. (2006, 2012, 2021); Lelieveld et al. (2012); Xoplaki et al. (2018); Labuhn et al. (2019); Finné et al. (2019); Luterbacher and Xoplaki (2019); Sinha et al. (2019) and Jones et al. (2019) provide recent reviews of proxy availability, distribution, potential, challenges, opportunities and limitations of palaeoclimatic data across the EMME region. Figure 6 presents the most recent and updated distribution of natural proxy records, including speleothems, lake and marine sediments, tree rings and documentary evidence that resolve annual to multidecadal hydroclimate variability covering the past two millennia for the EMME region. Amid the multitude of records, only a portion provides complete

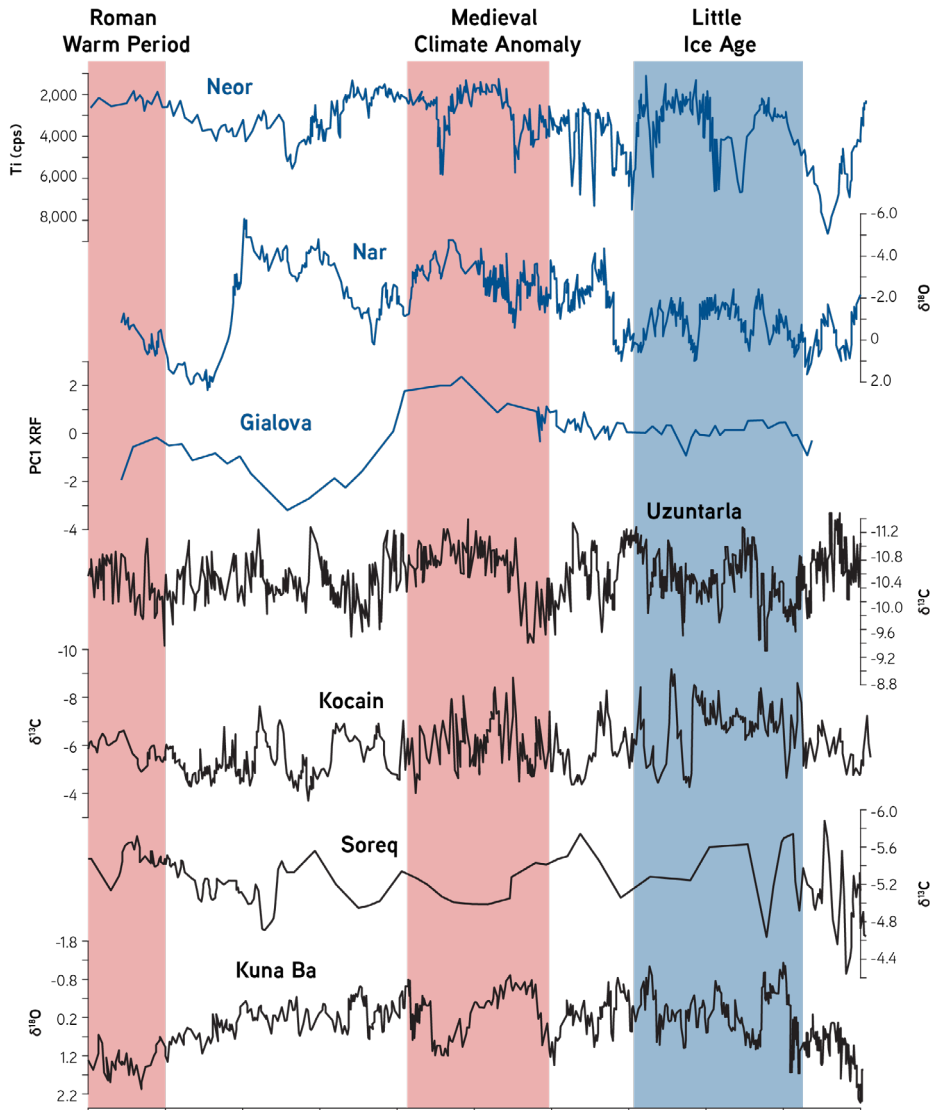
FIGURE 6. Natural and documentary proxies covering the past 2 000 years in the EMME region (adopted from Zittis et al., 2022)



information for two millennia, much of it focused on the southern and southeastern areas of the EMME. Detailed palaeoclimate information on Northern Africa, the Nile basin and the Arabian Peninsula that covers the past 2000 years is currently limited (Figure 7), in large part due to the prevalence of semi- to hyper-arid environments in parts of these areas over the time period. Dry climates generally preclude the long-term existence of lakes and wetlands that typically preserve long records of environmental change. Existing reconstructions are primarily based on lake sediments, which have a multidecadal resolution and suffer from considerable chronological uncertainties and changing sampling resolution. Speleothemes, deliver annually resolved records of hydroclimate in some areas of EMME (e.g. Fleitmann et al., 2004, 2007; Baker et al., 2010; Flohr et al., 2017).

Oxygen ($\delta^{18}O$) and carbon ($\delta^{13}C$) isotopes are the most frequent palaeoclimate proxies obtained from stalagmites. $\delta^{18}O$ is often used as indicator for the amount of precipitation above the cave (more negative $\delta^{18}O$ values indicate wetter climatic conditions) and changes in the seasonality of rainfall. $\delta^{13}C$ values mainly influenced by vegetation and soil microbial activity above the cave, they are both strongly governed by moisture and temperature. Mediterranean lakes record changes in past climate and water balance through a range of proxy indicators that are preserved in their sediments. Lakes lose water mainly

FIGURE 7. Regional hydroclimate proxy records of the past 2 000 years (adopted from Zittis et al., 2022)



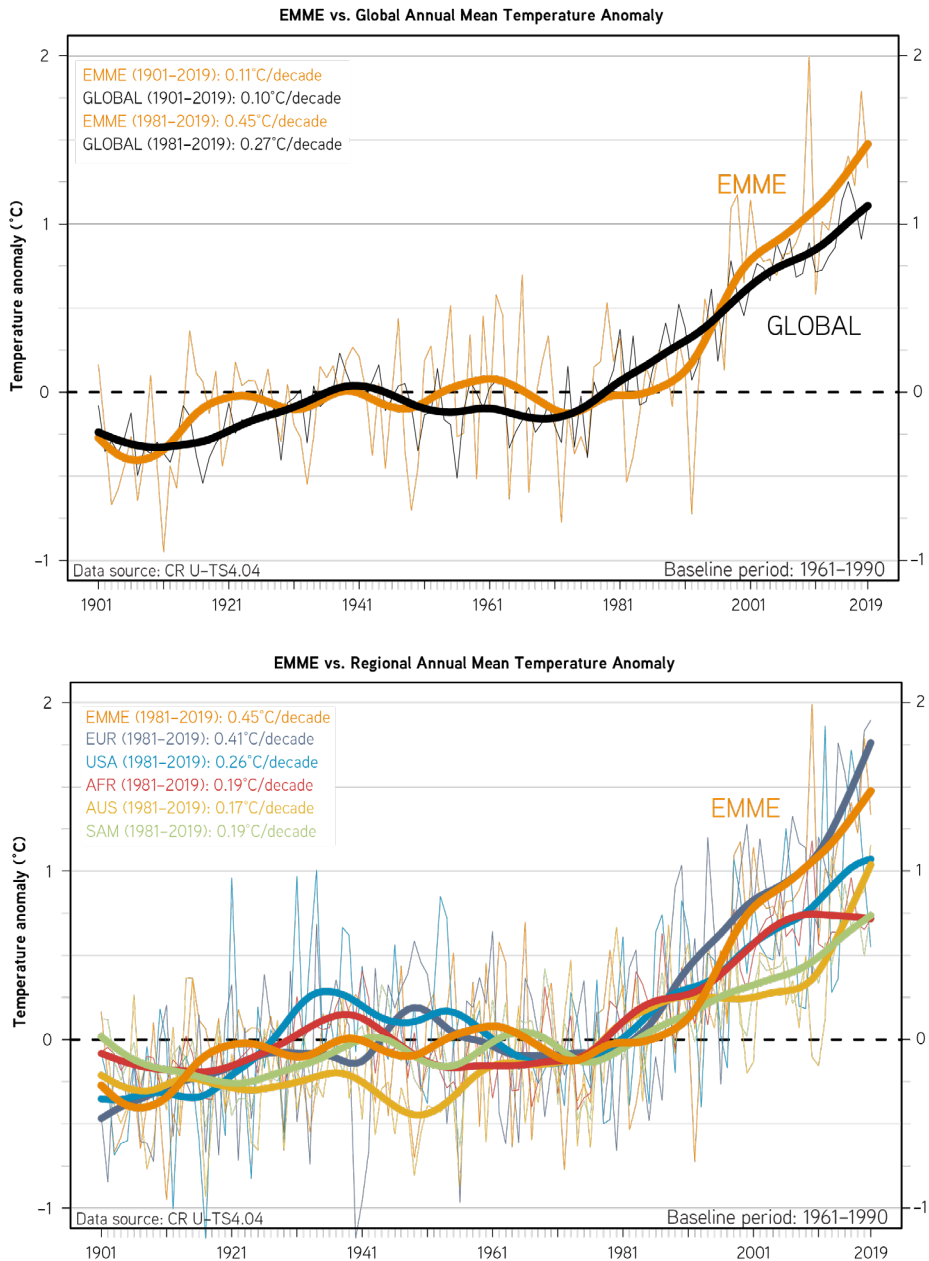
through evaporation and may become hydrologically closed, and thus their waters saline. During periods of negative water balance, the region of a closed lake shrinks, water levels fall and salinity increases, while the opposite occurs at times of positive water balance. Lake records from across the Mediterranean are of great value for reconstructing fluctuations in climate over multi-decadal and longer timescales. A few hydroclimatic reconstructions from marine and lake sediment with various temporal resolutions are available

for the Balkans, central and eastern Mediterranean (Figures 7 and 8). A variety of proxies can be used for reconstructing hydroclimate, such as oxygen isotopes, pollen, and concentration of certain trace elements (e.g., titanium (Ti) in lake sediments as an indicator for aridity; Luterbacher et al. 2021).

We present a selection of several well-dated, two-millennia-long and highly resolved proxy records that cover the area in transects from west to east and north to south (Figures 7 and 8). Oxygen ($\delta^{18}\text{O}$) and carbon ($\delta^{13}\text{C}$) isotope records, as well as titanium (Ti) from lake sediments and stalagmites, show multidecadal fluctuations (Figure 8). For example, for the Gialova Lagoon, a shallow coastal ecosystem in southwest Peloponnese (Katrantsiotis et al., 2018), the first principal component (PC1) of the X-ray fluorescence (XRF) data reflects hydroclimatic variations. The Nar Lake's (Jones et al., 2006) $\delta^{18}\text{O}$ record, through its precipitation-evaporation balance signal, presents information on the amount of precipitation. The aeolian input to the peripheral peat of the Neor Lake (Sharifi et al., 2015) increases during dry periods as defined by the Ti records. The $\delta^{13}\text{C}$ stalagmite records of the Uzuntarla and Kocain caves (Göktürk, 2011), and the $\delta^{18}\text{O}$ record of the Soreq (Bar-Matthews et al., 2003) and the Kuna Ba (Sinha et al., 2019) caves present effective moisture (P-ET) variations, indicative of precipitation. The caves are located in different climatic zones, and therefore some inconsistencies exist between their effective humidity records. These inconsistencies may be exacerbated by chronological uncertainties of up to several decades.

The first two centuries of the first millennium were characterised by less variable, warm and humid climatic conditions that coincided with the Roman Empire. While the Kuna Ba cave had a tendency towards more humid conditions for almost the entire first millennium, most proxy records indicate a continuous path to drier conditions over the first six centuries. The Nar Lake indicates a rapid and extreme shift to a humid 4th century followed by a drier period until almost the end of the 7th century. A century earlier, all other records present increased humidity that lasted during most of the Medieval Climate Anomaly period (MCA, ~950 to ~1250; Masson-Delmotte et al., 2013). At the beginning of the MCA, abundant rainfall and a mild climate characterised the northern EMME and the Byzantium. Favourable conditions for the local societies prevailed up to the early to mid-12th century, when in some cases abrupt drying is observed (Xoplaki et al., 2016). Highly variable hydro-climatological conditions prevailed during the transition period between the MCA and the Little Ice Age (LIA, ~1400 to ~1850; Mann et al., 2009). During nearly 400 years of this period, strong hydroclimate variability occurred across almost the entire region covered by the proxy records. Multiple natural and documentary records substantiate cooler and rainier conditions over the Eastern Mediterranean during the past nearly two

FIGURE 8. EMME vs. global (top panel) and regional (bottom panel) time series of temperature anomalies since 1901 (redrawn from Zittis et al., 2022)



Source: Based on the CRU gridded observations (Harris et al., 2020) over land (annual values: thin curves and cubic smoothing splines: thick curves).

Note: Linear trends are also presented for Eastern Mediterranean and Middle East (EMME), Europe (EUR), the United States of America (USA), Africa (AFR), Australia (AUS), South America (SAM) and the globe (GLOBAL).

centuries (Xoplaki et al., 2001). All proxies and their adjacent areas, except the lakes Neor and Nar, experienced strong variability and a clear drying trend. It is worth noting that the Neor Lake record presents the last major atmospheric dust event as late as in the 1930s, while the Nar Lake's humid 20th century corresponds to a combination of the influence of the Indian monsoon and the North Atlantic Oscillation over the area.

3.2. Recent changes

3.2.1. Temperature

Following the global trend, observed regional changes in climate parameters over the past 120 years are characterised by pronounced warming (Figure 8, top panel). There is unequivocal evidence that this is related to anthropogenic activities and elevated concentrations of GHG gases in the atmosphere (IPCC, 2013). This warming accelerated over the past four decades to reach about 1.4-1.5°C compared to the beginning of the 20th century (Figure 8, top panel). For example, during the past three decades, the surface temperature of the Sahara Desert increased at a rate two to four times greater than that of the tropical-mean temperature (Cook and Vizzy, 2015). This recent acceleration in regional warming is tracked by several studies, based on various observational data sources (Christensen et al., 2013; Zittis and Hadjinicolaou, 2017; Cramer et al., 2018; Lionello and Scarascia, 2018). Because of various global, regional or local meteorological processes and feedbacks (e.g. modes of internal climate variability, land-atmosphere and land-sea interactions, urbanisation and other land-use changes), the sign, magnitude and significance level of observed temperature trends vary. These can depend on 1) location and geographical characteristics, 2) the type of dataset investigated, 3) the season under consideration and 4) the period of analysis. Nevertheless, significant positive trends of the order of 0.1-0.6°C/decade have been identified for most EMME territories, including Egypt, Turkey, Greece, Israel, Jordan, Lebanon, the Arabian Peninsula and more (Feidas et al., 2007; Freiwan and Radioğlu, 2008; Shohami et al., 2011; Tanarhte et al., 2012; Ramadan et al., 2013; Almazroui et al., 2014; Donat et al., 2014; Mariotti et al., 2015; Xoplaki et al., 2016; Mostafa et al., 2019; El Kenawy et al., 2019; Mohammed and Fallah, 2019; Almazroui, 2020a).

Our updated analysis reveals an indicative EMME region-average trend of 0.45°C/decade for 1981-2019, which is nearly twice the global trend for the same period (0.27°C/decade) (Figure 8, top panel). These values are based on the latest version of the Climate Research Unit dataset (CRU-TS4.04) of the University of East Anglia (Harris et al., 2020). Considering the dataset's entire time frame of 1901-2019, the global and regional temperature trends are similar (0.11°C/decade). When regional warming in the EMME is compared with other parts of the world, including Europe, the United States, Africa, South America and

Australia (Figure 8, bottom panel), warming trends of the past four decades (i.e. 1981–2019) are found to be strongest in the EMME (0.45°C/decade) and Europe (0.41°C/decade). Regions of the southern hemisphere (e.g. South America and Australia) are found to warm at a relatively slower pace.

Besides changes in the mean temperature conditions, the frequency and intensity of high-impact, extreme events (e.g. severe heatwaves) have also increased in the recent past (Cherif et al., 2020). In the past decades, extreme weather events' characteristics, including the frequency, duration and intensity of heatwaves, have amplified across the EMME (Kostopoulou and Jones, 2005; Kuglitsch et al., 2010; Donat et al., 2014; Lelieveld et al., 2016; Ceccherini et al., 2017; Nashwan et al., 2018; Abbasnia and Toros, 2019; Tolika, 2019; Hochman et al., 2021). Particularly in the Middle East, the observed trend of cumulative heat (i.e. the product of all seasonal heatwave days, including heatwave frequency and average heatwave intensity) is 50% per decade, among the highest in the world (Perkins-Kirkpatrick and Lewis, 2020). Parts of the region (e.g. Greece) were affected by some of the most severe, record-breaking hot weather events of the past decade (Coumou and Rahmstorf, 2012). On 4 September 2020, the surface temperature records in Athalassa, Cyprus, hit a record of 46.2°C, which is the highest temperature officially recorded on the island. On 21 July 2016, in the hottest year on record so far, the temperature in Mitribah, Kuwait, reached a record of 54°C (Merlone et al., 2019). The following summer, on 29 June 2017, a temperature of 53.7°C was recorded at Ahwaz, Iran. In the arid regions of EMME (mainly in the Arabian Peninsula and east Iran), summer land surface temperature, usually derived by satellite sensors, routinely soared above 60°C (Mildrexler et al., 2011). In 2018, the world's highest land surface temperature of 80.8°C was observed in the Lut Desert in Iran (Zhao et al., 2021b). The Arabian or Persian Gulf recently also experienced record-breaking sea surface temperatures. On 30 July 2020, extreme sea surface temperatures in Kuwait Bay reached 37.6°C (Alosairi et al., 2020).

Cold-weather extremes in the region (e.g. cold spell duration, number of ice and frost days) were also subject to warming trends; however, these are not as significant as the trends for hot-weather extremes (Donat et al., 2014; Yosef et al., 2019; Abbasnia and Toros, 2020; Ntoumos et al., 2020).

3.2.2. Precipitation

In addition to the dominant warming trends, changes in the hydrological cycle have also occurred in the past century in the EMME region (Cherif et al., 2020). However, the alterations between relatively drier and wetter periods were mainly driven by natural climate variability, while the role of anthropogenic climate change and external forcing has only recently become more evident (Xoplaki et al., 2000, 2004; Mariotti et al., 2002, 2015;

Mariotti and Dell’Aquila, 2012; Hoerling et al., 2012; Seager et al., 2014). Several observation-based studies have investigated past precipitation trends in the EMME region. The sign, magnitude and significance of trends vary strongly and depend on the location and period under consideration. For example, precipitation in Greece declined across the years 1950-2018, yet in the last 30 years of this period, the precipitation trend is mostly positive (Cherif et al., 2020). Nonetheless, the majority of analyses suggests a reduction of mean precipitation across the EMME region, most importantly during the wet part of the year, with an observed transition to drier conditions (Xoplaki et al., 2004; Maheras et al., 2004; Partal and Kahya, 2006; Shaban, 2009; Philandras et al., 2011; Sousa et al., 2011; Almazroui et al., 2012; Tanarhte et al., 2012; Ziv et al., 2014; Güner Bacanlı, 2017; Zittis, 2018; Yosef et al., 2019). In most climate analyses, in contrast with temperature, regional precipitation trends appear to be less statistically significant (Partal and Kahya, 2006; Shohami et al., 2011; Ouarda et al., 2014; Donat et al., 2014; Khadr, 2017; Zittis, 2018; Gado et al., 2019; Yosef et al., 2019). Similar declining trends are identified in other sub-tropical, Mediterranean-type climate regimes around the globe (Deitch et al., 2017).

There is strong evidence that the frequency and intensity of droughts in many countries of the EMME region have increased since the second half of the 20th century (Pashiardis and Michaelides, 2008; Hoerling et al., 2012; Nastos et al., 2013; Donat et al., 2014; Güner Bacanlı, 2017; Caloiero et al., 2018; Seager et al., 2019; Spinoni et al., 2019). Recent mega-drought events in the eastern Mediterranean and the Levant have received great attention, and their magnitude cannot be fully explained by natural climate variability (Kelley et al., 2015; Cook et al., 2016; Mathbout et al., 2018a). Between 1951 and 2016, about 10% of the most extreme macro-regional drought events globally occurred in the broader EMME region (Spinoni et al., 2019). This list includes high-impact events, such as the 1989-91 drought in the southern Balkans, the 2000-02 drought in Cyprus and Greece, the 2007-08 drought in Turkey and Cyprus and the more recent multiyear drought events in the Middle East. Other examples include the drought that hit the Fertile Crescent, Iraq, during 2007-08 (Notaro et al., 2015) and the prolonged drought in southeast Iran from 1999 to 2002 (Rashki et al., 2013b).

Despite the observed decrease in precipitation totals, for some Mediterranean regions, a paradoxical increase of extreme rainfall magnitude or in the number of heavy precipitation days is evident (Alpert et al., 2002; Founda et al., 2013). Particularly for the Middle East, extreme precipitation events can be the result of tropical-extratropical interactions, for example, Active Red Sea Troughs (de Vries et al., 2013). Stratospheric potential vorticity streamers, as indicators of Rossby wave breaking, combined with intense moisture transport, can contribute substantially to this type of extreme event in the region (de Vries

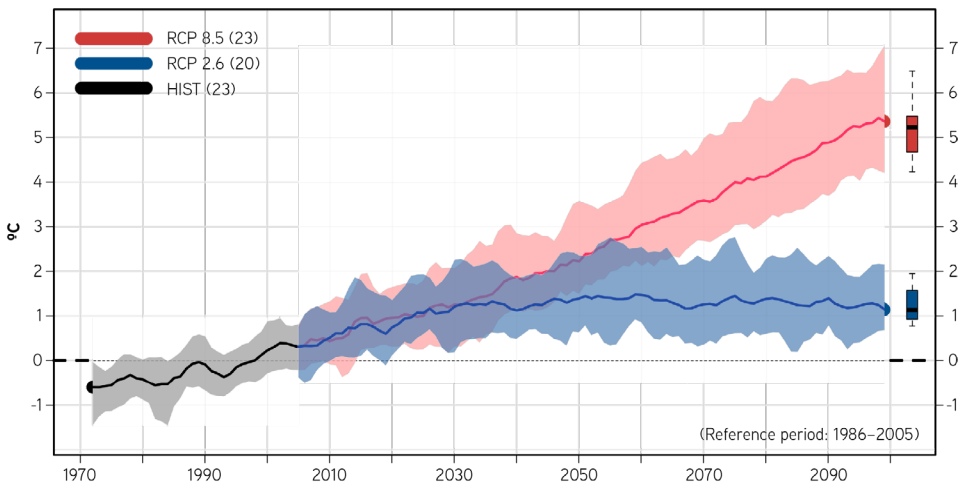
et al, 2018, 2021). Dust radiative forcing can also shift the ITCZ northwards, thus affecting extreme precipitation in the southwest Arabian Peninsula (Bangalath and Stenchikov, 2015). Such torrential rains can trigger flash floods with dramatic societal impacts, including major economic damage and loss of life (de Vries et al., 2013, 2018; Spyrou et al., 2020). At the same time, such rains can replenish freshwater resources that are of crucial importance for agriculture and ecosystems (de Vries et al, 2018). Nevertheless, due to the rare and local nature of such events, observed trends and changes in their severity and frequency are not always statistically significant, and therefore, it is difficult to derive robust conclusions (Mathbout et al., 2018b; Nashwan et al., 2018; Zittis, 2018; Yosef et al., 2019; Abbasnia and Toros, 2020). It is likely that mean and extreme precipitation trends are masked due to strong temporal variability (a signal-to-noise ratio issue) along with the selection of the study period length and the trend magnitude (Yosef et al., 2019).

4. Future climate

4.1. Temperature – averages and extremes

According to the CORDEX-CORE⁸ regional climate projections (Coppola et al., 2021b) (see Annex A for methods and datasets), the EMME will continue to warm during the 21st century (Figure 9). Global and regional models corroborate that this rise will continue to be faster than the global rate of increase (Lionello and Scarascia, 2018; Zittis et al., 2019). For the business-as-usual Representative Concentration Pathway (RCP8.5) (see Annex A for the definition of climate scenarios), the increase is expected to follow a linear trend and exceed 5°C by the year 2100, compared to the 1986–2005 reference period. For the more optimistic RCP2.6 (close to meeting the main Paris Agreement targets), the mean annual temperature anomaly will peak by the mid-21st century and then stabilise or slightly decrease to 1–1.5°C. Temperature projections for both pathways are very similar up until the 2030s and only then start to diverge significantly. The end-of-century spread of models is more evident for the RCP8.5, indicating that the climate sensitivity to GHG forcing varies among the different models. To approximate the warming levels since pre-industrial

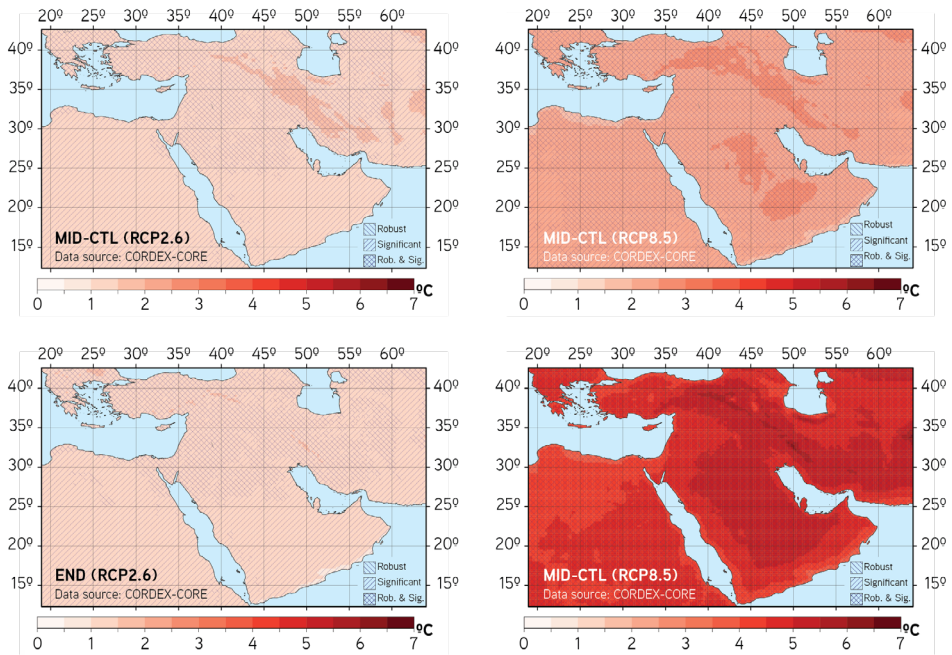
FIGURE 9. Projections of mean annual temperature anomalies in EMME (with respect to the 1986–2005 reference period)



Source: Based on CORDEX-CORE climate projections and two Representative Concentration Pathways (redrawn from Zittis et al., 2022).

8. Coordinated Regional Climate Downscaling Experiment–Coordinated Output for Regional Evaluations.

FIGURE 10. Projected changes of mean annual temperature (with respect to the 1986–2005 reference period)



Source: Based on CORDEX-CORE climate projections, for RCP2.6 (left panels) and RCP8.5 (right panels) and for mid-21st (2041–60, top panels) and end-of-century projections (2081–2100, bottom panels). (redrawn from Zittis et al., 2022)

times (e.g. from 1880–99 onwards), about 0.8°C, estimated from observations, should be added to these values (Cramer et al., 2018; Zittis et al., 2019). Time series of projected temperature anomalies, averaged across the 17 individual countries of the region, are provided in Figure A.7 of the Annex.

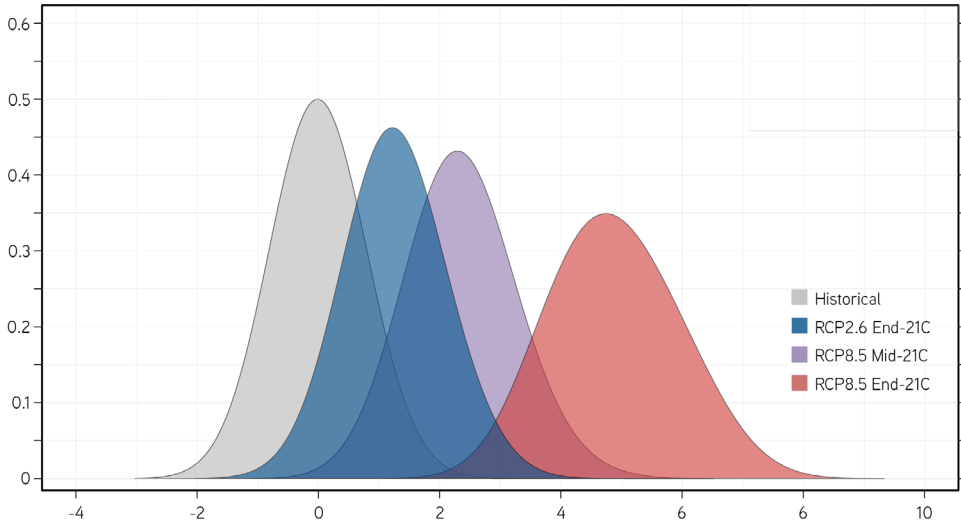
Regional maps of projected changes in the 2-m mean annual temperature are presented in Figure 10. The simulated temperature climatology of the historical period is presented in Figure A.2 for reference. For both pathways and time horizons under investigation (middle and end of the 21st century), the projected changes are found to be significant. This means that the signal of change is larger than the inter-annual variability of the control reference period, whereas, particularly for RCP8.5, the models tend to agree on the sign and magnitude of changes (i.e. high level of robustness). RCP2.6 implies a more uniform regional warming, which will likely not exceed 1.5°C (with respect to the 1986–2005 reference period) for most of the EMME region. This is about 2–2.5°C since pre-industrial times.

Exceptions are found in some mountainous regions (e.g. the Zagros Mountains), where the projected warming can exceed these values in the middle of the current century. Instead, RCP8.5 suggests a strong mean annual temperature warming by 2-3°C for the 2050s. This is expected to reach 5-6°C by the end of the century relative to 1986-2005 (and >6°C relative to the pre-industrial period). Generally, the temperature increases are projected to be strongest in mountainous areas, probably due to reduced snow cover and alterations in the snow-albedo positive climate feedbacks. This is supported by the fact that this regional response is most evident in projections for the winter and spring seasons when snow cover is more widespread (Figures A.3 and A.4 of the Annex). The continental part of the Arabian Peninsula is also projected to warm more strongly, particularly by the end-of-century and under RCP8.5.

Maps of detailed seasonal projections are presented in Figures A.3-A.6 of the Annex. For most of the EMME region, changes are expected to be most pronounced (up to 6-8°C) during the summer season and to a lesser extent in the autumn (Figures A.5-A.6). This seasonal warming response is more evident in the relatively wetter parts of the EMME that are expected to become drier (see the following section). This is partially explained by land-atmosphere interactions and amplification feedbacks related to the hydrologic cycle (Zittis et al., 2014). For example, when precipitation, soil water content, and thus evapotranspiration decrease, near-surface air temperature is enhanced due to reduced evaporative cooling. The exceptional summertime warming is also associated with a thermal low (expansion of the Indo/Pakistan monsoon thermal low over the EMME region), which is conceived as a widening of the Persian trough that extends from South Asia to the eastern Mediterranean, and is projected to further expand westwards and combine with the intensifying thermal low over the Sahara (Lelieveld et al., 2016).

Annual temperature anomalies, averaged across the EMME region (with respect to the 1986-2005 mean conditions), for the various periods and future pathways are presented as probability density plots (Figure 11). For RCP8.5, the comparison with the historical simulations indicates a median shift to warmer conditions (+5°C) by the end of the century. This implies that under a business-as-usual scenario and by 2100, the coolest years will be comparable to the very warmest years of the reference period. At the same time, the width of the distribution is also projected to change to a more platykurtic shape, indicating greater year-to-year variability and thus more pronounced extreme years or seasons. This is an indication that the EMME region will be subjected to unprecedented heat extremes. Median changes under the optimistic RCP2.6 are projected to be milder (1-1.5°C). Nevertheless, temperatures in the warmest years will still be well in excess of the range of historical values. The mid-century projections for RCP8.5 are in between (2-2.5°C).

FIGURE 11. Probability density curves of annual temperature anomalies (with respect to the 1986–2005 mean conditions), averaged across the region (redrawn from Zittis et al., 2022)



Previous national or regional assessments and modelling studies have been developed for the region or parts of it (Zanis et al., 2009; Hadjinicolaou et al., 2011; Lelieveld et al., 2016, 2012; Önel and Unal, 2014; Jacob et al., 2014; Bucchignani et al., 2018; Ozturk et al., 2018; Hochman et al., 2018c; Mostafa et al., 2019; Zittis et al., 2019, 2020; Almazroui et al., 2020; Driouech et al., 2020a; Drobinski et al., 2020; Giannakis et al., 2020; Varotsos et al., 2021; Coppola et al., 2021a). Although a different selection of models, pathways and/or scenarios might have been used, the ranges of projected temperature trends, warming patterns and levels of significance are in close agreement with the present, updated analysis. A comparison between RCP-driven global projections (CMIP5⁹) and the Shared Socio-economic Pathways (SSPs) that will be discussed in the 6th Assessment Report of the IPCC (AR6) reveals a slightly warmer temperature response in the more advanced SSP-driven experiments (CMIP6) (Tebaldi et al. 2020). For the EMME region, this difference between the two generations of global projections is up to 0.2°C per 1.0°C of global warming.

The projected changes for each period and pathway, averaged for the 17 EMME countries, are presented in Table 1 as ensemble means. In addition, the ranges of change (i.e. model experiments with the lowest/highest climate sensitivity) are also provided in the same table. For the 2081–2100 period and RCP2.6, Greece and Turkey, at the northern edges of the EMME, are expected to experience the strongest warming (1.5°C) on average. For

⁹ Climate Model Intercomparison Project.

these countries, individual projections range between 0.7°C and 2.1°C. In the case of the stronger radiative forcing scenario (RCP8.5), the highest annual temperature increases (4.8-4.9°C) are projected in Iran, Saudi Arabia and the United Arab Emirates. According to the climate sensitivity models at the highest end of the range, the expected increase is 6.5°C. Somewhat milder temperature increases (near 4°C) are projected for the island nations of Bahrain and Cyprus. This is related to the moderating effect of the surrounding seas. Similar seasonal temperature projections are provided in Tables A.3-A.6 of the Annex. For the majority of EMME countries, summer warming is expected to be significantly stronger than in the other seasons.

Simulated temperature (and precipitation) and end-of-century projections on an annual and monthly basis are presented in Figure 12 for two representative capital cities of the EMME region. Similar plots for all the capitals of the region, as well as projections for the more optimistic RCP2.6 are presented in Figure A.8 of the Annex. Cyprus’s capital city of Nicosia (Figure 12, top panels) represents a typical Mediterranean climate regime, while

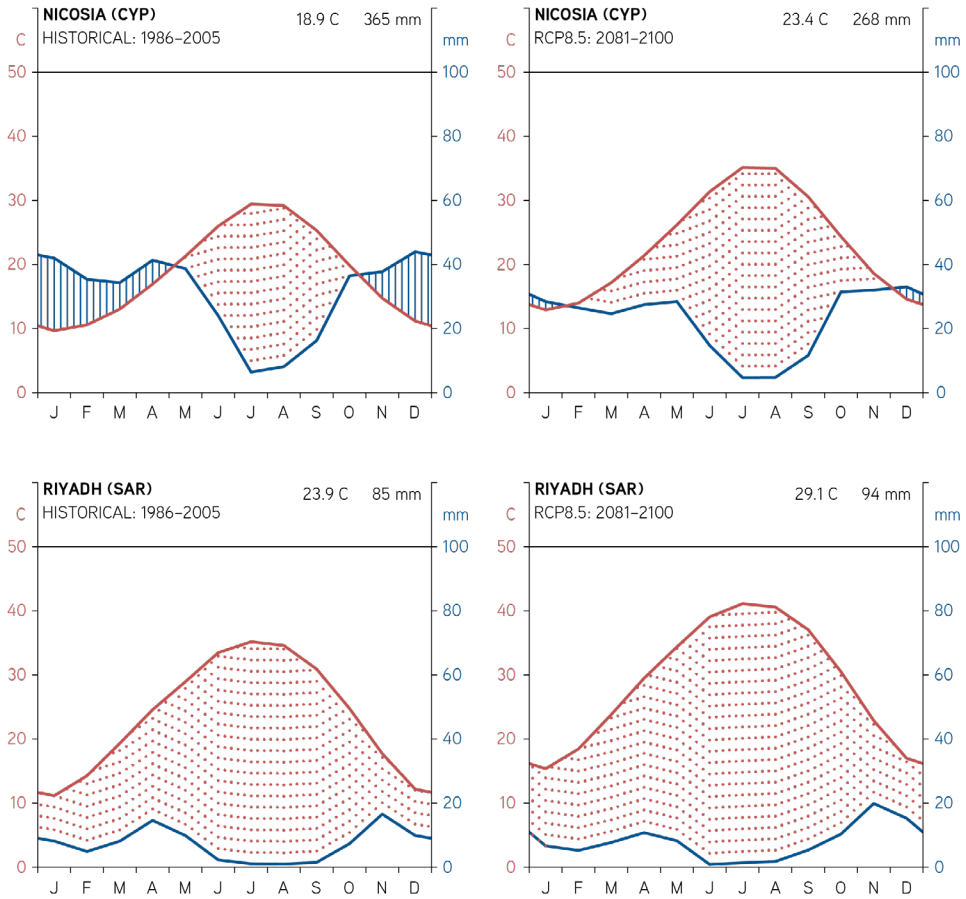
TABLE 1. Simulated annual temperature and projected changes, averaged for 17 EMME countries

Annual Temperature			TAS (CTL) °C	DELTA RCP2.6 MID		DELTA RCP2.6 END		DELTA RCP8.5 MID		DELTA RCP8.5 END	
				MEAN	(MIN, MAX)						
1	Bahrain	(BHR)	25.3	1.2	(0.7, 2.1)	1.1	(0.7, 2.0)	2.0	(1.7, 2.9)	4.2	(3.6, 5.9)
2	Cyprus	(CYP)	18.7	1.2	(0.5, 2.1)	1.3	(0.6, 2.0)	2.1	(1.6, 2.9)	4.1	(3.3, 5.7)
3	Greece	(GRC)	14.5	1.3	(0.5, 2.2)	1.4	(0.7, 2.1)	2.1	(1.4, 2.9)	4.4	(3.1, 5.9)
4	Egypt	(EGY)	21.5	1.3	(0.6, 2.2)	1.3	(0.6, 2.2)	2.2	(1.6, 3.1)	4.4	(3.4, 5.8)
5	Iran	(IRN)	16.1	1.5	(0.9, 2.5)	1.3	(0.6, 2.2)	2.4	(1.7, 3.3)	4.9	(3.9, 6.5)
6	Iraq	(IRQ)	21.8	1.4	(0.9, 2.4)	1.3	(0.7, 2.1)	2.4	(1.9, 3.3)	5.0	(4.1, 6.4)
7	Israel	(ISR)	19.7	1.2	(0.6, 2.1)	1.2	(0.6, 2.0)	2.1	(1.6, 3.0)	4.3	(3.3, 5.7)
8	Jordan	(JOR)	18.4	1.4	(0.8, 2.4)	1.3	(0.7, 2.1)	2.4	(1.7, 3.3)	4.7	(3.6, 6.3)
9	Kuwait	(KWT)	25	1.4	(0.8, 2.3)	1.2	(0.7, 2.1)	2.4	(1.7, 3.2)	4.8	(3.7, 6.2)
10	Lebanon	(LBN)	14.6	1.3	(0.6, 2.4)	1.3	(0.6, 2.1)	2.3	(1.8, 3.2)	4.6	(3.5, 6.3)
11	Oman	(OMN)	26.2	1.2	(0.8, 1.8)	1.1	(0.7, 1.8)	2.1	(1.6, 2.8)	4.4	(3.4, 5.6)
12	Palestine	(PSE)	19.7	1.3	(0.6, 2.2)	1.3	(0.6, 2.1)	2.2	(1.6, 3.1)	4.4	(3.4, 6.0)
13	Qatar	(QAT)	26.5	1.3	(0.8, 2.2)	1.2	(0.7, 2.1)	2.3	(1.9, 3.1)	4.7	(4.0, 6.0)
14	Saudi Arabia	(SAU)	23.7	1.4	(0.8, 2.3)	1.2	(0.7, 2.1)	2.4	(1.7, 3.3)	4.9	(3.8, 6.5)
15	Syria	(SYR)	18	1.4	(0.7, 2.3)	1.3	(0.7, 2.3)	2.3	(1.8, 3.2)	4.7	(3.7, 6.2)
16	Turkey	(TUR)	10.3	1.3	(0.6, 2.3)	1.4	(0.8, 2.1)	2.4	(1.7, 3.2)	4.7	(3.6, 6.2)
17	UAE	(UAE)	26.8	1.4	(0.9, 2.2)	1.2	(0.7, 2.1)	2.4	(1.9, 3.2)	4.8	(4.0, 6.2)

Source: The ensemble means and ranges of the CORDEX-CORE regional projections for each country and for RCP2.6 and RCP8.5.

Note: CTL: 1986-2005; MID: 2041-60; END: 2081-2100.

FIGURE 12. Monthly temperature and precipitation climatologies for Nicosia (Cyprus) and Riyadh (Saudi Arabia)



Source: Based on CORDEX-CORE climate projections for the 1986-2005 reference period (left panels) and the end of the century period (2081-2100) under RCP8.5 (right panels) for Nicosia, Cyprus (top panels), and Riyadh, Saudi Arabia (bottom panels).

Note: Monthly temperature (red curve) and precipitation (blue curve) climatologies. Red-shaded areas indicate the dry part of the year, while blue-shaded areas indicate the wet part of the year.

Riyadh, Saudi Arabia, represents a more arid environment. For Nicosia, the ensemble-mean projections under a business-as-usual pathway suggest a 4.5°C temperature increase, with greater warming in the summer than the winter months. For Riyadh, the mean annual temperature conditions are projected to increase by 5.2°C, with respect to the 1986-2005 reference period. This is among the highest projected warming rates across capital cities in the EMME; a similar rate is expected for Baghdad, Iraq. For the other capitals, the warming is expected to range between 3.6°C and 4.9°C (Figure A.8). These changes refer to the 30-year mean, while temperature anomalies in individual extreme warm years can

be much higher. RCP2.6 (Figure A.8 of the Annex) implies slower increases of mean annual temperature. Such a case would provide a wider window for the adaptation of local societies and ecosystems.

A peculiarity of the EMME region is that days are observed and projected to warm more strongly than nights. Minimum and maximum daily temperatures in the global 30–46°N latitudinal zone increase at a similar rate, or the minimum temperature increases more strongly than the maximum temperature (Lionello and Scarascia, 2018). In the broader Mediterranean area, maximum temperature increases are expected to be stronger than minimum temperature. Particularly under high-emission pathways, there is consensus that the enhanced warming during the hot part of the year will further augment the extreme heat conditions and cause increases in the frequency, magnitude and duration of heatwaves. The projected heat stress intensification and related impacts have received great attention in the scientific community, and there are a large number of available regional studies, based on a wide range of extreme temperature indicators, heatwave definitions and various sources of climate information (Goubanova and Li, 2007; Diffenbaugh et al., 2007; Fischer and Schär, 2010; Diffenbaugh and Giorgi, 2012; Jacob et al., 2014, 2018; Lelieveld et al., 2014; Russo et al., 2014; Zittis et al., 2016; Pal and Eltahir, 2016; Almazroui, 2020b; Molina et al., 2020; Ntoumos et al., 2020).

For most of the region, very hot summers that occurred only rarely in the recent past are projected to become commonplace by the middle and the end of the century (Lelieveld et al., 2014). Indicatively for the city of Athens in Greece, historical 1-in-20-year heatwaves will likely become 1-in-5-year events under global warming levels of 1.5°C (Jacob et al., 2018). In the scenario of 3°C global warming since the pre-industrial era, such events are projected to occur annually. Particularly in the Middle East and North Africa, exceptional heatwaves have been observed early in the century, and these thus far unprecedented events could become the norm by the end of the century (Molina et al., 2020; Zittis et al., 2021). Compared to present-day standards, extreme heatwave characteristics in the region are projected to increase tremendously (Zittis et al., 2016). The annual number of events is projected to increase by a factor of 3–6 times, their amplitude to increase to 6–7°C, while the duration of the longest-lasting events will likely be several weeks to months. Under high-emission pathways, by the end of the century, 80% of the most populated cities of the EMME are expected to suffer from heatwave conditions for at least 50% of the warm-season days (Varela et al., 2020). Besides daytime conditions, parts of the region will likely face an increase of more than 60% in the number of tropical nights, augmenting potential adverse effects on society and ecosystems (Sillmann et al., 2013; Lelieveld et al., 2016; Zittis et al., 2016; Dosio and Fischer, 2018). Peak temperatures during

extreme future heatwaves could exceed 56°C in some locations in the Middle East and the Gulf region (Zittis et al., 2021).

These model estimations might be conservative since they do not consider the urban heat island (UHI) phenomenon. Typical present-day UHI magnitudes for the region (e.g. Santamouris 2015) could add another 3-4°C. If such high temperatures become a reality, parts of the EMME region may become uninhabitable for some species. These will likely include humans and even animals tolerant of high temperatures, such as camels. Dangerous heat-stress conditions in parts of the region, mainly in the Arabian Peninsula (i.e. days with wet-bulb temperature $\geq 27^\circ\text{C}$), increase in frequency by 10-20% due to irrigation and the associated increase of humidity in the atmosphere (Krakauer et al., 2020). Widespread adverse impacts on public health, the water-energy-food nexus and other socio-economic sectors and indicators are expected (Zachariadis and Hadjinicolaou, 2014; McGeehin and Mirabelli, 2001; Habib et al., 2010; Dunne et al., 2013; Constantinidou et al., 2016; Waha et al., 2017; Ahmadalipour and Moradkhani, 2018; Abel et al., 2019; Lange, 2019; Drobinski et al., 2020). Mass gathering events in the region, such as the Muslim Pilgrimage or Hajj, may be particularly affected by extreme heat conditions (Kang et al., 2019; Saeed et al., 2021). For example, Kang et al. (2019) cautioned that there may be future increases in the frequency and intensity of heat stress in Mecca during the Hajj, with pronounced health consequences under both business-as-usual and mitigation scenarios.

Extreme ocean-warming events, known as marine heatwaves (MHWs), can be critical since they severely affect marine ecosystems and fisheries, while they can also induce an amplifying feedback on atmospheric heatwaves by limiting the moderating effect of the surrounding seas and suppressing cooling mechanisms such as land-sea breezes (Zittis et al., 2016; Darmaraki et al., 2019b). The projections for MHWs suggest longer and more intense events for the whole Mediterranean, including the eastern part of the basin. By the end of the century and under business-as-usual pathways, at least one long-lasting MHW every year, up to several weeks longer and about four times more intense than present-day events is expected (Darmaraki et al., 2019a).

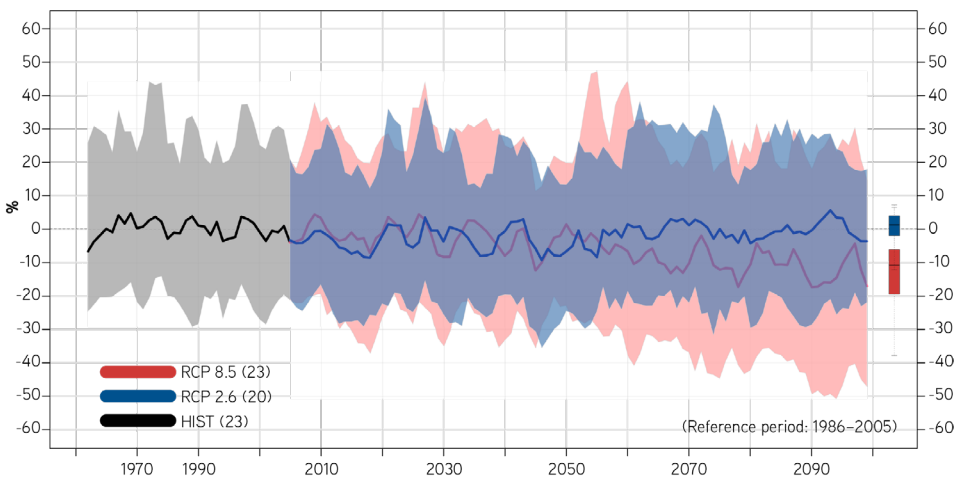
Cold-weather extremes are expected to decline throughout the EMME region. The decreases will likely be most profound in the mountainous areas of Greece, Turkey and Iran (Kostopoulou et al., 2014). For example, under an intermediate warming scenario, the number of frost nights per year will be likely reduced by 50-60 days. Moreover, glaciers in the mountainous parts of the region (e.g. Anatolia, Caucasus, Alborz and Zagros mountains) are projected to rapidly continue losing mass in the 21st century (even under RCP2.6) and will likely completely diminish by 2100 under RCP8.5 warming conditions (Hock et al., 2019).

4.2. Precipitation – averages and extremes

Global warming is associated with the Hadley Cell circulation expansion and the poleward shift of the westerlies and associated storm tracks (IPCC, 2013). This creates easterly wind anomalies at the mid-latitudes (Lu et al., 2007). Normally, westerlies are associated with moisture convergence in Mediterranean latitudes; however, the easterly shift weakens this phenomenon and induces drying (Seager et al., 2019). About 85% of the reduction in precipitation during the wet season, averaged across the Mediterranean, is attributed to such atmospheric circulation responses (Zappa et al., 2015). In addition, the drying of the eastern Mediterranean is largely caused by enhanced warming over land (Drobinski et al., 2020).

Time series of annual precipitation anomalies (with respect to the 1986–2005 climatic means), averaged for the EMME region, are presented in Figure 13. The inter-annual variability and spread of the model results are more pronounced than of annual temperatures, highlighting the greater uncertainty of precipitation projections. For RCP2.6, no significant change in precipitation is projected. In contrast, the business-as-usual RCP8.5 projects a 10–20% precipitation decrease for the region by the end of the century. For the eastern Mediterranean, this range is in very good agreement with other assessments, suggesting that the mean rate of the decrease in land precipitation across the Mediterranean is 4% per degree of global warming (Cherif et al., 2020). In addition to the overall drying trend,

FIGURE 13. Projections of EMME annual precipitation anomalies (for the 1986–2005 reference period)

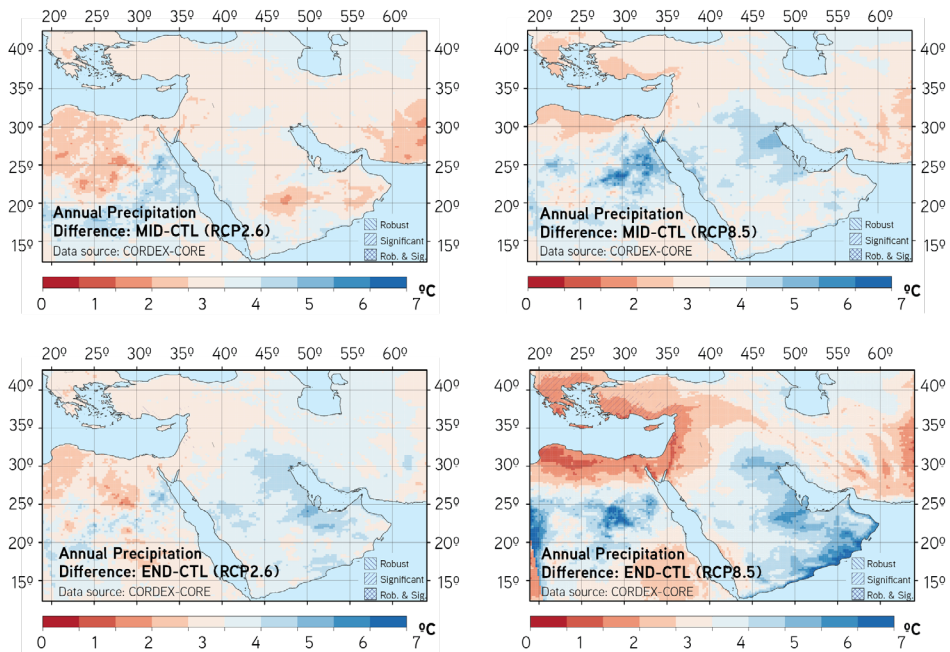


Source: Based on CORDEX-CORE climate projections and two Representative Concentration Pathways (redrawn from Zittis et al., 2022).

individual years, at least according to some models, could be drier or wetter than the present-day mean conditions as a result of the increased variability, combined with alterations in atmospheric thermodynamics and circulation drivers.

The spatial pattern of annual precipitation changes is presented in Figure 14, whereas changes on a seasonal basis are presented in Figures A.9-A.12 (Annex). The simulated precipitation climatology of the historical period is presented in Figure A.2 for reference. For RCP2.6 and both time horizons, annual precipitation changes are limited to about $\pm 10\%$, with increases projected mainly for the EMME’s southern and southeastern territories. The levels of robustness and significance are low, indicating that under this pathway, projected changes are within the present-day variability, and the model spread comparable to the climate change signal. Under RCP8.5, the mid-century conditions are similar to RCP2.6 and associated with low levels of significance and inter-model agreement, and hence have low robustness. However, the end-of-century signal is stronger. For regions adjacent to the Mediterranean Sea (for instance, Greece, Turkey, Cyprus, Lebanon, Israel, Palestine, north Egypt, etc.), the ensemble suggests a significant and occasionally robust

FIGURE 14. Projected changes (%) in annual precipitation (with respect to the 1986-2005 reference period)



Source: Based on CORDEX-CORE climate projections for RCP2.6 (left panels) and RCP8.5 (right panels) and for mid-21st-century (2041-60, top panels) and end-of-century projections (208-2100, bottom panels) (redrawn from Zittis et al., 2022).

precipitation decrease (20-40%). This decrease is greater for precipitation amounts in the winter season. Conversely, in the southern regions (e.g. parts of the Arabian Peninsula and south Egypt), the annual precipitation is expected to increase (up to 50%). Although the percentage increase seems large, it is not always significant in terms of rainfall amounts. Under the business-as-usual pathway, the rainfall increase in the southern parts of the domain is mainly projected for the transition seasons of spring and autumn (Figures A.11 and A.13), coinciding with the seasonal displacement of the ITCZ. The contribution of the rainiest days of the year to the annual precipitation total is projected to increase (Zittis et al., 2021).

Country-level information on the projected annual precipitation changes is presented in Table 2. Ensemble means and ranges (i.e. driest and wettest model projections) are indicated. Time series of projected precipitation anomalies for the 17 individual countries of the region are also provided in Figure A.7 of the Annex. Under RCP2.6 conditions, and

TABLE 2. Simulated annual precipitation (in mm) and projected changes (in %), averaged for 17 EMME countries

Annual Precipitation			PR (CTL) mm	DELTA RCP2.6 MID		DELTA RCP2.6 END		DELTA RCP8.5 MID		DELTA RCP8.5 END	
				MEAN (%)	(MIN, MAX)						
1	Bahrain	(BHR)	89	22	(-15, 43)	43	(-6, 80)	37	(-11, 86)	74	(-7, 144)
2	Cyprus	(CYP)	504	-3	(-12, 4)	-3	(-13, 6)	-11	(-21, -2)	-26	(-43, -12)
3	Greece	(GRC)	857	-6	(-15, 3)	-5	(-13, 2)	-11	(-21, -1)	-24	(-37, -11)
4	Egypt	(EGY)	30	8	(-42, 57)	7	(-34, 54)	21	(-33, 70)	33	(-57, 101)
5	Iran	(IRN)	331	-5	(-19, 11)	5	(-10, 22)	0	(-17, 19)	-5	(-31, 22)
6	Iraq	(IRQ)	212	-3	(-19, 11)	6	(-14, 24)	4	(-16, 23)	-1	(-34, 33)
7	Israel	(ISR)	305	-6	(-26, 11)	-5	(-17, 8)	-7	(-27, 11)	-26	(-45, -7)
8	Jordan	(JOR)	119	-9	(-30, 9)	-4	(-20, 13)	-4	(-26, 19)	-22	(-47, 4)
9	Kuwait	(KWT)	118	7	(-17, 33)	21	(-6, 48)	14	(-12, 43)	22	(-18, 76)
10	Lebanon	(LBN)	801	-6	(-22, 4)	-5	(-14, 4)	-9	(-22, 3)	-27	(-42, 13)
11	Oman	(OMN)	94	6	(-45, 65)	18	(-28, 80)	17	(-42, 92)	52	(-38, 165)
12	Palestine	(PSE)	278	-6	(-27, 10)	-5	(-18, 5)	-9	(-25, 7)	-29	(-45, -16)
13	Qatar	(QAT)	80	29	(-16, 65)	41	(-14, 80)	45	(-18, 167)	58	(-15, 125)
14	Saudi Arabia	(SAU)	97	8	(-26, 50)	16	(-19, 54)	17	(-21, 63)	22	(-36, 78)
15	Syria	(SYR)	272	-7	(-21, 4)	-4	(-15, 6)	-8	(-21, 6)	-19	(-38, 0)
16	Turkey	(TUR)	851	-4	(-11, 3)	-2	(-9, 5)	-6	(-14, 2)	-14	(-29, -3)
17	UAE	(UAE)	69	9	(-29, 61)	18	(-21, 60)	16	(-34, 89)	31	(-29, 112)

Source: The ensemble means and ranges of the CORDEX-CORE regional projections are presented for each country and for RCP2.6 and RCP8.5.

Note: CTL: 1986-2005; MID: 2041-60; END: 2081-2100.

for most countries, the projected changes are within the natural inter-annual variability and are in the $\pm 10\%$ range. Exceptions are Bahrain and Qatar, which, however, according to CORDEX-CORE models, have very low reference precipitation (about 40 mm/year), leading to relatively greater percentage changes. For RCP8.5 and mid-21st century conditions, some precipitation increases in the Gulf countries with low rainfall in the reference period are also expected (e.g. in Bahrain, Kuwait, Qatar, Saudi Arabia and the United Arab Emirates). In eastern Mediterranean countries (e.g. Cyprus, Greece, Israel, Lebanon, Turkey), annual precipitation is expected to decrease, by up to 11%, under the high-emission pathway. This precipitation decrease is projected to intensify towards the end of the current century and reach up to 30%. A hotspot of precipitation decrease is the Levant region, with areas such as Palestine, Israel and Cyprus being most strongly affected. The confidence in this end-of-century drying is high, as indicated by the consistency across the different projections. Under this pathway, the precipitation increase in some Middle East territories is also expected to continue. Nonetheless, any potential benefits for water resources will be by far outweighed by the strong temperature (and thus evapotranspiration) increases (see Table 1).

End-of-century climate projections for the EMME capitals are presented on a monthly basis (Figures 12 and A.8). For the more temperate climates, the blue-shaded areas represent the wet period of the year, while the red-shaded areas represent the dry months. For cities with typical Mediterranean climate conditions (e.g. Athens, Nicosia, Beirut, Tel Aviv, Amman, Ramallah), the combined warming and strong precipitation decrease, suggested by RCP8.5, implies an up to two months' expansion of the dry season of the year. For some hyper-arid Middle East regions (e.g. the capitals of Kuwait, Oman, Qatar and the United Arab Emirates), the projected increase in precipitation is mainly due to increases in individual autumn months (Figure A.8). These months (e.g., October, November) coincide with the displacement of the ITCZ that under global warming conditions is expected to expand poleward. A northward shift of the ITCZ may cause changes in the atmospheric circulation over the region, in wind regimes, dust emissions and accumulation (Rashki et al., 2019). This precipitation increase could also be the result of extreme single-day precipitation events; however, this hypothesis should be further investigated. Under RCP2.6, much milder changes in rainfall are projected for all cities under investigation.

In terms of direction, magnitude and location as well as the uncertainty range of precipitation changes, these updated estimates are in good agreement with and corroborate previous studies and assessments for the region (Lelieveld et al., 2012, 2016; Önoğlu and Unal, 2014; ESCWA et al., 2017; Bucchignani et al., 2018; Öztürk et al., 2018; Zittis et al.,

2019, 2020; Driouech et al., 2020a; Varotsos et al., 2021). Especially for the Middle East, the current analysis provides additional details, particularly for the RCP2.6 projections.

Several global and regional studies, based on a variety of drought indicators, suggest a future increase in the severity, length and impact of future drought events across the broader Mediterranean and Middle East region (Sen et al., 2012; Prudhomme et al., 2014; Dubrovský et al., 2014; Touma et al., 2015; Waha et al., 2017; Liu et al., 2018; Naumann et al., 2018; Tabari and Willems, 2018; Spinoni et al., 2018, 2020; Driouech et al., 2020a; Danandeh Mehr et al., 2020). For example, the Aridity Index, which considers both precipitation and potential evapotranspiration, is projected to increase by up to 50% for most of the eastern Mediterranean coastal regions, while the signal of changes is weaker for the already hyper-arid parts of the region (Waha et al., 2017). In addition, drought periods are projected to last longer (up to 90%) in about 80% of the Middle East area (Tabari and Willems, 2018). High-resolution projections for Israel and Cyprus also highlight that the number of consecutive dry days per year is expected to increase by up to 20-40 additional days per year (Hochman et al., 2018c; Zittis et al., 2020). In Cyprus, for example, the dry period of the year is projected to expand by one to two months by the end of the current century. This can be partly attributed to the projections for a shorter wet season and a longer dry season due to the projected (and significant) decrease in the occurrence of Cyprus Lows and the projected increase in the frequency of the Persian Trough (Hochman et al., 2018b, 2018a). Towards the end of the century, droughts are anticipated to increase more under high-forcing pathways, while the projected changes in the severity of such events are more pronounced when the synergetic impact of temperature is also considered (Driouech et al., 2020b; Spinoni et al., 2020). For example, changes corresponding to an overall increase of 20-40% in the percentage of dry years with the highest values exceeding 40% lead to a doubling of the present-day ratio (Driouech et al., 2020b).

Extreme precipitation is expected to intensify with global warming over large parts of the globe as the concentration of atmospheric water vapor, which supplies the moisture for precipitation, increases in proportion to the atmospheric saturation vapour pressure at a rate of about 6-7% per degree rise in temperature (Allen and Ingram, 2002; Tabari, 2020). Parts of EMME lie in the transitional zone, where, on the one hand, decreases of weak to moderate precipitation are expected, while on the other hand, climate models suggest an increase in extremes. Besides the uncertainties involved in the precipitation projections and the contribution of internal climate variability, which cannot be neglected, several studies have highlighted that climate change is likely to affect the severity and frequency of high-impact extreme precipitation events in the region (Chen et al., 2014; Paxian

et al., 2015; Donat et al., 2016; Rajczak and Schär, 2017; Drobinski et al., 2018; Giorgi et al., 2019). In the Fertile Crescent (except for the southeastern coasts of the Mediterranean Sea), extremely wet days are expected to increase by approximately 25%, particularly for RCP8.5, by the end of the 21st century (Samuels et al., 2018).

For the semi-arid and arid parts of the EMME, global climate models suggest an increase of up to 5-10% in 1-in-30-year extreme precipitation intensity per degree of global warming in 2070-99 under RCP8.5, compared with 1971-2000 (Tabari, 2020). Such projections challenge the assumption of climate stationarity, a standard hypothesis in the estimation of extreme precipitation quantiles often used as key design criteria for infrastructure (Martel et al., 2020). Moreover, the contribution of the wettest day of the year to the annual precipitation total is projected to increase in the future throughout the Mediterranean region (Zittis et al., 2021b). Global and regional climate projections indicate a strong north/south gradient with a projected increase of extreme precipitation indicators in the northern Mediterranean and a decrease in the south (Tramblay and Somot, 2018; Lionello and Scarascia, 2020; Zittis et al., 2021b). It should be noted, however, that most of the available literature focuses on Mediterranean countries, and more research is needed to assess the future of extreme precipitation in more southern latitudes and regions of the Middle East.

Excluding the role of water management, nearly all rivers flowing into the Mediterranean are expected to see significant reductions in their natural discharges through the 21st century due to the projected rainfall reduction (Mariotti et al., 2008; Jin et al., 2010; Alpert et al., 2013). The Nile may be an exception since its water resources are in the tropical regions where some rainfall increases are projected. The Fertile Crescent is expected to dry, and its fertility is challenged by the end of the 21st century (Kitoh et al., 2008), with a significant drying of the Euphrates and Jordan rivers (streamflow decreases of 29-73% and 82-98%, respectively). The Euphrates discharge regime has changed substantially since the construction of its first dams in the 1970s, while the natural flow may be expected to drop by ~70% in high-warming scenarios (Kitoh et al., 2008; Alpert et al., 2014).

4.3. Other meteorological parameters

4.3.1. Atmospheric circulation

Global warming is accompanied by an expansion of the Hadley Cell circulation and a poleward shift of the westerlies and associated storm tracks (Evans, 2010). This creates easterly wind anomalies at mid-latitudes (Lu et al., 2007). Normally, westerlies lead to moisture convergence in the Mediterranean latitudes; however, the easterly shift weakens

this phenomenon and contributes to drying (Seager et al., 2019). Trends in recent cyclone numbers affecting the Mediterranean are largely absent; however, when trends are detected, these are mostly negative (Cherif et al., 2020). A reduction in the total number of cyclones crossing the Mediterranean region is expected under future climate change conditions (Nissen et al., 2014). Exceptions are parts of the Levant and the Arabian Peninsula, where climate models predict a statistically significant increase in the number of cyclones. A large fraction of the reduction in wet-season precipitation, averaged for the Mediterranean area, has been attributed to such atmospheric circulation responses (Zappa et al., 2015). In addition, a drying trend in the eastern Mediterranean is enhanced by warming over land (Drobinski et al., 2020). Local circulation patterns are also likely to be affected, particularly under high radiative forcing pathways. For example, Cyprus Lows (mid-latitude disturbances that tend to develop in the Levantine Basin during the wet season) are expected to weaken towards the end of the 21st century (Hochman et al., 2018b). These reductions may partially be compensated by increases in Persian Troughs and Red Sea Troughs, especially during the winter season, but these weather systems may nevertheless be less active in terms of precipitation. For Mediterranean tropical-like cyclones or Medicanes that might develop or generate impacts in parts of the eastern Mediterranean (e.g. in Greece), climate projections indicate decreasing frequency but increasing intensity (Romero and Emanuel, 2013; González-Alemán et al., 2019).

In addition to the projected changes in atmospheric circulation dynamics, it was recently suggested that the lengths of seasons may change dramatically through the 21st century. Of particular relevance is the duration of synoptic seasons (Alpert et al., 2004), especially the rainy winter relative to the warm and dry summer. The winter season may dwindle by up to two months, while the summer lengthens by up to five (Hochman et al., 2018a, 2018b).

4.3.2. Near-surface winds

Future wind speed changes over the continental parts of the EMME may vary in sign and magnitude and have a different seasonal response. Under an intermediate GHG emission scenario, the northern part of the EMME (e.g. the southern Balkans and Anatolia) is projected to experience decreased wind speeds during the winter (by about 10%), while the southern parts of the EMME are projected to experience increased speeds. Climate projections for the northern EMME suggest a wind speed increase in summer as well (also by about 10%), while for the southern EMME, the changes are expected to be relatively small (McInnes et al., 2011). One exception is the south parts of the Arabian Peninsula (including Yemen and Oman), where wind speeds are projected to increase, mostly during the

summer season (Feron et al., 2020). This is especially relevant for future changes in dust outbreaks from the southern Arabian deserts (e.g. Rub-Al Khali, Oman desert) towards the Arabian Sea (Francis et al., 2021). On average, off-shore wind speeds over the eastern Mediterranean Sea are projected to decrease by up to 10% (Dobrynin et al., 2012; Cherif et al., 2020). This will impose a general decrease in the mean wave height, as well as in the number and intensity of wave extremes, over a large part of the region, especially in winter (Cherif et al., 2020). The Etesian winds over the Aegean Sea, mainly active during summer, are an exception since increases in the wind speed are expected for the future (Dafka et al., 2019; Ezber, 2019). The wind speed along the western coast of the Arabian Sea is also expected to increase by the end of the century by about 5% to 10% (McInnes et al., 2011; Dobrynin et al., 2012). These changes are expected to have implications in several respects, including renewable energy resources in some parts of the region (Davy et al., 2018) and Aeolian dust activity. For example, in Crete, a future aeolian energy rise is expected in summer and fall, while in the adjacent island of Cyprus, wind energy production is projected to decrease in all seasons (Vara et al., 2020). Decreases in windstorm days are expected over most of the EMME region (Nissen et al., 2014). This overall reduction is due to a projected decrease in the number of events associated with local cyclones.

4.3.3. Total cloud cover

The projected poleward expansion of the Hadley Cell will likely induce a reduction (of up to 5-10%) in total cloud cover across the broader Mediterranean region (Enriquez-Alonso et al., 2016; Bartók et al., 2017; Hentgen et al., 2019). Nevertheless, this signal is not always significant, and is more evident in the results of global models than in regional models, and is projected to be stronger under high climate forcing pathways and towards the end of the century (Cherif et al., 2020). This reduction is mostly expected for the northern countries of the EMME and is projected to be statistically significant under intermediate and high-emission pathways such as RCP4.5 and RCP8.5 (IPCC, 2013). For the Arabian Peninsula, minor and insignificant changes in the mean cloudiness are projected, associated with an increase of about 5% in the cloudiness variability by mid-century (IPCC, 2013; Feron et al., 2020). This enhanced cloudiness variability will likely influence photovoltaic energy production. For example, summer days with very low photovoltaic power outputs are expected to double in the Arabian Peninsula. For the eastern Mediterranean (e.g. in Cyprus), a slight decrease in photovoltaic productivity is projected during spring, summer and fall, especially by the end of the century (Vara et al., 2020). During winter months, significant changes in future photovoltaic productivity are not expected.

4.3.4. Relative humidity

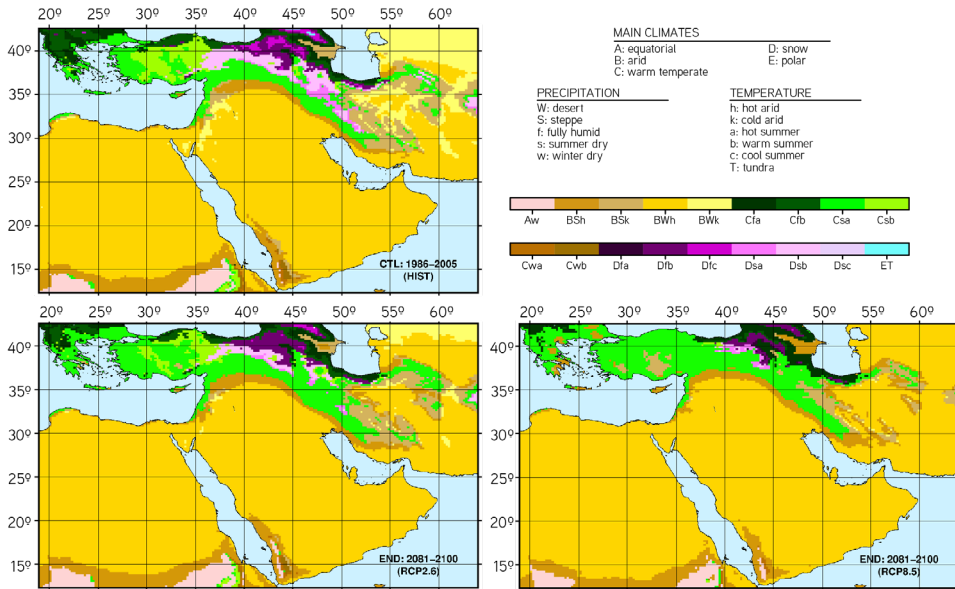
The relative humidity of the atmosphere is a critical weather parameter for ecosystems and human comfort in many parts of the EMME and particularly in the Gulf region. There, the shallow and warm waters are an abundant humidity source. As a result of atmospheric warming and circulation changes, relative humidity changes in the region are projected to have a strong seasonal response. Under a business-as-usual pathway, global climate models suggest a mild decrease (of up to 5%) throughout the region during the winter season (Collins et al., 2013). In summer, a stronger and statistically significant decrease in relative humidity is expected (by up to 10%) for the northern parts of the EMME (e.g. the Balkans and Anatolia), while for the southern parts of the region (including the Arabian Peninsula and the Gulf region), relative humidity is projected to increase by up to 5%. This increase will further increase heat discomfort and thermal stress in these areas, while it could potentially affect other human activities, for example, transportation, through decreased visibility. The projected relative humidity changes are expected to be more pronounced towards the end of the current century.

4.4. Changes in climate regimes

Climate classifications offer a systematic way of describing the main climatic features of a region. The Köppen-Geiger climate classification system, applied in the present assessment, is one of the most widely used. It is based on the concept that climate zone boundaries also describe the vegetation and ecosystem distribution. A detailed description of the Köppen-Geiger classification, including the climate constraints for its application, is presented in Section A.1.4 and Table A.2 of the Annex. The synergistic effects of temperature and precipitation changes, and alterations in their monthly and seasonal distribution, are expected to cause changes in the main climate characteristics of the EMME region. Such changes will likely introduce adverse impacts on both human and natural systems.

The classification results for the 1986-2005 control reference period are presented in the top-left panel of Figure 16. Most of the EMME (about 75%) is characterised as a hot desert (BWh) or steppe (BSh) (see Table A.2). Such regions involve large parts of the Arabian Peninsula and North Africa. The Balkan and Anatolia peninsulas, as well as parts of the Fertile Crescent, are identified as warm temperate climates across several subcategories (e.g. Cfa, Cfb, Csa, Csb; see Table A.2), with the cooler classes found in the northern part of the EMME. These areas represent about 18% of the surface area of the region. In the remaining 7%, snow climates prevail (i.e. the temperature of the warmest month is greater

FIGURE 15. Application of the Köppen-Geiger climate classification system

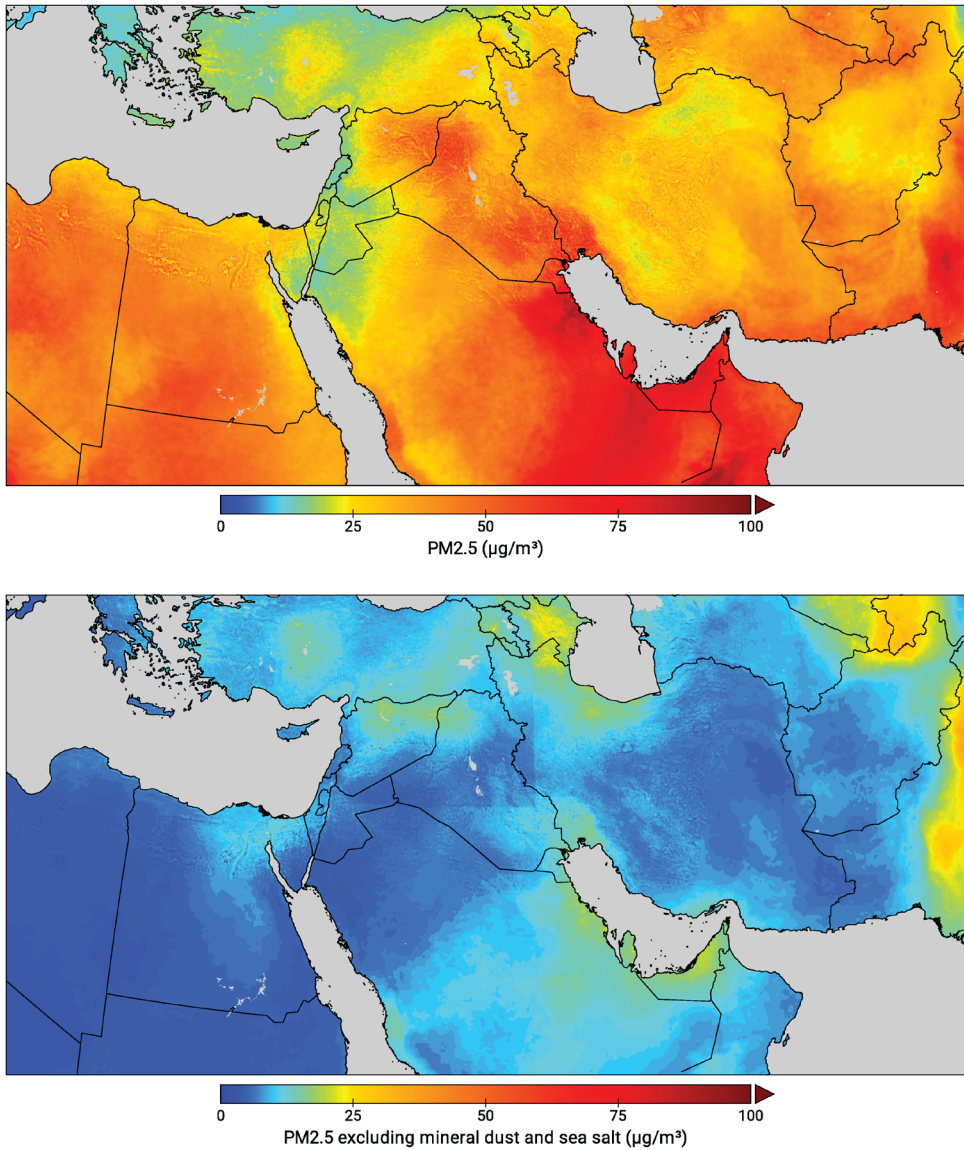


Source: Based on the CORDEX-CORE dataset for the 1986-2005 historical reference period (top left panel) and the end of the 21st century (2081-2100) under RCP2.6 (bottom left panel) and RCP8.5 (bottom right panel) (adopted from Zittis et al., 2022).

than 10°C, and the temperature of the coldest month is -3°C or lower). This class is mainly found at the highest elevations, for example, the Taurus, Caucasus and Zagros mountains.

Because of the projected warming and alterations in the hydrological cycle, by the end of the current century (2081-2100) and under the high-emission pathway (RCP8.5), the climate characteristics of the region are expected to change (Figure 15, bottom right panel). The most profound alterations include a northward expansion (by 5%) of the dry zones (BWh and BSh) against the more temperate climates (Cf and Cs; see Table A.2). Such arid zones will likely expand to parts of Cyprus, eastern Greece and Turkey, characterised as temperate zones in the historical simulations. Because of the strong winter warming in high-elevation regions, snow climates (Df and Ds; see Table A.2) are projected to mostly diminish to less than 2% of the EMME region. This will have a large impact on water resources, especially in places that rely on winter and spring snow cover upstream. On the contrary, under RCP2.6, the milder warming and less pronounced changes of precipitation seasonality and total amounts imply less significant changes in the climatic characteristics of the region (Figure 15, bottom left panel).

Figure 16. Annual mean distributions of PM2.5 over the EMME, derived from satellite observations



Source: Updated data from Van Donkelaar et al. (2016).

Note: The upper panel shows a total of PM2.5, and the lower panel without sea salt and aeolian dust, i.e. mostly dust of natural origin.

4.5. Regional sea-level rise

Over the past decades, the sea level has risen globally, primarily due to global warming, which has led to an increase in ocean warming and thermal expansion, as well as significant land and ice mass loss. The altimetry-based global mean sea level average trend was 3.1 ± 0.3 mm yr⁻¹ for the period 1993-2018, with ocean thermal expansion, glaciers, Greenland and Antarctica contributing 42%, 21%, 15% and 8% to the global mean sea level rise, respectively, over this period (Cazenave et al., 2018). Amid the ongoing energy uptake of the global ocean, this trend has high inertia and will continue in the future. Indications of Antarctic land ice destabilisation are steadily gaining support, strengthening the likelihood of the significant acceleration of sea-level rise (SLR) during the present and following centuries. This will potentially reach several metres by 2100, and could rise much further during the expected lifetime of current coastal settlements, infrastructure, agriculture and cultural heritage sites. Thermal expansion, ocean dynamics, land ice loss contributions, vertical land movements and the Earth's gravity field will shape regional differences under an SLR of the order of 0.1 m (Asariotis and Benamara, 2012; Oppenheimer et al., 2019). Given the magnitude of the expected SLR overall, these regional differences will have limited importance. This section focuses on observed and future changes in sea levels in three important basins of interest: the Arabian or Persian Gulf, the eastern part of the Mediterranean Sea and the Red Sea. Such changes may imply severe impacts on coastal infrastructure and the quality of the intensively exploited Mediterranean aquifers (Kron, 2013; Mazi et al., 2014; Izaguirre et al., 2020).

4.5.1. Arabian Gulf

The Arabian Gulf is located in the sub-tropics between 24°N and 30°N latitude and 48°E and 57°E longitude. It is considered a biogeographic sub-province of the northwestern Indian Ocean. The mean depth of this shallow water body is about 50 metres. The Gulf, particularly the shallow southern basins, is the warmest sea on the planet during summer, with sea surface temperatures regularly exceeding 35°C in August (Vaughan et al., 2018). An increase in sea surface temperatures by 0.7°C/decade along the western side of the Arabian Gulf is observed, a rate that substantially exceeds the annual global warming since pre-industrial times (Hereher, 2020). For a period of more than 28 years (1979-2007) and the northwestern part of the Arabian Gulf, a relative SLR of 2.2 ± 0.5 mm yr⁻¹ was estimated (Allothman et al., 2014). After considering the vertical land motion, the absolute rise for the same period is estimated at 1.5 ± 0.8 mm yr⁻¹, which is consistent with the global estimate of 1.9 ± 0.1 mm yr⁻¹ (Church and White, 2011). An analysis of tidal data from seven stations along the west coast of the Arabian Gulf in Saudi Arabia revealed an increase in

sea levels, reaching a maximum of 3.4 ± 0.98 mm yr⁻¹ for 1979-2008 (Siddig et al., 2019). More recent observations (1993-2019) report an average SLR rate of 2.85 mm per year (Naderi Beni et al., 2021). SLR projections are also available for the Arabian (Persian) Gulf and Oman Sea. The SimCLIM¹⁰ model, driven by data from 24 CMIP5 coupled climate models, projects an increase of regional mean sea levels by the end of the century. These projections range from about 84 to 181 centimetres (cm) for a low (RCP2.6) and a high (RCP8.5) emission pathway, respectively (Irani et al., 2017).

4.5.2. Mediterranean Sea

The Mediterranean Sea is a semi-enclosed overturning water body situated between Southern Europe, the Middle East and Northern Africa, connected to the global ocean by only the narrow Strait of Gibraltar. The average depth is about 1.5 kilometres (km), but in some areas it exceeds 5 km. The inflow of the Atlantic water through the strait compensates for the water deficit generated by the excess of evaporation over precipitation (Soto-Navarro et al., 2020). For the period 1993-2018, monitored by satellite altimetry, the Mediterranean Sea level was shown to have risen at a rate of 2.8 ± 0.1 mm yr⁻¹, consistent with the rise in global sea levels (3.1 ± 0.4 mm yr⁻¹) (Cherif et al., 2020, and references therein). Based on estimations from coupled regional climate models, the rise in the Mediterranean Sea level is expected to be close to that of the global mean sea level. The basin-level average will likely increase by 37-90 cm in the 21st century compared to the end of the 20th century, with a small probability of increasing more than 110 cm (Cherif et al., 2020, and references therein). Another calculation method, based on the sea-level projections of IPCC's "Special Report on the Ocean and Cryosphere in a Changing Climate" (Oppenheimer et al., 2019), confirms that the likely rise in the Mediterranean Sea level at the end of the century will be in the range of approximately 20 cm to 110 cm (Cherif et al., 2020). However, there is growing evidence for the higher values and also a multicentury lock-in that cannot be mitigated. Extreme sea level events are water-level heights that consist of contributions from mean sea levels, storm surges and tides. Such events in the eastern Mediterranean are projected to increase. For example, in Alexandria, Egypt, extreme sea level events with return periods of 100 years in the recent past will become annual or even more frequent (Oppenheimer et al., 2019).

4.5.3. Red Sea

The Red Sea is located between the African and Asian continents (12-30°N and 32-44°N), oriented from the north-northwest to the south-southeast. It is a semi-enclosed basin, with a length of about 2 000 km, an average width of 280 km and an average depth of

10. SimCLIM is a software tool designed to facilitate the assessment of risks from climate change.

about 500 metres. The sea-level variability of the Red Sea is mainly influenced by the exchange between the Red Sea and the Gulf of Aden. The Red Sea is one of the warmest and most saline water bodies in the world, due to the high evaporation rates and near-zero precipitation (Abdulla and Al-Subhi, 2020, and references therein). Several studies have investigated the annual sea level variation and characteristics of the seasonal cycle and circulation at certain locations in the Red Sea (Pugh and Abualnaja, 2015; Abdulla and Al-Subhi, 2020; Alothman et al., 2020); however, there is limited information on its projected rise.

5. Special topics

5.1. The interplay between atmospheric composition and climate

Global warming has strong impacts on the arid and semi-arid regions of the Middle East, which have physical geography and atmospheric conditions that make them particularly vulnerable to climate change (Barlow et al., 2002; Notaro et al., 2015; Klingmüller et al., 2016; Masoudi et al., 2018). Several studies investigate trends in dust activity, including seasonality, as the major factors behind degraded air quality in the Middle East (Rezazadeh et al., 2013; Mashat et al., 2018; Rashki et al., 2018). Figure 16 illustrates the contribution of mineral dust to concentrations of particulate matter with a diameter less than 2.5 microns (PM_{2.5}), revealing the southern Arabian deserts, the Iraqi Plains and regions in south-east Iran as dust sources contributing majorly to the PM_{2.5} mass. Chemical analysis of airborne dust is essential for questions related to emission inventories, source apportionment, climate modelling, air pollution monitoring and mitigation strategies. The majority of such studies emphasised trace metals, organics and micro-organisms in total suspended particulates or PM₁₀ and PM_{2.5} samples (Shahsavani et al., 2012; Al-Khashman, 2013; Heidari-Farsani et al., 2013; Rashki et al., 2013a; Mazar et al., 2016; Gat et al., 2017; Lang-Yona et al., 2020). Declining trends in precipitation and an increase in evapotranspiration over the Middle East may decrease vegetation cover and increase the bare surface, which becomes more susceptible to wind erosion, causing an increase in dust activity, and the frequency and intensity of dust storms (Gholami et al., 2020; Rashki et al., 2021). Consequently, land degradation and increased susceptibility to aeolian erosion have resulted in an observed increase in dust days (Middleton, 2019; Shaheen et al., 2020).

Scattering and absorption of solar radiation by atmospheric aerosols (such as dust, soot from the burning of biomass and pollution) can modify the radiation budget, atmospheric stability, latent and sensible heat fluxes and thus affect cloud formation, microphysics (albedo, droplet size distribution, lifetime) and precipitation (Ramanathan et al., 2001; Rosenfeld et al., 2001, 2007; Kaufman et al., 2005). On a global scale, desert dust exerts an estimated top of atmosphere (TOA) radiative forcing in the range of -0.6 to 0.4 Wm^{-2} , while in the EMME region, the forcing, both at the TOA and surface, is much more intense due to enhanced aerosol loading, especially during the summer season (Alpert et al., 1998; IPCC, 2007). Few studies have assessed the dust-induced radiative forcing over the region. In this respect, studies followed different modelling approaches (mostly based on satellite observations), revealing large surface radiative cooling, especially during intense

dust events (Papadimas et al., 2012; Mishra et al., 2014; Gkikas et al., 2018). Over areas not systematically affected by intense dust plumes, the surface cooling due to aerosols is mostly attributed to light absorption (atmospheric heating), due to the presence of highly absorbing aerosols (e.g. black carbon), as over the eastern Mediterranean (Mishra et al., 2014; Klingmüller et al., 2019). When dust is mixed with anthropogenic aerosols, atmospheric heating can amount to $17 \pm 8 \text{ W m}^{-2}$, influencing the ambient temperature in the lower atmosphere ($< 3 \text{ km}$) with heating rates ranging from 0.1°C/day to 0.9°C/day . The uptake of acids from the gas phase by the alkaline dust particles influences atmospheric composition, for example, by reducing nitrate, which in turn decreases the formation of ammonium nitrate aerosols (Karydis et al., 2016). The uptake of acids tends to reduce the lifetime of dust particles by enhancing the deposition and cloud scavenging efficiency (Abdelkader et al., 2015). Since aerosols act as cloud condensation nuclei, dust-pollution-cloud interactions cause cloud adjustments, which reduce the condensed water path, leading to a positive (warming) radiative forcing of climate (Klingmüller et al., 2020).

Absorbing dust aerosols over the EMME may stabilise the lower atmosphere via localised diabatic heating and may lead to accumulation of aerosols over the region and the formation of a “pollution pool” (Mishra et al., 2014). Shortwave and longwave radiative forcing assessment over the arid Middle East was also performed via numerical model simulations (Saeed et al., 2014; Jish Prakash et al., 2015). A considerable radiative effect of dust aerosols was observed at the surface due to large dust scattering, with significant warming during the night and cooling during the day. By modifying the radiative balance and earth-atmosphere fluxes, dust aerosols affect local climatic parameters such as temperature, winds and precipitation over the Middle East (Klingmüller et al., 2016; Yu et al., 2016; Francis et al., 2021). A severe dust storm over Arabia in March 2009 caused a large temperature decrease ($\sim 6^\circ\text{C}$) over Riyadh (Maghrabi et al., 2011; Alharbi et al., 2013). Similarly, Prakash et al. (2015) estimated a large reduction of -6.7°C in surface temperature over the Middle East during a severe dust storm in March 2012.

In addition, the vertical distribution of dust is particularly important for the radiative effects over the arid regions with multiple light reflections between the bright surface and dust layers. Several studies have also shown a strong linkage between elevated dust-induced atmospheric heating over the Arabian Sea and modulations in the monsoon circulation pattern and rainfall over the Indian sub-continent (Vinoj et al., 2014; Solmon et al., 2015; Jin et al., 2016; Kaskaoutis et al., 2018). This dust forcing and monsoon interaction, which may be a regulatory climatic factor in South Asia, has been investigated via satellite observations, ground measurements and numerical simulations. Radiation absorption by elevated dust layers can enhance cyclonicity over the western Arabian Sea, and therefore modulate

the pressure gradient across the north Indian Ocean that influences the monsoon circulation. The result is the intensification of the southwesterly summer monsoon flow over the Arabian Sea and increased rainfall over western and central India (Lawrence and Lelieveld, 2010; Jin et al., 2021). Therefore, short- or long-term changes in dust activity over Arabia may modulate the climate system over the whole of South Asia. Even small changes in the absorbing capability of dust – due to changes in mineralogy – may significantly affect the precipitation rates (Das et al., 2015).

Changes in pressure gradients between the Caspian Sea and the Hindu Kush–Pamir mountainous range may strongly affect the wind regime and dust activity over the eastern parts of Iran (Kaskaoutis et al., 2016, 2017). This area is highly affected by the Levant seasonal or “120-days” winds blowing with great intensity from mid-May to mid-September. Warmer conditions and accelerating desertification over Central Asia will affect the Caspian Sea High that mostly modulates the Levant wind and dust activity, causing a sequence of weather and climate forcing. More recently, high-resolution satellite data and in-situ observations were analysed for estimating the direct and semi-direct radiative effects of dust over the southern Arabian Peninsula during an intense dust storm (Francis et al., 2021). Apart from the reduction in incoming solar irradiance, the dust-induced radiative forcing was found to enhance the cyclonicity over the region due to intense lower-atmosphere heating, which in turn, triggered a new intense dust storm and convective clouds. It should be mentioned that regional climate model projections usually do not account for radiative feedbacks associated with desert dust and other aerosol types, including those from biomass burning (section 6.2.2), and a further integration of these processes in models will be needed.

5.2. Land-use change and climate

5.2.1. Urbanisation

In the wider area of the Middle East and North Africa, the total population is expected to grow to over 1 billion inhabitants by 2100. This demographic trend, in a region with scarce arable land and water resources, poses a significant socio-economic challenge, in addition to the imposed stress on the environment (McKee et al., 2017). The total population of the EMME countries has increased fivefold since the 1950s, from just under 85 million in 1950 to an estimated 432 million in 2020, and it is expected to grow further to nearly 600 million by 2050, following the medium variant projections (UNDESA, 2018). The corresponding urban population has risen ten-fold in the past seven decades. By 2050, the urban population is projected to account for 76% of the total. Some countries already have very high urbanisation levels (>80% in Kuwait and close to 100% in Qatar). One of the first-order

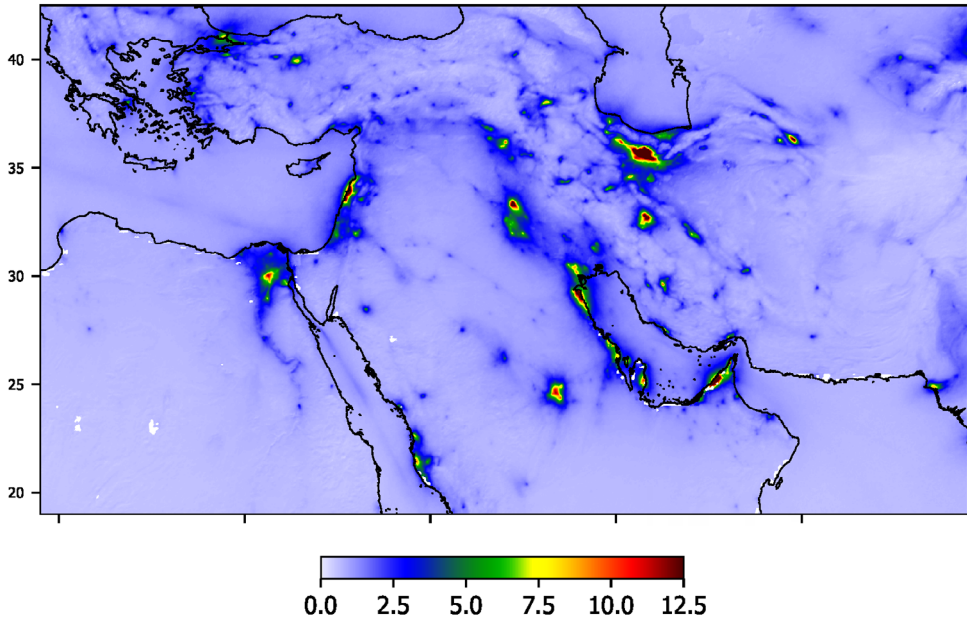
effects of urbanisation on the local climate is the urban heat island (UHI) phenomenon by which temperatures over a city are higher than the surroundings due to differences in the urban/rural energy balance, brought about by radiative and heat flux changes from the altered land cover and anthropogenic activities (Oke et al., 2017). This effect should be considered when deriving air temperature trends from station-based datasets (Kalnay and Cai, 2003); however, it contributes little to the global warming observed over the past four decades (Jones, 2016). Only a few studies of the connection between urbanisation and warming have focused on the EMME region. An analysis of 24 stations in Saudi Arabia showed that the observed increase in air temperature, of about 0.5–0.6°C/decade, is likely not due to urbanisation changes (Almazroui et al., 2013). Another analysis of observations from more than 200 stations in the Middle East and North Africa identified an average mean annual temperature trend of about 0.4°C/decade and a discernible, but small effect of urbanisation defined from a satellite-based land type (Hadjinicolaou et al., 2021).

The synergistic interaction of UHI effects and heatwaves has been studied for eastern Mediterranean cities. This interaction over Athens, Greece, results in a pronounced amplification of nocturnal UHI intensity (by 3°C) under exceptionally hot weather (Founda et al., 2015). UHI effects in Nicosia, Cyprus, raise the temperature by more than 1°C during the daytime under heatwave conditions due to urban/rural moisture contrast (Pyrgou et al., 2020). In Nicosia, urban warming has been linked to an increased probability of heat-related mortality during heatwaves (Pyrgou and Santamouris, 2018). It is thus important to be able to estimate local urban warming, in addition to the regional manifestation of global, large-scale warming, to assess the impacts of their combined magnitude on human health.

The accurate projection of urban warming in the context of global warming is a great challenge (Hamdi et al., 2020). Few estimates are available for the EMME. A population-driven urban warming estimation in four Israeli cities suggests that from 2015 to 2060, the UHI intensity will increase further by 2–4°C (Itzhak-Ben-Shalom et al., 2016). Another approach uses fully coupled global climate simulations and reduced-order urban modelling to project local urban climates (Zhao et al., 2021a). For a high-emission scenario, cities in the Middle East may experience additional warming of 4°C, on top of the predicted regional warming due to anthropogenic climate change. It will be needed to account for urbanisation trends and UHI effect in future climate projections.

Additionally, the intense urbanisation in the EMME region leads to severe, regionwide air pollution. Urban areas in hot and dry environments are prone to high levels of fossil fuel by-products and elevated emissions of pollutants, greenhouse gases and primary aerosols. Reactions of emitted organic and inorganic pollutants contribute by forming secondary aerosols. Photochemical reactions of organic pollutants, in the presence of nitrogen

Figure 17. Annual mean tropospheric NO₂ column concentrations in the EMME, observed by the TROPOMI satellite instrument



oxides, can form ozone pollution. These interactions are estimated to increase in the region, especially the Middle East, with harmful effects on people and vegetation in urban centres and downwind (Lelieveld et al., 2009). Figure 17 illustrates the strongly enhanced levels of NO₂ in urban areas. The dry and hot conditions also increase wildfires, which, together with chronic exposure to urban air pollution and high dust, deteriorate air quality and further contribute to respiratory and cardiovascular diseases in synergetic ways.

5.2.2. Forest fires

Wildfires are an integral component of Mediterranean landscapes and ecosystems. The occurrence of fires has markedly increased since the 1970s due to land use and climate change, but also changes in fire management (Wittenberg and Kutiel, 2016). Forest fires are most common during summertime. They are often intensified by the combined effect of droughts, high temperatures and strong winds (Koutsias et al., 2013). Eastern Mediterranean countries with relatively temperate climates that favour forest and shrubland biomes (e.g. Cyprus, Greece, Israel, Lebanon, Turkey) are among those most affected by forest fires. Severe drought events can create the pre-conditions for forest fires, predominantly during the warm and dry part of the year. Summer fires frequently rage across the

Mediterranean landscapes, while their impact is augmented by extraordinary high temperatures, as well as droughts that are found to regulate the fuel moisture (Turco et al., 2017b). For example, an increasing trend and a positive correlation are identified between the measures of fire activity (number of fires and area burned) and annual drought episodes in Greece (Dimitrakopoulos et al., 2011). Nevertheless, droughts also control fuel availability, making the relationships between fire activity and weather conditions more complex (Turco et al., 2017a).

High-impact wildfires were extensive in the summer of 2007 in southern Greece. That was the hottest summer on record for the country at the time, with temperatures in Athens exceeding the 1961-90 mean values by 3.3°C, corresponding to 3.7 standard deviations off the long-term mean (Founda and Giannakopoulos, 2009; Coumou and Rahmstorf, 2012). This coincided with massive forest fires that burned thousands of hectares of forested and agricultural land and caused the loss of 67 lives (Koutsias et al., 2012). It was considered the most extreme natural disaster in the country's recent history.

The December 2010 Mount Carmel forest fires in Israel (Paz et al., 2011) occurred following an unusually warm and dry autumn. More recently, extreme heat conditions in early October 2019 in Lebanon coincided with massive wildfires, indicating that the fire season has expanded towards the autumn months.

Across most forests in the EMME, days of critical fire risk, the length of the fire season and the extent of burnt areas have increased significantly in the past decades and are expected to continue doing so in the 21st century, especially under business-as-usual pathways (Karali et al., 2014; Levin et al., 2016; Palaiologou et al., 2018; Çolak and Sunar, 2020; Dupuy et al., 2020). This will be due to the combined warming and drying of the region, associated with more frequent and extreme heatwaves and drought events, projected to intensify (see Sections 6.1 and 6.2). For parts of the eastern Mediterranean, including Greece, under high warming scenarios, the burned area will increase proportionally, ranging from about 40% to 100% (Turco et al., 2018). This study highlights the significant benefits of limiting global warming levels to well below 2°C.

6. Challenges and recommendations

6.1. Critical sectors and impacts

6.1.1. Human health (air quality)

Degraded air quality in the region has serious impacts on human health, respiratory and cardiovascular diseases and lung cancer, especially at urban/industrialised centres, near oil industries, and in areas heavily affected by dust storms (Giannadaki et al., 2014; Stafoggia et al., 2016; Al-Hemoud et al., 2018; Soleimani et al., 2020). The human population in the Middle East is exposed regularly to PM levels characterised as very unhealthy or even hazardous, with daily PM_{2.5} and PM₁₀ levels above 150 and 250 micrograms per cubic metre of air ($\mu\text{g}/\text{m}^3$), respectively (Engelbrecht et al., 2009; Goudie, 2014; Goudarzi et al., 2018; Shahsavani et al., 2020). Air pollution and dust outbreaks increase hospital admissions, morbidity and mortality in countries of the region, including Saudi Arabia, Iran, Israel and Cyprus (Miri et al., 2007; Middleton et al., 2008; Al-Ghazawy, 2013; Gharehchahi et al., 2013; Neophytou et al., 2013; Gholampour et al., 2014; Vodonos et al., 2014; Nourmoradi et al., 2016; Pardo et al., 2017). The adverse health effects of dust in the arid Middle East can lead to hospital admissions due to asthma, respiratory and cardiovascular diseases (Tsiouri et al., 2015).

Toxic heavy metals like chromium, nickel and lead exist in both desert and resuspended anthropogenic dust (Philip et al., 2017) and may enter the human body through several pathways like inhalation, ingestion and dermal contact, causing serious neurotoxic and carcinogenic effects. Their concentrations are dramatically increased across the Middle East during periods of intense dust storms (Al-Harbi, 2015; Tsiouri et al., 2015; Dahmardeh Behrooz et al., 2021). Heavy metals extracted from airborne dust samples have been extensively analysed in the Middle East (Al-Khashman, 2013), and especially in Iran, revealing enhanced concentrations due to the combination of anthropogenic emissions in urban areas and oil refineries and dust storms (Zarasvandi et al., 2011; Shahsavani et al., 2012; Gholampour et al., 2014, 2016; Javed et al., 2015; Abbasi et al., 2019; Ziyadee et al., 2019). Occasionally, dust deposition, contaminated with heavy metals and other pollutants, adversely affects fish species and causes phytoplankton blooms in the Gulf (Keshavarzi et al., 2018). Many recent studies have underscored the health risks of potentially toxic metals and polycyclic aromatic hydrocarbons (PAHs) in airborne and street dust in Iran (Keshavarzi et al., 2018; Ghanavati et al., 2019; Motesaddi Zarandi et al., 2019; Najmeddin and Keshavarzi, 2019; Mihankhah et al., 2020). High carcinogenic risks were found in the

inhalation, ingestion and dermal contact pathways both for children and adults, while a comparative evaluation showed that cancer and other disease risks related to toxic contaminants in airborne dust in Iran were among the highest reported in the world (Behrooz et al., 2021). Furthermore, the cancer risks attributed to PAH exposure in the Middle East were found to exceed international standards (Soltani et al., 2015; Ghanavati et al., 2019; Jaafari et al., 2020). PAHs and other organic compounds found in smoke from wildfires can be carcinogenic and can also induce health effects when inhaled (Pardo et al., 2020). Resuspended road dust containing metals from brake and tire wear is also common in the region and can induce various health effects such as inflammation and oxidative stress that lead to diseases upon prolonged exposure in populated areas (Pardo et al., 2015, 2016; Shuster-Meiseles et al., 2016).

6.1.2. Human health (heat stress)

Warming, drying, more prolonged and more frequent extreme heat events and reduced precipitation will all exert substantial stress on the health and well-being of people in the EMME region. Exposure to elevated ambient temperatures, already commonplace in the region, is linked to heat cramps, heat syncope, heat exhaustion and heat stroke, especially among those with pre-existing illnesses, such as cardiovascular and respiratory diseases (McGeehin and Mirabelli, 2001). Associations between temperature increase and excess morbidity and mortality have been identified in several countries of the region, including Cyprus, Greece, Kuwait, Lebanon, Syria, while this is more evident along the coasts and in large urban centres (El-Zein et al., 2004; Nastos and Matzarakis, 2012; Peretz et al., 2012; Lubczyńska et al., 2015; Paravantis et al., 2017; Kouis et al., 2019; Alahmad et al., 2020a, 2020b). Continuous exposure to extreme heat through the nighttime has been associated with sleep disturbances, mental health issues, exhaustion and hyperthermia (Pal and Eltahir, 2016). Heat stress hotspots, especially in the coastal Middle East, may result from the interaction of hot desert air masses with onshore moisture advection from warm water bodies (Coffel et al., 2018). In parts of the EMME region, mainly in the Middle East, the climatic conditions during summer (but also late spring and early autumn) are expected to become particularly harsh. Particularly under business-as-usual scenarios, heat stress will intensify, and in combination with high humidity, ambient environmental conditions are likely to approach and exceed critical thresholds for human adaptability (Pal and Eltahir, 2016). Augmentation of heat stress conditions, particularly during extreme heatwaves (Lelieveld et al., 2016; Zittis et al., 2016; Varela et al., 2020), will substantially increase the heat-related mortality up to 8 to 20 times higher than historical values (Ahmadalipour and Moradkhani, 2018).

Vulnerable populations that include the elderly, children, pregnant women and people with chronic or pre-existing medical conditions are expected to be the most affected by the projected changes. Such extreme environmental conditions are also expected to augment the differences and inequalities between the more affluent and impoverished populations of the EMME region. The increasing temperatures may affect some cities in the region (e.g. the megacity Cairo) more than other cities, with increased adaptive capacity to withstand hot weather (Habib et al., 2010). At the rate of projected climate change over the next 50 years, heat-related losses in the region are unlikely to be offset by any cold-related gains (El-Zein et al., 2004). Outdoor labour activities such as construction and agriculture are already challenged in parts of the EMME region (Al-Bouwarthan et al., 2019). Environmental heat stress has reduced labour capacity to 90% in peak months over the past few decades in many parts of the world. Under future conditions, thermal stress will be augmented in many parts of the EMME (Dunne et al., 2013; Casanueva et al., 2020). Local industries should adapt to the projected changes to prevent major impacts on workers' health and, at the same time, preserve economic productivity.

The degree to which heat-related morbidity and mortality rates will increase in the next few decades will depend on the adaptive capacity of EMME population groups through acclimatisation, adaptation of the urban environment to reduce heat-island effects, implementation of public education programmes and the preparedness of health care systems.

6.1.3. Water resources and agriculture

Water resources in most of the Mediterranean and particularly in the EMME are scarce. They are also unevenly distributed and often do not match human and environmental needs (Fader et al., 2020). The dominance of evaporation over precipitation means that most of the region lacks surface and groundwater resources (Cullen et al., 2002). Many areas across the region consistently experience less than 100mm of precipitation per year (Hemming et al., 2010). Climate-change-driven alterations in precipitation patterns and seasonality, combined with warmer temperatures, stronger evapotranspiration, reduced snow cover in upstream areas, sea-level rise as well as increasing water demand have limited access to freshwater resources (Croke et al., 2000; Oroud, 2008; Shaban, 2008; Fujihara et al., 2008; Chenoweth et al., 2011; Chowdhury and Al-Zahrani, 2013; Schewe et al., 2014; Rajsekhar and Gorelick, 2017; Fader et al., 2021).

Surface and groundwater resources in most of the EMME region are projected to be further limited under climate change conditions and particularly when considering pathways of strong radiative forcing (Chenoweth et al., 2011; Hartmann et al., 2012; Al Qatarneh et al., 2018; Givati et al., 2019; Yıldırım et al., 2021). For example, climate projections for parts

of the region suggest an increase in the average seasonality and aridity indices affecting hydrologic regimes due to shorter humid seasons and earlier snowmelts (Allam et al., 2020). Particularly in the drier parts of the EMME region, the rise in temperatures appears to be the principal reason for water availability responses (Ajjur and Al-Ghamdi, 2021). Moreover, freshwater demand is expected to intensify as a result of regional population increases and changes in standards of living. Countries of the region where the required adaptation is likely to be particularly challenging include Turkey and Syria because of their reduced runoff projections and major agricultural activity, Iraq because of the magnitude of its change and its downstream location and Jordan because of its minor per capita water resources coupled with limited options for desalination (Chenoweth et al., 2011; Bozkurt and Sen, 2013).

The projected transition to warmer and drier bio-climatic conditions can be expected to severely affect agriculture, and thus food production, which is particularly sensitive to droughts (Hochman et al., 2021). Key Mediterranean crops (e.g. olives, vines, legumes, wheat, barley, maize) will be strongly affected by the combined effect of prolonged drought periods and increased thermal stress (Giannakopoulos et al., 2006; Al-Bakri et al., 2011; Sen et al., 2012; Constantinidou et al., 2016; Lazoglou and Anagnostopoulou, 2017; Verner et al., 2018; Papadaskalopoulou et al., 2020; Kitsara et al., 2021; Varotsos et al., 2021). This is mostly relevant for summer crops in the region. For example, a significant correlation between crop yield decrease and temperature increase is evident, regardless of whether the effects of CO₂ fertilisation or adaptation measures are considered (Waha et al., 2017). Other types of crops such as nut trees show a high response to climate change. For example, any changes in the air temperature pattern have negative consequences for pistachio cultivation in Iran, such as reduced yield, increased evapotranspiration and water requirements, increased pest infestation and increased risk of frost damage (Ahmadi et al., 2021).

Interestingly, for some crops (e.g. vines or cereals) in higher-altitude or higher-latitude regions, agricultural production might benefit from climate change (Giannakopoulos et al., 2006; Lazoglou and Anagnostopoulou, 2017). For some species and agro-ecosystems in the EMME, the projected climatic pressure will exceed the limits of resilience; vegetation will either adapt to the new conditions or be succeeded by cultivars more tolerant of heat and water stress (Daliakopoulos et al., 2017).

6.1.4. Impacts of sea-level rise

The impacts of sea-level rise (SLR) mainly include beach erosion, loss of wetlands, damage to coastal infrastructure and saltwater intrusion into coastal aquifers. These are negatively affecting ecosystems and a range of socio-economic activities such as agriculture,

tourism, water and energy management, urban planning and more. Low-elevation regions, flat sandy beaches and deltaic sediments, commonly found in the EMME coastal zones, are less resistant to SLR than elevated, hard and cliffy shores (Kumar et al., 2010).

A hotspot of such impacts in the eastern Mediterranean is the Nile Delta. The land elevation of approximately 25% of the deltaic region is equal to or beneath present-day sea levels (Shaltout et al., 2015). Even a moderate increase in mean SLR would dramatically damage the north coast of the region, which includes large lakes, tourist resorts, historical sites, fertile agricultural land and four populous cities. Egypt mainly depends on the Nile water for agricultural irrigation and economic use (Agoubi, 2021). However, the coastal areas, where economic activities intensify, depend mainly on groundwater, which ranks second after the Nile River on the list of water resources in Egypt (Mabrouk et al., 2013). If the SLR ranges between 0.5 and 1 metre, large areas of the Nile Delta will likely be submerged by seawater, and the coastline will shift landward by several kilometres on the delta's eastern and western sides (Sefelnasr and Sherif, 2014). Moreover, about 31% of the 1 200 km Red Sea coast in Egypt, mainly in the south, is extremely sensitive to SLR (Hereher, 2015). This region includes coastal flats, estuaries and bays over which most coastal cities, harbours and resort villages are located.

Similarly, in Turkey, numerous coastal cities, villages or towns are located within the 0-10 metre elevation zone and are highly vulnerable to SLR (Kuleli, 2010). In terms of potential land loss, the Mediterranean coast of Turkey is the most vulnerable, with islands of the eastern Mediterranean being particularly affected. In case of a moderate SLR (0.26 m), about 80% of the beaches in eastern Crete, Greece, are predicted to retreat by more than 20% (Monioudi et al. 2016). In the worst-case scenario of a 1.85-metre SLR, almost all beaches will retreat by 50%, while a large number of them will likely disappear.

Other parts of the Middle East, other than the Mediterranean coasts, will also be negatively affected. For example, in Oman, coastal regions highly vulnerable to SLR account for 805 km of the coast, mostly along the Al-Batinah plain in the north of the country (Hereher et al. 2020). Major settlements and key infrastructure (water desalination and power production plants, harbours, refineries) are located on this coastline. In the United Arab Emirates and Abu Dhabi in particular, nearly all human settlements are concentrated along the coastlines. In a scenario of a 0.5 metre SLR, about 1.5% of the urban areas will be affected (Ksiksi and Youssef, 2012). This percentage will increase tenfold if the SLR reaches 2 metres.

Besides infrastructure and human activities, the projected sea-level rise scenarios for the next century will deeply affect the fragile coastal ecosystems of the eastern Mediterranean,

especially within the context of more intense drought stress, increased human activities and diminished sediment supply by local rivers (Kaniewski et al., 2014). For example, mangrove forests and plantations in the Gulf region (e.g. in the United Arab Emirates) have a significant ecological, social and economic value (Ksiksi and Youssef, 2012). These coastal ecosystems are expected to be significantly affected by future SLR.

6.15. Human security and conflicts

Climate change can challenge human security by 1) undermining livelihood, culture and human rights; 2) increasing migration and 3) indirectly influencing armed conflict (Koubi et al., 2020). Climate-driven limitations in water and other resources (e.g. due to prolonged drought events) are found to directly or indirectly trigger or augment conflicts and disputes in the region (Gleick, 2014; Kelley et al., 2015); however, their relative importance, in comparison to other causes, remains controversial. The projected climatic changes will likely further increase regional energy demand and may lead to reduced crop yields. Such impacts will increase the already existing social contrasts between populations in the EMME region, potentially increasing food insecurity, prices and malnutrition. Such changes can increase political tensions and instabilities that may ultimately lead to conflicts and humanitarian crises. Regional economic, political, demographic and social drivers, as well as climate-related environmental stressors (including SLR, droughts, extreme heatwaves or vector-borne diseases), could contribute to migration flows, with climate change acting as a “push factor” (Black et al., 2011; Lelieveld et al., 2016; Tabari and Willems, 2018; Abel et al., 2019). The scale and geographic scope of this type of population displacement could be one of the greatest human rights challenges of our time (Koubi et al., 2020). Migration is not solely driven by climate change but also by a combination of climatic, socio-economic, cultural and political factors (Boas et al., 2019). Historically, in the arid to semi-arid areas of the Middle East, such changes have been drivers of human settlement and population migrations (Kaniewski et al., 2012). Nevertheless, at those times, migration may have been the only adaptation measure. The additional stress from climatic change to prevailing conflicts between countries and populations may have dire consequences for weakened populations, exposing them to high risks and contributing to migration, with the associated suffering from malnutrition, poor sanitation and a lack of medical and mental support.

6.2. Data limitations, uncertainties and needs

For parts of the EMME region (mainly in the north), station-based meteorological observations can include century-long records (Bellamy, 1903; Price et al., 1999; Founda et al., 2009; Morbidelli et al., 2020). However, for much of the southern part of the region, only

limited coverage exists, with gaps and inconsistencies in the meteorological data records. Therefore, considerable observational uncertainty surrounds analyses of the past. This is particularly the case for precipitation, which varies widely across space and time, and is poorly represented by the region's sparse rain gauge network (Tanarhte et al., 2012; Zittis, 2018). In the arid and semi-arid zones of the Mediterranean area, severely limited access to data is the rule rather than the exception. This has been most clearly demonstrated in the Middle East, and partially addressed by combining results from several thousands of rain gauges to build a new gridded precipitation dataset, entitled APHRODITE (Yatagai et al., 2007). This dataset offers gridded daily precipitation data for the Middle East in the period 1951-2007. The additional rain gauges are maintained regularly in many countries (but the resulting data are not submitted to the global World Meteorological Organization databases), and sometimes the data are obtained or purchased from local authorities, for example, in Turkey, Lebanon, Iran, Iraq, Syria, Jordan, Israel and other countries. These additions have been shown to greatly improve rainfall mapping.

In particular, the Fertile Crescent area is not satisfactorily represented in most global precipitation databases, including even high-resolution re-analyses, due to the scarcity of rain-gauge measurements. Furthermore, widespread and long-term records for ground-based measurements of pollutants, aerosol particles and other atmospheric components are lacking in parts of the EMME region, mainly in the Middle East (Klingmüller et al., 2016; Eger et al., 2019; Pikridas et al., 2019). Therefore, many studies are based on satellite or re-analysis products that are often not well validated for the region, complementing the scarce station time series.

Regional climate projections for the EMME are available through the modelling output of collaborative initiatives such as CORDEX. The broader region is partially resolved by the European, Mediterranean, African and West Asian domains. The only CORDEX domain that includes the full extent of the EMME region is the one dedicated to the Middle East and North Africa (MENA-CORDEX). Nevertheless, the currently available horizontal resolution (50 km) is relatively coarse, for example, in view of the pronounced topography and extended (and inhabited) coastal areas, while the number of participating models and calculations for multiple climate forcing pathways is limited compared to other parts of the world and multimodel ensembles. Several experiments of national or local interest are based on single models or relatively small numbers of them (Lelieveld et al., 2012; Zanis et al., 2015; Hochman et al., 2018c; Zittis et al., 2020). Moreover, many datasets are not open access. Therefore, there is a strong need for further co-ordination, dissemination of information and the promotion of data sharing in the EMME region.

6.3. Research recommendations and outlook for regional co-operation

6.3.1. Advancements in climate modelling

While future temperature projections appear to be quite robust, this is generally not the case for precipitation. Several factors contribute to modelling uncertainties, including 1) the very local nature of some rainfall events, 2) misrepresentation of orography and coastlines due to low model resolution and 3) sensitivity of modelled precipitation to the parameterisation methods of sub-grid-scale processes that contribute to rainfall generation (e.g. convection and cloud microphysics processes) (Zittis et al., 2017; Alpert et al., 2021). An increase in the vertical and horizontal resolution of climate models (global and regional) is a step forward, yet implies access to substantial computational resources. Improvements in the parameterisation schemes for physical processes, also considering the regional peculiarities and in-situ measurements of atmospheric properties, are also essential.

Most regional modelling efforts in the EMME region focus on the atmospheric component of the climate system. Additional components such as oceans, land and atmospheric chemistry processes are not yet sufficiently considered. For example, ocean properties (e.g. sea levels and sea surface temperatures) are prescribed, while vegetation and land-use components, including vegetation fires, are based on present-day inventories that are not dynamic (i.e. they are static over time). Furthermore, atmospheric chemistry components that have a strong impact on the regional climate (e.g. dust and other aerosols) are either prescribed or not considered. The consideration of additional modelling components (ocean circulation, dynamic vegetation and atmospheric chemistry) could eventually lead to regional earth system models. These could generate climate projections of increased accuracy and validity in representing mean climate conditions and extreme events of high societal impact. However, this type of coupled regional climate modelling implies substantial computational resources, multidisciplinary collaborations and expertise that is mostly not available in the region. For example, while there are significant advancements in the coupled atmosphere-ocean modelling for the Mediterranean, mainly through the Med-CORDEX initiative¹¹ (Ruti et al., 2016; Soto-Navarro et al., 2020), such regional initiatives do not exist for the Red Sea and the Gulf region.

The EMME region is characterised by rapid urbanisation, and population projections suggest this trend will intensify in the future. Dubai's dramatic urban evolution in just two decades is a case in point (Elhacham and Alpert, 2021). The combined effects of increased population density, anthropogenic climate warming, the urban heat island effect and poor air quality are expected to introduce additional challenges.

11. <https://www.medcordex.eu/>.

The current state-of-the-art climate models do not resolve urban scales, except for a few megacities. For developing suitable adaptation strategies and solutions, the representation of urban environments in climate change projections needs to be improved substantially. This can be partially addressed by higher-resolution modelling that considers at least some of the characteristics of urban environments (heat capacity, thermal conductivity, albedo, etc.) or offline coupling with more sophisticated micro-scale urban canopy models that can be applied for cities of specific interest (e.g. De Ridder et al., 2015; Oswald et al., 2020).

6.3.2. Sharing of data, knowledge and expertise

Depending on the economic development and political situation of each country, access to resources, funding for research activities, education opportunities and technological and innovation capacity are not equally distributed across the EMME region. Environmental matters in particular are often prioritised less than other regional challenges. These factors have a direct impact on each country's level of adaptive capacity (i.e. the potential to adapt to the effects or impacts of climate change) and climate resilience (i.e. the ability to anticipate, absorb, accommodate or recover from the effects of a potentially hazardous event in a timely and efficient manner). Since many of the regional outcomes of climate change are transboundary, stronger collaboration among the countries is indispensable to cope with the expected adverse impacts. Such synergies will be vital to achieving timely mitigation targets and concurrently ensuring energy security. Educational and research institutions in the region should play a leading role in promoting such collaborations, defying any political, cultural or religious barriers. Joint research activities; stronger partnerships between universities, meteorological services and research institutes in the region; the establishment of research and innovation funding tools; training activities; sharing of data, expertise and resources; analysis tools and computational resources and promotion of climate education are recommended for enhancing adaptive capacity and climate resilience regionwide. A co-benefit of such actions is the promotion of prosperity and collaboration in addressing challenges other than climate change. Toward these ends, the contribution of international organisations and funds for development in the region are already significant and are highly encouraged. Some successful examples include several United Nations commissions and organisations (ESCWA; the Food and Agriculture Organization; the United Nations Educational, Scientific and Cultural Organization; the World Meteorological Organization and the United Nations Office for Disaster Risk Reduction), the League of Arab States,¹² the Union for the Mediterranean¹³ and the MedECC

12. <http://www.lasportal.org/>.

13. <https://ufmsecretariat.org/>.

initiative, the European Union through projects such as EMME-CARE¹⁴ and other international initiatives and funding agencies such as the Deutsche Gesellschaft für Internationale Zusammenarbeit (GIZ),¹⁵ the Swedish International Development Cooperation Agency,¹⁶ the European Economic Area and Norway Funds¹⁷ and more.

6.3.3. Adaptation solutions and policy recommendations

As shown by the assessment of multiple future scenarios in this chapter, the magnitude of regional changes in climatic processes strongly depends on the pathway of greenhouse gas emissions and concentrations in the atmosphere, as well as on the presence of natural or anthropogenic particulate matter. This is also the case for the associated impacts on people's health, well-being and other important socio-economic factors. Since the EMME region is becoming an increasingly significant GHG emitter (particularly for CO₂ and CH₄) at the global scale, decarbonisation actions should be rapidly implemented in order to alleviate the regional impacts of climate change, which are otherwise projected to be devastating. Strengthening the global response to the threat of climate change and of efforts toward sustainable development and the eradication of poverty is critical for keeping global warming to well below 2°C since pre-industrial levels, and thus complying with the Paris Agreement's main targets (IPCC, 2018).

For the countries of the EMME, particular emphasis should be put on decarbonising the energy and transportation sectors, which dominate regional CO₂ emissions (see Section 4). A significant reduction in energy use and the full decarbonisation of energy production through renewables are required to achieve these goals. In terms of technical and economic feasibility, key options for the region include photovoltaics, wind power and concentrating solar power (Shawon et al., 2013; Hadjipanayi et al., 2016; Ciriminna et al., 2019; Azouzoute et al., 2020). Demand-side measures geared towards energy conservation and improvements in energy efficiency (e.g. in industry, transportation and buildings) are equally important (Riahi et al., 2017). Additionally, measures in the agricultural sector could support the reduction of CH₄ and N₂O emissions from various sources, including livestock and fertilisers (Riahi et al., 2017).

Besides substantial decreases in emissions, carbon dioxide removal technologies need to be developed and applied to reach net-zero or negative emissions, and thus alleviate the impacts of global and regional warming. Existing and potential measures include afforestation and reforestation, land restoration and soil carbon sequestration, direct air carbon capture and storage, enhanced weathering and ocean alkalisation (IPCC, 2018).

14. <https://emme-care.cyi.ac.cy/>.

15. <https://www.giz.de/en/>.

16. <https://www.sida.se/en/>.

17. <https://eeagrants.org/>.

Relevant technologies differ widely in terms of maturity, potential, cost, risks, co-benefits and trade-offs. For example, afforestation is considered a cost-effective and readily available climate change mitigation option; however, the arid regions of the Middle East show limited afforestation potential as forest growth rates are very low (Doelman et al., 2020).

Several Middle Eastern countries have experimented with carbon capture, utilisation and storage, including to enhance oil recovery and industrial facilities or integrate with energy and other industries (other than oil and gas) (Liu et al., 2012; ESCWA, 2017). However, none of these applications has been demonstrated to contribute sufficient gains at an appropriate scale. Appropriate policy and financing measures could help overcome political and commercial barriers to their further deployment (ESCWA, 2017).

Because of the long lifetime of GHGs in the atmosphere, the warming from anthropogenic emissions will persist for centuries to millennia and will continue to cause further long-term changes in the climate system (IPCC, 2018). Even if emissions were reduced in the short term, some of the global warming implications would persist, at least for the next few decades and most likely for the rest of the century. Countries in the EMME have no choice but adapt as environmentally harsh conditions become more challenging and likely even more societally disruptive.

For example, the limited water resources of the region will be further reduced. Demand is expected to increase, driven by the growth of population and food production, temperature increases and a decline in precipitation. Adaptation solutions include the use of non-conventional water resources, the treatment of wastewater, rainwater harvesting for irrigation, policies to reduce water demand, improved leakage detection in urban water distribution systems and more (Qadir et al., 2007; Rockström et al., 2010; Charalambous et al., 2019; Lange, 2019). Water resources, in particular, are frequently managed on a national basis, while cross-border river basins (e.g. the Tigris-Euphrates, Nile and Jordan rivers) additionally require international co-operation (Chenoweth et al., 2011). Some of these rivers are partially managed through international treaties; nevertheless, this international co-operation should be maintained and enhanced to increase climate resilience in the EMME region.

Other adaptation solutions for agriculture include the introduction of more heat- and water-stress-tolerant cultivars, the shifting of planting dates and the adoption of sustainable farming and irrigation. Such agro-ecological techniques could increase cropland productivity and satisfy future demand for food in the region (Rockström et al., 2010; Dalidakopoulos et al., 2017; Tzounis et al., 2017; Walter et al., 2017; Malek and Verburg, 2018; Lange, 2019; Adamides et al., 2020).

Dust-induced radiative forcing over the EMME region is a regulating climatic factor. The strong inter-relation between climate change, dust and precipitation trends over the Middle East calls for their further study under a warmer-world scenario that would further modify this inter-relation in the future. Implementing restoration and afforestation projects in suitable areas could reverse land degradation with a possible synergistic improvement of air quality, soils and water, as well as human health and societal indexes in the Middle East (Emamian et al., 2021). For the eastern Mediterranean environments, such restoration projects include mountain terrace rehabilitation, crop diversification and afforestation of abandoned and degraded land (Zoumides et al., 2017; Camera et al., 2018).

Around the world, extreme weather events are increasingly becoming the new normal, and are expected to increase in the 21st century as a result of climate change (Singh and Zommers, 2014). This is also the case for parts of the EMME region, where increasingly severe events include droughts, heatwaves, hydro-climate extremes, storm surges, wind-storms, dust storms, etc. To better cope with more severe and frequent extreme events, the development of accurate early-warning systems is vital. Early warnings and timely response play a major role in reducing vulnerability, limiting the casualties caused by disasters and enhancing the resilience of communities (Seng, 2012). These are key elements of climate change adaptation and disaster risk reduction and aim to avoid or reduce the damage caused by hazards, including extreme weather events and geoclimatic hazards.

Considering the strong urbanisation trends in the EMME region, sustainable spatial planning and the building of resilient cities are key measures for alleviating the adverse effects of climate change. The synergistic effect of global warming and the urban heat island effect makes such measures even more urgent. The substantial coastal developments in most countries of the region are particularly vulnerable to sea-level rise. Adaptation solutions include urban greening, use of cool surfaces, development of sustainable public transportation, improvements in the energy and water efficiency of the built environment, green building projects, coastal erosion protection measures and more (Abubakar and Dano, 2020; Salimi and Al-Ghamdi, 2020; Giannakis et al., 2020; Dimitriou et al., 2020; Serghides et al., 2020; Maggiotto et al., 2021). Urban forestry and the planting of other vegetation would mitigate climate change while also improving air quality, with consequent psychological and physical benefits for urban dwellers (Maggiotto et al., 2021).

References

- Abbasi S, Keshavarzi B, Moore F, et al (2019) Distribution and potential health impacts of microplastics and microrubbers in air and street dusts from Asaluyeh County, Iran. *Environ Pollut* 244:153–164. doi: 10.1016/j.envpol.2018.10.039
- Abbasnia M, Toros H (2019) Analysis of long-term changes in extreme climatic indices: a case study of the Mediterranean climate, Marmara Region, Turkey. In: Vilibić I, Horvath K, Palau JL (eds). Springer International Publishing, Cham, pp 141–153
- Abbasnia M, Toros H (2020) Trend analysis of weather extremes across the coastal and non-coastal areas (case study: Turkey). *J Earth Syst Sci* 129:. doi: 10.1007/s12040-020-1359-3
- Abdelkader M, Metzger S, Mamouri RE, et al (2015) Dust-air pollution dynamics over the eastern Mediterranean. *Atmos Chem Phys* 15:9173–9189. doi: 10.5194/acp-15-9173-2015
- Abdulla CP, Al-Subhi AM (2020) Sea level variability in the Red sea: A persistent east-west pattern. *Remote Sens* 12:. doi: 10.3390/rs12132090
- Abel GJ, Brottrager M, Crespo Cuarema J, Muttarak R (2019) Climate, conflict and forced migration. *Glob Environ Chang* 54:239–249. doi: 10.1016/j.gloenvcha.2018.12.003
- Abubakar IR, Dano UL (2020) Sustainable urban planning strategies for mitigating climate change in Saudi Arabia. *Environ Dev Sustain* 22:5129–5152. doi: 10.1007/s10668-019-00417-1
- Achilleos S, Mouzourides P, Kalivitis N, et al (2020) Spatio-temporal variability of desert dust storms in Eastern Mediterranean (Crete, Cyprus, Israel) between 2006 and 2017 using a uniform methodology. *Sci Total Environ* 714:136693. doi: 10.1016/j.scitotenv.2020.136693
- Adamides G, Kalatzis N, Stylianou A, et al (2020) Smart farming techniques for climate change adaptation in Cyprus. *Atmosphere (Basel)* 11:1–17. doi: 10.3390/ATMOS11060557
- Agoubi B (2021) A review: saltwater intrusion in North Africa's coastal areas—current state and future challenges. *Environ Sci Pollut Res* 28:17029–17043. doi: 10.1007/s11356-021-12741-z
- Ahmadalipour A, Moradkhani H (2018) Escalating heat-stress mortality risk due to global warming in the Middle East and North Africa (MENA). *Env Int* 117:215–225. doi: 10.1016/j.envint.2018.05.014
- Ahmadi H, Baaghideh M, Dadashi-Roudbari A (2021) Climate change impacts on pistachio cultivation areas in Iran: a simulation analysis based on CORDEX-MENA multi-model ensembles. *Theor Appl Climatol* 145:109–120. doi: 10.1007/s00704-021-03614-z
- Ajjur SB, Al-Ghamdi SG (2021) Evapotranspiration and water availability response to climate change in the Middle East and North Africa. *Clim Change* 166:1–18
- Al-Bakri J, Suleiman A, Abdulla F, Ayad J (2011) Potential impact of climate change on rainfed agriculture of a semi-arid basin in Jordan. *Phys Chem Earth* 36:125–134. doi: 10.1016/j.pce.2010.06.001
- Al-Bouwarthan M, Quinn MM, Kriebel D, Wegman DH (2019) Assessment of heat stress exposure among construction workers in the hot desert climate of Saudi Arabia. *Ann Work Expo Heal* 63:505–520. doi: 10.1093/annweh/wxz033
- Al-Ghazawy O (2013) The rising danger of asthma. *Nat Middle East*. doi: 10.1038/nmiddleeast.2013.79
- Al-Harbi M (2015) Characteristics and composition of the falling dust in urban environment. *Int J Environ Sci Technol* 12:641–652. doi: 10.1007/s13762-013-0440-8
- Al-Hemoud A, Al-Dousari A, Al-Shatti A, et al (2018) Health impact assessment associated with exposure to PM10 and dust storms in Kuwait. *Atmosphere (Basel)* 9:. doi: 10.3390/atmos9010006
- Al-Khashman OA (2013) Assessment of heavy metals contamination in deposited street dusts in different urbanized areas in the city of Ma'an, Jordan. *Environ Earth Sci* 70:2603–2612. doi: 10.1007/s12665-013-2310-6
- Al Qatarneh GN, Al Smadi B, Al-Zboon K, Shatanawi KM (2018) Impact of climate change on water resources in Jordan: a case study of Azraq basin. *Appl Water Sci* 8:1–14. doi: 10.1007/s13201-018-0687-9

- Alahmad B, Khraishah H, Shakarchi AF, et al (2020a) Cardiovascular mortality and exposure to heat in an inherently hot region: Implications for climate change. *Circulation* 1271–1273. doi: 10.1161/CIRCULATIONAHA.119.044860
- Alahmad B, Tomasso LP, Al-Hemoud A, et al (2020b) Spatial distribution of land surface temperatures in Kuwait: Urban heat and cool Islands. *Int J Environ Res Public Health* 17:. doi: 10.3390/ijerph17092993
- Alharbi BH, Maghrabi A, Tapper N (2013) The march 2009 dust event in Saudi Arabia: Precursor and supportive environment. *Bull Am Meteorol Soc* 94:515–528. doi: 10.1175/BAMS-D-11-00118.1
- Ali MA, Nichol JE, Bilal M, et al (2020) Classification of aerosols over Saudi Arabia from 2004–2016. *Atmos Environ* 241:117785. doi: 10.1016/j.atmosenv.2020.117785
- Allam A, Moussa R, Najem W, Bocquillon C (2020) Specific Climate Classification for Mediterranean Hydrology and Future Evolution Under Med-CORDEX RCM Scenarios. *Hydrol Earth Syst Sci Discuss* 1–26. doi: 10.5194/hess-2020-71
- Allen MR, Ingram WJ (2002) Constraints on future changes in climate and the hydrologic cycle. *Nature* 419:228–232
- Almazroui M (2020a) Changes in Temperature Trends and Extremes over Saudi Arabia for the Period 1978–2019. *Adv Meteorol* 2020:. doi: 10.1155/2020/8828421
- Almazroui M (2020b) Summer maximum temperature over the gulf cooperation council states in the twenty-first century: multimodel simulations overview. *Arab J Geosci* 13:. doi: 10.1007/s12517-020-05537-x
- Almazroui M, Islam MN, Dambul R, Jones PD (2014) Trends of temperature extremes in Saudi Arabia. *Int J Climatol* 34:808–826. doi: 10.1002/joc.3722
- Almazroui M, Islam MN, Jones PD (2013) Urbanization effects on the air temperature rise in Saudi Arabia. *Clim Change* 120:109–122. doi: 10.1007/s10584-013-0796-2
- Almazroui M, Nazrul Islam M, Athar H, et al (2012) Recent climate change in the Arabian Peninsula: Annual rainfall and temperature analysis of Saudi Arabia for 1978–2009. *Int J Climatol* 32:953–966. doi: 10.1002/joc.3446
- Almazroui M, Saeed F, Saeed S, et al (2020) Projected Change in Temperature and Precipitation Over Africa from CMIP6. *Earth Syst Environ* 4:455–475. doi: 10.1007/s41748-020-00161-x
- Alosairi Y, Alsulaiman N, Rashed A, Al-Houti D (2020) World record extreme sea surface temperatures in the northwestern Arabian/Persian Gulf verified by in situ measurements. *Mar Pollut Bull* 161:111766. doi: 10.1016/j.marpolbul.2020.111766
- Allothman AO, Bos M, Fernandes R, et al (2020) Annual sea level variations in the Red Sea observed using GNSS. *Geophys J Int* 221:826–834. doi: 10.1093/gji/ggaa032
- Allothman AO, Bos MS, Fernandes RMS, Ayhan ME (2014) Sea level rise in the north-western part of the Arabian Gulf. *J Geodyn* 81:105–110. doi: 10.1016/j.jog.2014.09.002
- Alpert P, Ben-Gai T, Baharad A, et al (2002) The paradoxical increase of Mediterranean extreme daily rainfall in spite of decrease in total values. *Geophys Res Lett* 29:31-1-31-4. doi: 10.1029/2001GL013554
- Alpert P, Hemming D, Jin F, et al (2013) The Hydrological Cycle of the Mediterranean. In: Navarra A, Tubiana L (eds) *Advances in Global Change Research*. Springer Netherlands, Dordrecht, pp 201–239
- Alpert P, Jin F, Kitoh A (2014) The projected death of the Fertile Crescent. In: Norwine J (ed) *A World After Climate Change and Culture-Shift*. Springer Netherlands, Dordrecht, pp 193–203
- Alpert P, Kaufman YJ, Shay-El Y, et al (1998) Quantification of dust-forced heating of the lower troposphere. *Nature* 395:367–370. doi: 10.1038/26456
- Alpert P, Osetinsky I, Ziv B, Shafir H (2004) A new seasons definition based on classified daily synoptic systems: An example for the eastern Mediterranean. *Int J Climatol* 24:1013–1021. doi: 10.1002/joc.1037
- Alpert P, Shafir H, Elhacham E (2021) An Unknown Maximum Lag-Correlation Between Rainfall and Aerosols at 140–160 Minutes. *Geophys Res Lett* 48:e2020GL089334. doi: 10.1029/2020GL089334
- Aydin M, Verhulst KR, Saltzman ES, et al (2011) Recent decreases in fossil-fuel emissions of ethane and methane derived from firn air. *Nature* 476:198–201. doi: 10.1038/nature10352
- Azouzoute A, Alami Merrouni A, Touili S (2020) Overview of the integration of CSP as an alternative energy source in the MENA region. *Energy Strateg Rev* 29:100493. doi: 10.1016/j.esr.2020.100493

- Baker A, Asrat A, Fairchild IJ, et al (2010) Decadal-scale rainfall variability in Ethiopia recorded in an annually laminated, Holocene-age, stalagmite. *Holocene* 20:827–836. doi: 10.1177/0959683610365934
- Bangalath HK, Stenchikov G (2015) Role of dust direct radiative effect on the tropical rain belt over middle east and North Africa: A high-resolution AGCM study. *J Geophys Res* 120:4564–4584. doi: 10.1002/2015JD023122
- Bar-Matthews M, Ayalon A, Gilmour M, et al (2003) Sea - land oxygen isotopic relationships from planktonic foraminifera and speleothems in the Eastern Mediterranean region and their implication for paleorainfall during interglacial intervals. *Geochim Cosmochim Acta* 67:3181–3199. doi: 10.1016/S0016-7037(02)01031-1
- Barlow M, Cullen H, Lyon B (2002) Drought in Central and Southwest Asia: La Niña, the warm pool, and Indian Ocean precipitation. *J Clim* 15:697–700. doi: 10.1175/1520-0442(2002)015<0697:DICASA>2.0.CO;2
- Bartók B, Wild M, Folini D, et al (2017) Projected changes in surface solar radiation in CMIP5 global climate models and in EURO-CORDEX regional climate models for Europe. *Clim Dyn* 49:2665–2683. doi: 10.1007/s00382-016-3471-2
- Basart S, Pérez C, Cuevas E, et al (2009) Aerosol characterization in Northern Africa, Northeastern Atlantic, mediterranean basin and middle east from direct-sun AERONET observations. *Atmos Chem Phys* 9:8265–8282. doi: 10.5194/acp-9-8265-2009
- Beirle S, Borger C, Dörner S, et al (2021) Catalog of NO_x emissions from point sources as derived from the divergence of the NO_x flux for TROPOMI. *Earth Syst Sci Data Discuss* 2021:1–28. doi: 10.5194/essd-2020-280
- Belda M, Holtanová E, Halenka T, Kalvová J (2014) Climate classification revisited: From Köppen to Trewartha. *Clim Res* 59:1–13. doi: 10.3354/cr01204
- Bellamy C V. (1903) Notes on the climate of cyprus. *Q J R Meteorol Soc* 29:29–46. doi: 10.1002/qj.49702912506
- Black R, Adger WN, Arnell NW, et al (2011) The effect of environmental change on human migration. *Glob Environ Chang* 21:S3–S11. doi: 10.1016/j.gloenvcha.2011.10.001
- Boas I, Farbotko C, Adams H, et al (2019) Climate migration myths. *Nat Clim Chang* 9:901–903. doi: 10.1038/s41558-019-0633-3
- Bodenheimer S, Nirel R, Lensky IM, Dayan U (2018) Relationship between AOD and synoptic circulation over the Eastern Mediterranean: A comparison between subjective and objective classifications. *Atmos Environ* 177:253–261. doi: 10.1016/j.atmosenv.2018.01.016
- Bou Karam Francis D, Flamant C, Chaboureaud JP, et al (2017) Dust emission and transport over Iraq associated with the summer Shamal winds. *Aeolian Res* 24:15–31. doi: 10.1016/j.aeolia.2016.11.001
- Bozkurt D, Sen OL (2013) Climate change impacts in the Euphrates-Tigris Basin based on different model and scenario simulations. *J Hydrol* 480:149–161. doi: 10.1016/j.jhydrol.2012.12.021
- Bucchignani E, Mercogliano P, Panitz HJ, Montesarchio M (2018) Climate change projections for the Middle East–North Africa domain with COSMO-CLM at different spatial resolutions. *Adv Clim Chang Res* 9:66–80. doi: 10.1016/j.accre.2018.01.004
- Caloiero T, Veltri S, Caloiero P, Frustaci F (2018) Drought analysis in Europe and in the Mediterranean basin using the standardized precipitation index. *Water* 10:1043. doi: 10.3390/w10081043
- Camera C, Djuma H, Bruggeman A, et al (2018) Quantifying the effectiveness of mountain terraces on soil erosion protection with sediment traps and dry-stone wall laser scans. *Catena* 171:251–264. doi: 10.1016/j.catena.2018.07.017
- Cao H, Liu J, Wang G, et al (2015) Identification of sand and dust storm source areas in Iran. *J Arid Land* 7:567–578. doi: 10.1007/s40333-015-0127-8
- Casanueva A, Kotlarski S, Fischer AM, et al (2020) Escalating environmental summer heat exposure—a future threat for the European workforce. *Reg Environ Chang* 20:40. doi: 10.1007/s10113-020-01625-6
- Cazenave A, Meyssignac B, Ablain M, et al (2018) Global sea-level budget 1993-present. *Earth Syst Sci Data* 10:1551–1590. doi: 10.5194/essd-10-1551-2018
- Ceccherini G, Russo S, Ameztoy I, et al (2017) Heat waves in Africa 1981–2015, observations and reanalysis. *Nat Hazards Earth Syst Sci* 17:115–125. doi: 10.5194/nhess-17-115-2017

- Charalambous K, Bruggeman A, Eliades M, et al (2019) Stormwater retention and reuse at the residential plot level-green roof experiment and water balance computations for long-term use in Cyprus. *Water (Switzerland)* 11:1–11. doi: 10.3390/w11051055
- Chen H, Sun J, Chen X (2014) Projection and uncertainty analysis of global precipitation-related extremes using CMIP5 models. *Int J Climatol* 34:2730–2748. doi: 10.1002/joc.3871
- Chenoweth J, Hadjinicolaou P, Bruggeman A, et al (2011) Impact of climate change on the water resources of the eastern Mediterranean and Middle East region: Modeled 21st century changes and implications. *Water Resour Res* 47:W06506. doi: 10.1029/2010WR010269
- Chowdhury S, Al-Zahrani M (2013) Implications of Climate Change on Water Resources in Saudi Arabia. *Arab J Sci Eng* 38:1959–1971. doi: 10.1007/s13369-013-0565-6
- Christensen JH, Kanikicharla KK, Aldrian E, et al (2013) Climate phenomena and their relevance for future regional climate change. *Clim Chang* 2013 Phys Sci Basis Work Gr I Contrib to Fifth Assess Rep Intergov Panel Clim Chang 9781107057:1217–1308. doi: 10.1017/CBO9781107415324.028
- Church JA, White NJ (2011) Sea-Level Rise from the Late 19th to the Early 21st Century. *Surv Geophys* 32:585–602. doi: 10.1007/s10712-011-9119-1
- Ciriminna R, Albanese L, Pecoraino M, et al (2019) Solar Energy and New Energy Technologies for Mediterranean Countries. *Glob Challenges* 3:1900016. doi: 10.1002/gch2.201900016
- Coffel ED, Horton RM, De Sherbinin A (2018) Temperature and humidity based projections of a rapid rise in global heat stress exposure during the 21st century. *Environ Res Lett* 13:. doi: 10.1088/1748-9326/aaa00e
- Çolak E, Sunar F (2020) Evaluation of forest fire risk in the Mediterranean Turkish forests: A case study of Menderes region, Izmir. *Int J Disaster Risk Reduct* 45:101479. doi: 10.1016/j.ijdrr.2020.101479
- Constantinidou K, Hadjinicolaou P, Zittis G, Lelieveld J (2016) Effects of climate change on the yield of winter wheat in the eastern Mediterranean and Middle East. *Clim Res* 69:129–141. doi: 10.3354/cr01395
- Cook BI, Anchukaitis KJ, Touchan R, et al (2016) Spatiotemporal drought variability in the mediterranean over the last 900 years. *J Geophys Res* 121:2060–2074. doi: 10.1002/2015JD023929
- Cook KH, Vizy EK (2015) Detection and analysis of an amplified warming of the Sahara Desert. *J Clim* 28:6560–6580. doi: 10.1175/JCLI-D-14-00230.1
- Coppola E, Nogherotto R, Ciarlo' JM, et al (2021a) Assessment of the European Climate Projections as Simulated by the Large EURO-CORDEX Regional and Global Climate Model Ensemble. *J Geophys Res Atmos* 126:1–20. doi: 10.1029/2019JD032356
- Coppola E, Raffaele F, Giorgi F, et al (2021b) Climate hazard indices projections based on CORDEX-CORE, CMIP5 and CMIP6 ensemble
- Coumou D, Rahmstorf S (2012) A decade of weather extremes. *Nat Clim Chang* 2:491–496. doi: 10.1038/nclimate1452
- Cramer W, Guiot J, Fader M, et al (2018) Climate change and interconnected risks to sustainable development in the Mediterranean. *Nat Clim Chang* 8:972–980. doi: 10.1038/s41558-018-0299-2
- Croke B, Cleridou N, Kolovos A, et al (2000) Water resources in the desertification-threatened Messara Valley of Crete: Estimation of the annual water budget using a rainfall-runoff model. *Environ Model Softw* 15:387–402. doi: 10.1016/S1364-8152(00)00018-9
- Cullen HM, Kaplan A, Arkin PA, DeMenocal PB (2002) Impact of the North Atlantic Oscillation on Middle Eastern climate and streamflow. *Clim Change* 55:315–338. doi: 10.1023/A:1020518305517
- Dafka S, Toreti A, Zanis P, et al (2019) Twenty-First-Century Changes in the Eastern Mediterranean Ete-sians and Associated Midlatitude Atmospheric Circulation. *J Geophys Res Atmos* 124:12741–12754. doi: 10.1029/2019JD031203
- Dahmardeh Behrooz R, Kaskaoutis DG, Grivas G, Mihalopoulos N (2021) Human health risk assessment for toxic elements in the extreme ambient dust conditions observed in Sistan, Iran. *Chemosphere* 262:. doi: 10.1016/j.chemosphere.2020.127835

- Daliakopoulos IN, Panagea IS, Tsanis IK, et al (2017) Yield Response of Mediterranean Rangelands under a Changing Climate. *L Degrad Dev* 28:1962–1972. doi: 10.1002/ldr.2717
- Danandeh Mehr A, Sorman AU, Kahya E, Hesami Afshar M (2020) Climate change impacts on meteorological drought using SPI and SPEI: case study of Ankara, Turkey. *Hydrol Sci J* 65:254–268. doi: 10.1080/02626667.2019.1691218
- Darmaraki S, Somot S, Sevault F, et al (2019a) Future evolution of Marine Heatwaves in the Mediterranean Sea. *Clim Dyn* 53:1371–1392. doi: 10.1007/s00382-019-04661-z
- Darmaraki S, Somot S, Sevault F, Nabat P (2019b) Past Variability of Mediterranean Sea Marine Heatwaves. *Geophys Res Lett* 46:9813–9823. doi: 10.1029/2019GL082933
- Das S, Dey S, Dash SK, et al (2015) Dust aerosol feedback on the Indian summer monsoon: Sensitivity to absorption property. *J Geophys Res* 120:9642–9652. doi: 10.1002/2015JD023589
- Davy R, Gnaniuk N, Pettersson L, Bobylev L (2018) Climate change impacts on wind energy potential in the European domain with a focus on the Black Sea. *Renew Sustain Energy Rev* 81:1652–1659. doi: 10.1016/j.rser.2017.05.253
- De Meij A, Lelieveld J (2011) Evaluating aerosol optical properties observed by ground-based and satellite remote sensing over the Mediterranean and the Middle East in 2006. *Atmos Res* 99:415–433. doi: 10.1016/j.atmosres.2010.11.005
- De Meij A, Pozzer A, Lelieveld J (2012) Trend analysis in aerosol optical depths and pollutant emission estimates between 2000 and 2009. *Atmos Environ* 51:75–85. doi: 10.1016/j.atmosenv.2012.01.059
- De Ridder K, Lauwaet D, Maiheu B (2015) UrbClim - A fast urban boundary layer climate model. *Urban Clim* 12:21–48. doi: 10.1016/j.uclim.2015.01.001
- de Vries AJ (2021) A global climatological perspective on the importance of Rossby wave breaking and intense moisture transport for extreme precipitation events. *Weather Clim Dyn* 2:129–161. doi: 10.5194/wcd-2-129-2021
- De Vries AJ, Tyrlis E, Edry D, et al (2013) Extreme precipitation events in the Middle East: Dynamics of the Active Red Sea Trough. *J Geophys Res Atmos* 118:7087–7108. doi: 10.1002/jgrd.50569
- de Vries, AJ, Ouwersloot HG, Feldstein SB et al (2018) Identification of tropical-extratropical interactions and extreme precipitation events in the Middle East based on potential vorticity and moisture transport. *J. Geophys. Res.* 123, 861-881
- Deitch MJ, Sapundjieff MJ, Feirer ST (2017) Characterizing precipitation variability and trends in the world's mediterranean-climate areas. *Water* 9:259. doi: 10.3390/w9040259
- Diffenbaugh NS, Giorgi F (2012) Climate change hotspots in the CMIP5 global climate model ensemble. *Clim Change* 114:813–822. doi: 10.1007/s10584-012-0570-x
- Diffenbaugh NS, Pal JS, Giorgi F, Gao X (2007) Heat stress intensification in the Mediterranean climate change hotspot. *Geophys Res Lett* 34:L11706. doi: 10.1029/2007GL030000
- Dimitrakopoulos AP, Vlahou M, Anagnostopoulou CG, Mitsopoulos ID (2011) Impact of drought on wildland fires in Greece: Implications of climatic change? *Clim Change* 109:331–347. doi: 10.1007/s10584-011-0026-8
- Dimitriou S, Kyprianou I, Papanicolas CN, Serghides D (2020) A new approach in the refurbishment of the office buildings—from standard to alternative nearly zero energy buildings. *Int J Sustain Energy* 39:761–778. doi: 10.1080/14786451.2020.1749629
- Dobrynin M, Murawsky J, Yang S (2012) Evolution of the global wind wave climate in CMIP5 experiments. *Geophys Res Lett* 39:2–7. doi: 10.1029/2012GL052843
- Doelman JC, Stehfest E, van Vuuren DP, et al (2020) Afforestation for climate change mitigation: Potentials, risks and trade-offs. *Glob Chang Biol* 26:1576–1591. doi: 10.1111/gcb.14887
- Donat MG, Lowry AL, Alexander L V., et al (2016) More extreme precipitation in the world's dry and wet regions. *Nat Clim Chang* 6:508–513. doi: 10.1038/nclimate2941
- Donat MG, Peterson TC, Brunet M, et al (2014) Changes in extreme temperature and precipitation in the Arab region: Long-term trends and variability related to ENSO and NAO. *Int J Climatol* 34:581–592. doi: 10.1002/joc.3707

- Dosio A, Fischer EM (2018) Will Half a Degree Make a Difference? Robust Projections of Indices of Mean and Extreme Climate in Europe Under 1.5°C, 2°C, and 3°C Global Warming. *Geophys Res Lett* 45:935–944. doi: 10.1002/2017GL076222
- Driouech F, ElRhazi K, Moufouma-Okia W, et al (2020a) Assessing Future Changes of Climate Extreme Events in the CORDEX-MENA Region Using Regional Climate Model ALADIN-Climate. *Earth Syst Environ* 4:477–492. doi: 10.1007/s41748-020-00169-3
- Driouech F, ElRhazi K, Moufouma-Okia W, et al (2020b) Assessing Future Changes of Climate Extreme Events in the CORDEX-MENA Region Using Regional Climate Model ALADIN-Climate. *Earth Syst Environ* 4:477–492. doi: 10.1007/s41748-020-00169-3
- Drobinski P, Da Silva N, Bastin S, et al (2020) How warmer and drier will the Mediterranean region be at the end of the twenty-first century? *Reg Environ Chang* 20. doi: 10.1007/s10113-020-01659-w
- Drobinski P, Silva N Da, Panthou G, et al (2018) Scaling precipitation extremes with temperature in the Mediterranean: past climate assessment and projection in anthropogenic scenarios. *Clim Dyn* 51:1237–1257. doi: 10.1007/s00382-016-3083-x
- Dubrovský M, Hayes M, Duce P, et al (2014) Multi-GCM projections of future drought and climate variability indicators for the Mediterranean region. *Reg Environ Chang* 14:1907–1919. doi: 10.1007/s10113-013-0562-z
- Dunne JP, Stouffer RJ, John JG (2013) Reductions in labour capacity from heat stress under climate warming. *Nat Clim Chang* 3:563–566. doi: 10.1038/nclimate1827
- Dupuy J luc, Fargeon H, Martin-StPaul N, et al (2020) Climate change impact on future wildfire danger and activity in southern Europe: a review. *Ann For Sci* 77. doi: 10.1007/s13595-020-00933-5
- Eger PG, Friedrich N, Schuladen J, et al (2019) Shipborne measurements of CINO_x in the Mediterranean Sea and around the Arabian Peninsula during summer. *Atmos Chem Phys* 19:12121–12140. doi: 10.5194/acp-19-12121-2019
- El-Zein A, Tewfel-Salem M, Nehme G (2004) A time-series analysis of mortality and air temperature in Greater Beirut. *Sci Total Environ* 330:71–80. doi: 10.1016/j.scitotenv.2004.02.027
- El Kenawy AM, Lopez-Moreno JI, McCabe MF, et al (2019) Daily temperature extremes over Egypt: Spatial patterns, temporal trends, and driving forces. *Atmos Res* 226:219–239. doi: 10.1016/j.atmosres.2019.04.030
- Elhacham E, Alpert P (2021) Temperature patterns along an arid coastline experiencing extreme and rapid urbanization, case study: Dubai. *Sci Total Environ* 784:147168. doi: 10.1016/j.scitotenv.2021.147168
- Emamian A, Rashki A, Kaskaoutis DG, et al (2021) Assessing vegetation restoration potential under different land uses and climatic classes in northeast Iran. *Ecol Indic* 122. doi: 10.1016/j.ecolind.2020.107325
- Engelbrecht JP, McDonald E V., Gillies JA, et al (2009) Characterizing mineral dusts and other aerosols from the Middle East - Part 1: Ambient sampling. *Inhal Toxicol* 21:297–326. doi: 10.1080/08958370802464273
- Enriquez-Alonso A, Sanchez-Lorenzo A, Calbó J, et al (2016) Cloud cover climatologies in the Mediterranean obtained from satellites, surface observations, reanalyses, and CMIP5 simulations: validation and future scenarios. *Clim Dyn* 47:249–269. doi: 10.1007/s00382-015-2834-4
- Evans JP (2010) Global warming impact on the dominant precipitation processes in the Middle East. *Theor Appl Climatol* 99:389–402. doi: 10.1007/s00704-009-0151-8
- Ezber Y (2019) Assessment of the changes in the Etesians in the EURO-CORDEX regional model projections. *Int J Climatol* 39:1213–1229. doi: 10.1002/joc.5872
- Feidas H, Nouloupoulou C, Makrogiannis T, Bora-Senta E (2007) Trend analysis of precipitation time series in Greece and their relationship with circulation using surface and satellite data: 1955–2001. *Theor Appl Climatol* 87:155–177. doi: 10.1007/s00704-006-0200-5
- Feron S, Cordero RR, Damiani A, Jackson RB (2020) Climate change extremes and photovoltaic power output. *Nat Sustain* 4. doi: 10.1038/s41893-020-00643-w
- Finné M, Woodbridge J, Labuhn I, Roberts CN (2019) Holocene hydro-climatic variability in the Mediterranean: A synthetic multi-proxy reconstruction. *Holocene* 29:847–863. doi: 10.1177/0959683619826634
- Fischer EM, Schär C (2010) Consistent geographical patterns of changes in high-impact European heatwaves. *Nat Geosci* 3:398–403. doi: 10.1038/ngeo866

- Fleitmann D, Burns SJ, Mangini A, et al (2007) Holocene ITCZ and Indian monsoon dynamics recorded in staghmites from Oman and Yemen (Socotra). *Quat Sci Rev* 26:170–188. doi: 10.1016/j.quascirev.2006.04.012
- Fleitmann D, Burns SJ, Neff U, et al (2004) Palaeoclimatic interpretation of high-resolution oxygen isotope profiles derived from annually laminated speleothems from Southern Oman. *Quat Sci Rev* 23:935–945. doi: 10.1016/j.quascirev.2003.06.019
- Flohr P, Fleitmann D, Zorita E, et al (2017) Late Holocene droughts in the Fertile Crescent recorded in a speleothem from northern Iraq. *Geophys Res Lett* 44:1528–1536. doi: 10.1002/2016GL071786
- Floutsi AA, Korras-Carraca MB, Matsoukas C, et al (2016) Climatology and trends of aerosol optical depth over the Mediterranean basin during the last 12 years (2002–2014) based on Collection 006 MODIS-Aqua data. *Sci Total Environ* 551–552:292–303. doi: 10.1016/j.scitotenv.2016.01.192
- Founda D, Giannakopoulos C (2009) The exceptionally hot summer of 2007 in Athens, Greece - A typical summer in the future climate? *Glob Planet Change* 67:227–236. doi: 10.1016/j.gloplacha.2009.03.013
- Founda D, Giannakopoulos C, Pierros F, et al (2013) Observed and projected precipitation variability in Athens over a 2.5 century period. *Atmos Sci Lett* 14:72–78. doi: 10.1002/asl2.419
- Founda D, Kambezidis HD, Petrakis M, et al (2009) A correction of the recent air-temperature record at the historical meteorological station of the National Observatory of Athens (NOA) due to instrument change. *Theor Appl Climatol* 97:385–389. doi: 10.1007/s00704-008-0084-7
- Founda D, Pierros F, Petrakis M, Zerefos C (2015) Interdecadal variations and trends of the Urban Heat Island in Athens (Greece) and its response to heat waves. *Atmos Res* 161–162:1–13. doi: 10.1016/j.atmosres.2015.03.016
- Francis D, Chaboureaux JP, Nelli N, et al (2021) Summertime dust storms over the Arabian Peninsula and impacts on radiation, circulation, cloud development and rain. *Atmos Res* 250:. doi: 10.1016/j.atmosres.2020.105364
- Freiwan M, Kadioglu M (2008) Climate variability in Jordan. *Int J Climatol* 28:69–89. doi: 10.1002/joc.1512
- Fritz HM, Blount CD, Albusaidi FB, Al-Harthy AHM (2010) Cyclone Gonu storm surge in Oman. *Estuar Coast Shelf Sci* 86:102–106. doi: 10.1016/j.ecss.2009.10.019
- Fujihara Y, Tanaka K, Watanabe T, et al (2008) Assessing the impacts of climate change on the water resources of the Seyhan River Basin in Turkey: Use of dynamically downscaled data for hydrologic simulations. *J Hydrol* 353:33–48. doi: 10.1016/j.jhydrol.2008.01.024
- Gado TA, El-Hagrsy RM, Rashwan IMH (2019) Spatial and temporal rainfall changes in Egypt
- Ganor E, Osetinsky I, Stupp A, Alpert P (2010) Increasing trend of African dust, over 49 years, in the eastern Mediterranean. *J Geophys Res Atmos* 115:. doi: 10.1029/2009JD012500
- Gat D, Mazar Y, Cytryn E, Rudich Y (2017) Origin-Dependent Variations in the Atmospheric Microbiome Community in Eastern Mediterranean Dust Storms. *Environ Sci Technol* 51:6709–6718. doi: 10.1021/acs.est.7b00362
- Georgoulas AK, Alexandri G, Kourtidis KA, et al (2016) Spatiotemporal variability and contribution of different aerosol types to the aerosol optical depth over the Eastern Mediterranean. *Atmos Chem Phys* 16:13853–13884. doi: 10.5194/acp-16-13853-2016
- Ghanavati N, Nazarpour A, Watts MJ (2019) Status, source, ecological and health risk assessment of toxic metals and polycyclic aromatic hydrocarbons (PAHs) in street dust of Abadan, Iran. *Catena* 177:246–259. doi: 10.1016/j.catena.2019.02.022
- Gharehchahi E, Mahvi AH, Amini H, et al (2013) Health impact assessment of air pollution in Shiraz, Iran: a two-part study. *J Environ Heal Sci Eng* 11:. doi: 10.1186/2052-336x-11-11
- Gholami H, Mohammadifar A, Bui DT, Collins AL (2020) Mapping wind erosion hazard with regression-based machine learning algorithms. *Sci Rep* 10:. doi: 10.1038/s41598-020-77567-0
- Gholampour A, Nabizadeh R, Hassanvand MS, et al (2016) Characterization and source identification of trace elements in airborne particulates at urban and suburban atmospheres of Tabriz, Iran. *Environ Sci Pollut Res* 23:1703–1713. doi: 10.1007/s11356-015-5413-7
- Gholampour A, Nabizadeh R, Yunesian M, et al (2014) Physicochemical characterization of ambient air particulate matter in Tabriz, Iran. *Bull Environ Contam Toxicol* 92:738–744. doi: 10.1007/s00128-014-1276-8
- Giannadaki D, Pozzer A, Lelieveld J (2014) Modeled global effects of airborne desert dust on air quality and premature mortality. *Atmos Chem Phys* 14:957–968. doi: 10.5194/acp-14-957-2014

- Giannakis E, Serghides D, Dimitriou S, Zittis G (2020) Land transport CO₂ emissions and climate change: evidence from Cyprus. *Int J Sustain Energy* 39:634–647. doi: 10.1080/14786451.2020.1743704
- Giannakopoulos C, Le Sager P, Bindi M, et al (2009) Climatic changes and associated impacts in the Mediterranean resulting from a 2°C global warming. *Glob Planet Change* 68:209–224. doi: 10.1016/j.gloplacha.2009.06.001
- Ginoux P, Prospero JM, Gill TE, et al (2012) Global-scale attribution of anthropogenic and natural dust sources and their emission rates based on MODIS Deep Blue aerosol products. *Rev Geophys* 50:. doi: 10.1029/2012RG000388
- Giorgi F (2006) Climate change hot-spots. *Geophys Res Lett* 33:L08707. doi: 10.1029/2006GL025734
- Giorgi F, Gutowski WJ (2016) Coordinated Experiments for Projections of Regional Climate Change. *Curr Clim Chang Reports* 2:202–210. doi: 10.1007/s40641-016-0046-6
- Giorgi F, Lionello P (2008) Climate change projections for the Mediterranean region. *Glob Planet Change* 63:90–104. doi: 10.1016/j.gloplacha.2007.09.005
- Giorgi F, Raffaele F, Coppola E (2019) The response of precipitation characteristics to global warming from climate projections. *Earth Syst Dyn* 10:73–89. doi: 10.5194/esd-10-73-2019
- Givati A, Thirel G, Rosenfeld D, Paz D (2019) Climate change impacts on streamflow at the upper Jordan River based on an ensemble of regional climate models. *J Hydrol Reg Stud* 21:92–109. doi: 10.1016/j.ejrh.2018.12.004
- Gkikas A, Hatzianastassiou N, Mihalopoulos N, et al (2013) The regime of intense desert dust episodes in the Mediterranean based on contemporary satellite observations and ground measurements. *Atmos Chem Phys* 13:12135–12154. doi: 10.5194/acp-13-12135-2013
- Gkikas A, Obiso V, Pérez García-Pando C, et al (2018) Direct radiative effects during intense Mediterranean desert dust outbreaks. *Atmos Chem Phys* 18:8757–8787. doi: 10.5194/acp-18-8757-2018
- Gleick PH (2014) Water, Drought, Climate Change, and Conflict in Syria. *Weather Clim Soc* 6:331–340. doi: 10.1175/WCAS-D-13-00059.1
- González-Alemán JJ, Pascale S, Gutierrez-Fernandez J, et al (2019) Potential Increase in Hazard From Mediterranean Hurricane Activity With Global Warming. *Geophys Res Lett* 46:1754–1764. doi: 10.1029/2018GL081253
- Goubanova K, Li L (2007) Extremes in temperature and precipitation around the Mediterranean basin in an ensemble of future climate scenario simulations. *Glob Planet Change* 57:27–42. doi: 10.1016/j.gloplacha.2006.11.012
- Goudarzi G, Alavi N, Geravandi S, et al (2018) Health risk assessment on human exposed to heavy metals in the ambient air PM₁₀ in Ahvaz, southwest Iran. *Int J Biometeorol* 62:1075–1083. doi: 10.1007/s00484-018-1510-x
- Goudie AS (2014) Desert dust and human health disorders. *Environ Int* 63:101–113. doi: 10.1016/J.ENVINT.2013.10.011
- Güner Bacanlı Ü (2017) Trend analysis of precipitation and drought in the Aegean region, Turkey. *Meteorol Appl* 24:239–249. doi: 10.1002/met.1622
- Gütschow J, Jeffery ML, Gieseke R, et al (2016) The PRIMAP-hist national historical emissions time series. *Earth Syst Sci Data* 8:571–603. doi: 10.5194/essd-8-571-2016
- Habib RR, Zein K El, Ghanawi J (2010) Climate change and health research in the Eastern Mediterranean Region. *Ecohealth* 7:156–175. doi: 10.1007/s10393-010-0330-1
- Hadjinicolaou P, Giannakopoulos C, Zerefos C, et al (2011) Mid-21st century climate and weather extremes in Cyprus as projected by six regional climate models. *Reg Environ Chang* 11:441–457. doi: 10.1007/s10113-010-0153-1
- Hadjipanayi M, Koumparou I, Philippou N, et al (2016) Prospects of photovoltaics in southern European, Mediterranean and Middle East regions. *Renew Energy* 92:58–74. doi: 10.1016/j.renene.2016.01.096
- Haldon J, Roberts N, Izdebski A, et al (2014) The climate and environment of Byzantine Anatolia: Integrating science, history, and archaeology. *J Interdiscip Hist* 45:113–161. doi: 10.1162/JINH_a_00682
- Hamdi R, Kusaka H, Doan Q Van, et al (2020) The State-of-the-Art of Urban Climate Change Modeling and Observations. *Earth Syst Environ* 4:631–646. doi: 10.1007/s41748-020-00193-3
- Hamidi M, Kavianpour MR, Shao Y (2013) Synoptic analysis of dust storms in the Middle East. *Asia-Pacific J Atmos Sci* 49:279–286. doi: 10.1007/s13143-013-0027-9

- Hamill P, Giordano M, Ward C, et al (2016) An AERONET-based aerosol classification using the Mahalanobis distance. *Atmos Environ* 140:213–233. doi: 10.1016/j.atmosenv.2016.06.002
- Harris I, Osborn TJ, Jones P, Lister D (2020) Version 4 of the CRU TS monthly high-resolution gridded multivariate climate dataset. *Sci Data* 7:1–18. doi: 10.1038/s41597-020-0453-3
- Hartmann A, Lange J, Vivó Aguado À, et al (2012) A multi-model approach for improved simulations of future water availability at a large Eastern Mediterranean karst spring. *J Hydrol* 468–469:130–138. doi: 10.1016/j.jhydrol.2012.08.024
- Heidari-Farsani M, Shirmardi M, Goudarzi G (2013) The evaluation of heavy metals concentration related to PM 10 in ambient air of Ahvaz city, Iran. *J Adv Environ Heal Res* 1:1–9
- Hemming D, Buontempo C, Burke E, et al (2010) How uncertain are climate model projections of water availability indicators across the Middle East? *Philos Trans R Soc A Math Phys Eng Sci* 368:5117–5135. doi: 10.1098/rsta.2010.0174
- Hentgen L, Ban N, Kröner N, et al (2019) Clouds in Convection Resolving Climate Simulations Over Europe. *J Geophys Res Atmos* 124:3849–3870. doi: 10.1029/2018JD030150
- Hereher M, Al-Awadhi T, Al-Hatrushy S, et al (2020) Assessment of the coastal vulnerability to sea level rise: Sultanate of Oman. *Environ Earth Sci* 79:1–12. doi: 10.1007/s12665-020-09113-0
- Hereher ME (2020) Assessment of climate change impacts on sea surface temperatures and sea level rise-The Arabian Gulf. *Climate* 8
- Hereher ME (2015) Assessment of Egypt's Red Sea coastal sensitivity to climate change. *Environ Earth Sci* 74:2831–2843. doi: 10.1007/s12665-015-4304-z
- Hermida L, Merino A, Sánchez JL, et al (2018) Characterization of synoptic patterns causing dust outbreaks that affect the Arabian Peninsula. *Atmos Res* 199:29–39. doi: 10.1016/j.atmosres.2017.09.004
- Hochman A, Harpaz T, Saaroni H, Alpert P (2018a) The seasons' length in 21st century CMIP5 projections over the eastern Mediterranean. *Int J Climatol* 38:2627–2637. doi: 10.1002/joc.5448
- Hochman A, Harpaz T, Saaroni H, Alpert P (2018b) Synoptic classification in 21st century CMIP5 predictions over the eastern Mediterranean with focus on cyclones. *Int J Climatol* 38:1476–1483. doi: 10.1002/joc.5260
- Hochman A, Mercogliano P, Alpert P, et al (2018c) High-resolution projection of climate change and extremity over Israel using COSMO-CLM. *Int J Climatol* 38:5095–5106. doi: 10.1002/joc.5714
- Hock R, Bliss A, Marzeion BEN, et al (2019) GlacierMIP-A model intercomparison of global-scale glacier mass-balance models and projections. *J Glaciol* 65:453–467. doi: 10.1017/jog.2019.22
- Hoerling M, Eischeid J, Perlwitz J, et al (2012) On the increased frequency of mediterranean drought. *J Clim* 25:2146–2161. doi: 10.1175/JCLI-D-11-00296.1
- Hsu NC, Gautam R, Sayer AM, et al (2012) Global and regional trends of aerosol optical depth over land and ocean using SeaWiFS measurements from 1997 to 2010. *Atmos Chem Phys* 12:8037–8053. doi: 10.5194/acp-12-8037-2012
- Huang Y, Liu X, Yin Z-Y, An Z (2021) Global Impact of ENSO on Dust Activities with Emphasis on the Key Region from the Arabian Peninsula to Central Asia. *J Geophys Res Atmos* 126:e2020JD034068. doi: <https://doi.org/10.1029/2020JD034068>
- Irani M, Massah Bavani A, Bohluly A, Alizadeh Katak Lahijani H (2017) Sea Level Rise in Persian Gulf and Oman Sea Due to Climate Change in the Future Periods. *Phys Geogr Res Q* 49:603–614. doi: 10.22059/jphgr.2018.2211011006966
- Itzhak-Ben-Shalom H, Samuels R, Potchter O, Alpert P (2016) Recent Trends and Future Predictions until 2060 of Urban Warming in Four Israeli Cities Employing the RegCM Climate Model. *Am J Clim Chang* 05:464–484. doi: 10.4236/ajcc.2016.54034
- Izaguirre C, Losada IJ, Camus P, et al (2020) Climate change risk to global port operations. *Nat Clim Chang*. doi: 10.1038/s41558-020-00937-z
- Izdebski A, Holmgren K, Weiberg E, et al (2016a) Realising consilience: How better communication between archaeologists, historians and natural scientists can transform the study of past climate change in the Mediterranean. *Quat Sci Rev* 136:5–22. doi: 10.1016/j.quascirev.2015.10.038

- Izdebski A, Pickett J, Roberts N, Waliszewski T (2016b) The environmental, archaeological and historical evidence for regional climatic changes and their societal impacts in the Eastern Mediterranean in Late Antiquity. *Quat Sci Rev* 136:189–208. doi: 10.1016/j.quascirev.2015.07.022
- Jaafari J, Naddafi K, Yunesian M, et al (2020) Characterization, risk assessment and potential source identification of PM10 in Tehran. *Microchem J* 154:104533. doi: 10.1016/j.microc.2019.104533
- Jacob D, Kotova L, Teichmann C, et al (2018) Climate Impacts in Europe Under +1.5°C Global Warming. *Earth's Futur* 6:264–285. doi: 10.1002/2017EF000710
- Jacob D, Petersen J, Eggert B, et al (2014) EURO-CORDEX: New high-resolution climate change projections for European impact research. *Reg Environ Chang* 14:563–578. doi: 10.1007/s10113-013-0499-2
- Javed W, Wexler AS, Murtaza G, et al (2015) Spatial, temporal and size distribution of particulate matter and its chemical constituents in Faisalabad, Pakistan. *Atmosfera* 28:99–116. doi: 10.1016/s0187-6236(15)30003-5
- Jin F, Kitoh A, Alpert P (2010) Water cycle changes over the Mediterranean: A comparison study of a super-high-resolution global model with CMIP3. *Philos Trans R Soc A Math Phys Eng Sci* 368:5137–5149. doi: 10.1098/rsta.2010.0204
- Jin Q, Wei J, Lau WKM, et al (2021) Interactions of Asian mineral dust with Indian summer monsoon: Recent advances and challenges. *Earth-Science Rev* 215:103562. doi: 10.1016/j.earscirev.2021.103562
- Jin Q, Yang ZL, Wei J (2016) Seasonal responses of Indian summer monsoon to dust aerosols in the middle East, India, and China. *J Clim* 29:6329–6349. doi: 10.1175/JCLI-D-15-0622.1
- Jish Prakash P, Stenichkov G, Kalenderski S, et al (2015) The impact of dust storms on the Arabian Peninsula and the Red Sea. *Atmos Chem Phys* 15:199–222. doi: 10.5194/acp-15-199-2015
- Jones MD, Abu Jaber N, AlShdaifat A, et al (2019) 20,000 years of societal vulnerability and adaptation to climate change in southwest Asia. *WIREs Water* 6:e1330. doi: 10.1002/wat2.1330
- Jones P (2016) The reliability of global and hemispheric surface temperature records. *Adv Atmos Sci* 33:269–282. doi: 10.1007/s00376-015-5194-4
- Kalnay E, Cai M (2003) Impact of urbanization and land-use change on climate. *Nature* 423:528–531. doi: 10.1038/nature01675
- Kang S, Pal JS, Eltahir EAB (2019) Future Heat Stress During Muslim Pilgrimage (Hajj) Projected to Exceed “Extreme Danger” Levels. *Geophys Res Lett* 46:10094–10100. doi: 10.1029/2019GL083686
- Kaniewski D, Van Campo E, Morhange C, et al (2014) Vulnerability of mediterranean ecosystems to long-term changes along the coast of Israel. *PLoS One* 9:1–9. doi: 10.1371/journal.pone.0102090
- Kaniewski D, Van Campo E, Weiss H (2012) Drought is a recurring challenge in the Middle East. *Proc Natl Acad Sci U S A* 109:3862–3867. doi: 10.1073/pnas.1116304109
- Karali A, Hatzaki M, Giannakopoulos C, et al (2014) Sensitivity and evaluation of current fire risk and future projections due to climate change: The case study of Greece. *Nat Hazards Earth Syst Sci* 14:143–153. doi: 10.5194/nhess-14-143-2014
- Karydis VA, Tsimpidi AP, Pozzer A, et al (2016) Effects of mineral dust on global atmospheric nitrate concentrations. *Atmos Chem Phys* 16:1491–1509. doi: 10.5194/acp-16-1491-2016
- Kaskaoutis DG, Houssos EE, Rashki A, et al (2016) The Caspian Sea–Hindu Kush Index (CasHKI): A regulatory factor for dust activity over southwest Asia. *Glob Planet Change* 137:10–23. doi: 10.1016/j.gloplacha.2015.12.011
- Kaskaoutis DG, Houssos EE, Solmon F, et al (2018) Impact of atmospheric circulation types on southwest Asian dust and Indian summer monsoon rainfall. *Atmos Res* 201:189–205. doi: 10.1016/j.atmosres.2017.11.002
- Kaskaoutis DG, Kambezidis HD, Hatzianastassiou N, et al (2007) Aerosol climatology: dependence of the Angstrom exponent on wavelength over four AERONET sites. *Atmos. Chem. Phys. Discuss.* 7:7347–7397
- Kaskaoutis DG, Rashki A, Houssos EE, et al (2017) Assessment of changes in atmospheric dynamics and dust activity over southwest Asia using the Caspian Sea–Hindu Kush Index. *Int J Climatol* 37:1013–1034. doi: 10.1002/joc.5053
- Kaufman YJ, Koren I, Remer LA, et al (2005) The effect of smoke, dust, and pollution aerosol on shallow cloud development over the Atlantic Ocean. *Proc Natl Acad Sci U S A* 102:11207–11212. doi: 10.1073/pnas.0505191102

- Kelley CP, Mohtadi S, Cane MA, et al (2015) Climate change in the Fertile Crescent and implications of the recent Syrian drought. *Proc Natl Acad Sci U S A* 112:3241–3246. doi: 10.1073/pnas.1421533112
- Keshavarzi B, Abbasi S, Moore F, et al (2018) Contamination Level, Source Identification and Risk Assessment of Potentially Toxic Elements (PTEs) and Polycyclic Aromatic Hydrocarbons (PAHs) in Street Dust of an Important Commercial Center in Iran. *Environ Manage* 62:803–818. doi: 10.1007/s00267-018-1079-5
- Khadr M (2017) Recent trends and fluctuations of rainfall in the Upper Blue Nile River Basin. In: Negm AM (ed) *Handbook of Environmental Chemistry*. Springer International Publishing, Cham, pp 451–466
- Kitoh A, Yatagai A, Alpert P (2008) First super-high-resolution model projection that the ancient “Fertile Crescent” will disappear in this century. *Hydrol Res Lett* 2:1–4. doi: 10.3178/hrl.2.1
- Kitsara G, Schriek T Van Der, Varotsos K V, Giannakopoulos C (2021) Future changes in climate indices relevant to agriculture in the Aegean islands (Greece). *Euro-Mediterranean J Environ Integr* 4:1–12. doi: 10.1007/s41207-020-00233-4
- Klingmüller K, Karydis VA, Bacer S, et al (2020) Weaker cooling by aerosols due to dust-pollution interactions. *Atmos Chem Phys* 20:15285–15295. doi: 10.5194/acp-20-15285-2020
- Klingmüller K, Lelieveld J, Karydis VA, Stenchikov GL (2019) Direct radiative effect of dust-pollution interactions. *Atmos Chem Phys* 19:7397–7408. doi: 10.5194/acp-19-7397-2019
- Klingmüller K, Pozzer A, Metzger S, et al (2016) Aerosol optical depth trend over the Middle East. *Atmos Chem Phys* 16:5063–5073. doi: 10.5194/acp-16-5063-2016
- Knutti R, Sedláček J (2013) Robustness and uncertainties in the new CMIP5 climate model projections. *Nat Clim Chang* 3:369–373. doi: 10.1038/nclimate1716
- Kostopoulou E, Giannakopoulos C, Hatzaki M, et al (2014) Spatio-temporal patterns of recent and future climate extremes in the eastern Mediterranean and Middle East region. *Nat Hazards Earth Syst Sci* 14:1565–1577. doi: 10.5194/nhess-14-1565-2014
- Kostopoulou E, Jones PD (2005) Assessment of climate extremes in the Eastern Mediterranean. *Meteorol Atmos Phys* 89:69–85. doi: 10.1007/s00703-005-0122-2
- Kottek M, Grieser J, Beck C, et al (2006) World map of the Köppen-Geiger climate classification updated. *Meteorol Zeitschrift* 15:259–263. doi: 10.1127/0941-2948/2006/0130
- Kouis P, Kakkoura M, Ziogas K, et al (2019) The effect of ambient air temperature on cardiovascular and respiratory mortality in Thessaloniki, Greece. *Sci Total Environ* 647:1351–1358. doi: 10.1016/j.scitotenv.2018.08.106
- Koutsias N, Arianoutsou M, Kallimanis AS, et al (2012) Where did the fires burn in Peloponnisos, Greece the summer of 2007? Evidence for a synergy of fuel and weather. *Agric For Meteorol* 156:41–53. doi: 10.1016/j.agrformet.2011.12.006
- Koutsias N, Xanthopoulos G, Founda D, et al (2013) On the relationships between forest fires and weather conditions in Greece from long-term national observations (1894–2010). *Int J Wildl Fire* 22:493–507. doi: 10.1071/WF12003
- Krakauer NY, Cook BI, Puma MJ (2020) Effect of irrigation on humid heat extremes. *Environ Res Lett* 15:. doi: 10.1088/1748-9326/ab9ecf
- Krasnov H, Katra I, Friger M (2016) Increase in dust storm related PM10 concentrations: A time series analysis of 2001–2015. *Environ Pollut* 213:36–42. doi: 10.1016/j.envpol.2015.10.021
- Krichak SO, Tsidulko M, Alpert P (2000) Monthly synoptic patterns associated with wet/dry conditions in the Eastern Mediterranean. *Theor Appl Climatol* 65:215–229. doi: 10.1007/s007040070045
- Kron W (2013) Coasts: The high-risk areas of the world. *Nat Hazards* 66:1363–1382. doi: 10.1007/s11069-012-0215-4
- Ksikis TS, Youssef T (2012) Sea Level Rise and Abu Dhabi Coastlines: An Initial Assessment of the Impact on Land and Mangrove Areas. *J Ecosyst Ecography* 02: doi: 10.4172/2157-7625.1000115
- Kuglitsch FG, Toreti A, Xoplaki E, et al (2010) Heat wave changes in the eastern mediterranean since 1960. *Geophys Res Lett* 37:L04802. doi: 10.1029/2009GL041841
- Kuleli T (2010) City-based risk assessment of sea level rise using topographic and census data for the Turkish Coastal zone. *Estuaries and Coasts* 33:640–651. doi: 10.1007/s12237-009-9248-7

- Kumar TS, Mahendra RS, Nayak S, et al (2010) Coastal vulnerability assessment for Orissa State, East Coast of India. *J Coast Res* 26:523–534. doi: 10.2112/09-1186.1
- Labban AH, Mashat AWS, Awad AM (2021) The variability of the Siberian high ridge over the Middle East. *Int J Climatol* 41:104–130. doi: 10.1002/joc.6611
- Labuhn I, Finné M, Izdebski A, et al (2019) Climatic Changes and Their Impacts in the Mediterranean during the First Millennium AD. Brill, Leiden, The Netherlands, pp 247–270
- Lang-Yona N, Öztürk F, Gat D, et al (2020) Links between airborne microbiome, meteorology, and chemical composition in northwestern Turkey. *Sci Total Environ* 725:138227. doi: 10.1016/j.scitotenv.2020.138227
- Lange MA (2019) Impacts of climate change on the Eastern Mediterranean and the Middle East and North Africa region and the water-energy nexus. *Atmosphere (Basel)* 10:455. doi: 10.3390/atmos10080455
- Lawrence MG, Lelieveld J (2010) Atmospheric pollutant outflow from southern Asia: A review. *Atmos Chem Phys* 10:11017–11096. doi: 10.5194/acp-10-11017-2010
- Legasa MN, Manzanos R, Fernández J, et al (2020) Assessing multi domain overlaps and grand ensemble generation in CORDEX regional projections. *Geophys Res Lett*. doi: 10.1029/2019gl086799
- Lelieveld J, Beirle S, Hörmann C, et al (2015) Abrupt recent trend changes in atmospheric nitrogen dioxide over the Middle East. *Sci Adv* 1:e1500498–e1500498. doi: 10.1126/sciadv.1500498
- Lelieveld J, Hadjinicolaou P, Kostopoulou E, et al (2012) Climate change and impacts in the Eastern Mediterranean and the Middle East. *Clim Change* 114:667–687. doi: 10.1007/s10584-012-0418-4
- Lelieveld J, Hadjinicolaou P, Kostopoulou E, et al (2014) Model projected heat extremes and air pollution in the eastern Mediterranean and Middle East in the twenty-first century. *Reg Environ Chang* 14:1937–1949. doi: 10.1007/s10113-013-0444-4
- Lelieveld J, Hoor P, Jöckel P, et al (2009) Severe ozone air pollution in the Persian Gulf region. *Atmos Chem Phys* 9:1393–1406. doi: 10.5194/acp-9-1393-2009
- Lelieveld J, Proestos Y, Hadjinicolaou P, et al (2016) Strongly increasing heat extremes in the Middle East and North Africa (MENA) in the 21st century. *Clim Change* 137:245–260. doi: 10.1007/s10584-016-1665-6
- Levin N, Tessler N, Smith A, McAlpine C (2016) The Human and Physical Determinants of Wildfires and Burnt Areas in Israel. *Environ Manage* 58:549–562. doi: 10.1007/s00267-016-0715-1
- Lionello P, Malanotte-Rizzoli P, Boscolo R, et al (2006) The Mediterranean climate: An overview of the main characteristics and issues. In: Lionello P, Malanotte-Rizzoli P, Boscolo R (eds) *Developments in Earth and Environmental Sciences*. Elsevier, pp 1–26
- Lionello P, Scarascia L (2018) The relation between climate change in the Mediterranean region and global warming. *Reg Environ Chang* 18:1481–1493. doi: 10.1007/s10113-018-1290-1
- Lionello P, Scarascia L (2020) The relation of climate extremes with global warming in the Mediterranean region and its north versus south contrast. *Reg Environ Chang* 20:31. doi: 10.1007/s10113-020-01610-z
- Liu H, Tellez BG, Atallah T, Barghouty M (2012) The role of CO₂ capture and storage in Saudi Arabia' s energy future. *Int J Greenh Gas Control* 11:163–171. doi: 10.1016/j.ijggc.2012.08.008
- Liu W, Sun F, Ho Lim W, et al (2018) Global drought and severe drought-affected populations in 1.5 and 2 C warmer worlds. *Earth Syst Dyn* 9:267–283. doi: 10.5194/esd-9-267-2018
- Lu J, Vecchi GA, Reichler T (2007) Expansion of the Hadley cell under global warming. *Geophys Res Lett* 34:L06J805. doi: 10.1029/2006GL028443
- Lubczyńska MJ, Christophi CA, Lelieveld J (2015) Heat-related cardiovascular mortality risk in Cyprus: A case-crossover study using a distributed lag non-linear model. *Environ Heal A Glob Access Sci Source* 14:1–11. doi: 10.1186/s12940-015-0025-8
- Luterbacher J, García-Herrera R, Akcer-On S, et al (2012) A Review of 2000 Years of Paleoclimatic Evidence in the Mediterranean. In: Lionello PBT-TC of the MR (ed) *The Climate of the Mediterranean Region*. Elsevier, Oxford, pp 87–185
- Mabrouk MB, Jonoski A, Solomatine D, Uhlenbrook S (2013) A review of seawater intrusion in the Nile Delta groundwater system – the basis for assessing impacts due to climate changes and water resources development. *Hydrol Earth Syst Sci Discuss* 10:10873–10911. doi: 10.5194/hessd-10-10873-2013

- Maggiotto G, Miani A, Rizzo E, et al (2021) Heat waves and adaptation strategies in a mediterranean urban context. *Environ Res* 197:111066. doi: 10.1016/j.envres.2021.111066
- Maghrabi A, Alharbi B, Tapper N (2011) Impact of the March 2009 dust event in Saudi Arabia on aerosol optical properties, meteorological parameters, sky temperature and emissivity. *Atmos Environ* 45:2164–2173. doi: 10.1016/j.atmosenv.2011.01.071
- Maheras P, Tolika K, Anagnostopoulou C, et al (2004) On the relationships between circulation types and changes in rainfall variability in Greece. *Int J Climatol* 24:1695–1712. doi: 10.1002/joc.1088
- Malek Ž, Verburg PH (2018) Adaptation of land management in the Mediterranean under scenarios of irrigation water use and availability. *Mitig Adapt Strateg Glob Chang* 23:821–837. doi: 10.1007/s11027-017-9761-0
- Marinou E, Amiridis V, Biniotoglou I, et al (2017) Three-dimensional evolution of Saharan dust transport towards Europe based on a 9-year EARLINET-optimized CALIPSO dataset. *Atmos Chem Phys* 17:5893–5919. doi: 10.5194/acp-17-5893-2017
- Mariotti A, Dell'Aquila A (2012) Decadal climate variability in the Mediterranean region: roles of large-scale forcings and regional processes. *Clim Dyn* 38:1129–1145. doi: 10.1007/s00382-011-1056-7
- Mariotti A, Pan Y, Zeng N, Alessandri A (2015) Long-term climate change in the Mediterranean region in the midst of decadal variability. *Clim Dyn* 44:1437–1456. doi: 10.1007/s00382-015-2487-3
- Mariotti A, Zeng N, Lau KM (2002) Euro-Mediterranean rainfall and ENSO—a seasonally varying relationship. *Geophys Res Lett* 29:1621. doi: 10.1029/2001GL014248
- Mariotti A, Zeng N, Yoon JH, et al (2008) Mediterranean water cycle changes: Transition to drier 21st century conditions in observations and CMIP3 simulations. *Environ Res Lett* 3:. doi: 10.1088/1748-9326/3/4/044001
- Martel JL, Mailhot A, Brissette F (2020) Global and regional projected changes in 100-yr subdaily, daily, and multiday precipitation extremes estimated from three large ensembles of climate simulations. *J Clim* 33:1089–1103. doi: 10.1175/JCLI-D-18-0764.1
- Mashat AWS, Alamoudi AO, Awad AM, Assiri ME (2018) Seasonal variability and synoptic characteristics of dust cases over southwestern Saudi Arabia. *Int J Climatol* 38:105–124. doi: 10.1002/joc.5164
- Masoudi M, Jokar P, Pradhan B (2018) A new approach for land degradation and desertification assessment using geospatial techniques. *Nat Hazards Earth Syst Sci* 18:1133–1140. doi: 10.5194/nhess-18-1133-2018
- Mathbout S, Lopez-Bustins JA, Martin-Vide J, et al (2018a) Spatial and temporal analysis of drought variability at several time scales in Syria during 1961–2012. *Atmos Res* 200:153–168. doi: 10.1016/j.atmosres.2017.09.016
- Mathbout S, Lopez-Bustins JA, Royé D, et al (2018b) Observed Changes in Daily Precipitation Extremes at Annual Timescale Over the Eastern Mediterranean During 1961–2012. *Pure Appl Geophys* 175:3875–3890. doi: 10.1007/s00024-017-1695-7
- Mazar Y, Cytryn E, Erel Y, Rudich Y (2016) Effect of Dust Storms on the Atmospheric Microbiome in the Eastern Mediterranean. *Environ Sci Technol* 50:4194–4202. doi: 10.1021/acs.est.5b06348
- Mazi K, Koussis AD, Destouni G (2014) Intensively exploited mediterranean aquifers: Resilience to seawater intrusion and proximity to critical thresholds. *Hydrol Earth Syst Sci* 18:1663–1677. doi: 10.5194/hess-18-1663-2014
- McGeehin MA, Mirabelli M (2001) The potential impacts of climate variability and change on temperature-related morbidity and mortality in the United States. *Environ Health Perspect* 109:185–189. doi: 10.2307/3435008
- McInnes KL, Erwin TA, Bathols JM (2011) Global Climate Model projected changes in 10 m wind speed and direction due to anthropogenic climate change. *Atmos Sci Lett* 12:325–333. doi: 10.1002/asl.341
- Merlone A, Al-Dashti H, Faisal N, et al (2019) Temperature extreme records: World Meteorological Organization metrological and meteorological evaluation of the 54.0°C observations in Mitribah, Kuwait and Turbat, Pakistan in 2016/2017. *Int J Climatol* 39:5154–5169. doi: 10.1002/joc.6132
- Middleton N (2019) Variability and trends in dust storm frequency on decadal timescales: Climatic drivers and human impacts. *Geosci* 9:. doi: 10.3390/geosciences9060261
- Middleton N, Yiallouros P, Kleanthous S, et al (2008) A 10-year time-series analysis of respiratory and cardiovascular morbidity in Nicosia, Cyprus: the effect of short-term changes in air pollution and dust storms. *Environ Heal* 7:39. doi: 10.1186/1476-069X-7-39

- Mihankhah T, Saeedi M, Karbassi A (2020) A comparative study of elemental pollution and health risk assessment in urban dust of different land-uses in Tehran's urban area. *Chemosphere* 241:. doi: 10.1016/j.chemosphere.2019.124984
- Mildrexler DJ, Zhao M, Running SW (2011) Satellite finds highest land skin temperatures on Earth. *Bull Am Meteorol Soc* 92:855–860. doi: 10.1175/2011BAMS3067.1
- Miri A, Ahmadi H, Ghanbari A, Moghaddamnia A (2007) Dust Storms Impacts on Air Pollution and Public Health under Hot and Dry Climate. *Int J Energy Environ* 1:5
- Miri A, Maleki S, Middleton N (2021) An investigation into climatic and terrestrial drivers of dust storms in the Sistan region of Iran in the early twenty-first century. *Sci Total Environ* 757:143952. doi: 10.1016/j.scitotenv.2020.143952
- Mishra AK, Klingmueller K, Fredj E, et al (2014) Radiative signature of absorbing aerosol over the eastern Mediterranean basin. *Atmos Chem Phys* 14:7213–7231. doi: 10.5194/acp-14-7213-2014
- Mohammed SA, Fallah RQ (2019) Climate change indicators in AlSheikh-Badr basin (Syria). *Geogr Environ Sustain* 12:87–96. doi: 10.24057/2071-9388-2018-63
- Molina MO, Sánchez E, Gutiérrez C (2020) Future heat waves over the Mediterranean from an Euro-CORDEX regional climate model ensemble. *Sci Rep* 10:1–10. doi: 10.1038/s41598-020-65663-0
- Monioudi IN, Karditsa A, Chatzipavlis A, et al (2016) Assessment of vulnerability of the eastern Cretan beaches (Greece) to sea level rise. *Reg Environ Chang* 16:1951–1962. doi: 10.1007/s10113-014-0730-9
- Morbidelli R, García-marín AP, Al A, et al (2020) The history of rainfall data time-resolution in a wide variety of geographical areas. *J Hydrol* 590:. doi: 10.1016/j.jhydrol.2020.125258
- Mostafa AN, Wheida A, El Nazer M, et al (2019) Past (1950–2017) and future (–2100) temperature and precipitation trends in Egypt. *Weather Clim Extrem* 26:100225. doi: 10.1016/j.wace.2019.100225
- Motesaddi Zarandi S, Shahsavani A, Khodaghali F, Fakhri Y (2019) Concentration, sources and human health risk of heavy metals and polycyclic aromatic hydrocarbons bound PM_{2.5} ambient air, Tehran, Iran. *Environ Geochem Health* 41:1473–1487. doi: 10.1007/s10653-018-0229-2
- Nabat P, Somot S, Mallet M, et al (2013) A 4-D climatology (1979–2009) of the monthly tropospheric aerosol optical depth distribution over the Mediterranean region from a comparative evaluation and blending of remote sensing and model products. *Atmos Meas Tech* 6:1287–1314. doi: 10.5194/amt-6-1287-2013
- Nabat P, Somot S, Mallet M, et al (2014) Contribution of anthropogenic sulfate aerosols to the changing Euro-Mediterranean climate since 1980. *Geophys Res Lett* 41:5605–5611. doi: 10.1002/2014GL060798
- Nabavi SO, Haimberger L, Samimi C (2016) Climatology of dust distribution over West Asia from homogenized remote sensing data. *Aeolian Res* 21:93–107. doi: 10.1016/j.aeolia.2016.04.002
- Naderi Beni A, Marriner N, Sharifi A, et al (2021) Climate change: A driver of future conflicts in the Persian Gulf Region? *Heliyon* 7:e06288. doi: 10.1016/j.heliyon.2021.e06288
- Najmeddin A, Keshavarzi B (2019) Health risk assessment and source apportionment of polycyclic aromatic hydrocarbons associated with PM₁₀ and road deposited dust in Ahvaz metropolis of Iran. *Environ Geochem Health* 41:1267–1290. doi: 10.1007/s10653-018-0209-6
- Nashwan MS, Shahid S, Abd Rahim N (2018) Unidirectional trends in annual and seasonal climate and extremes in Egypt. *Theor Appl Climatol* 1–17. doi: 10.1007/s00704-018-2498-1
- Nasrallah HA, Balling RC (1993) Spatial and temporal analysis of Middle Eastern temperature changes. *Clim Change* 25:153–161. doi: 10.1007/BF01661203
- Nastos PT, Matzarakis A (2012) The effect of air temperature and human thermal indices on mortality in Athens, Greece. *Theor Appl Climatol* 108:591–599. doi: 10.1007/s00704-011-0555-0
- Nastos PT, Politi N, Kapsomenakis J (2013) Spatial and temporal variability of the Aridity Index in Greece. *Atmos Res* 119:140–152. doi: 10.1016/j.atmosres.2011.06.017
- Naumann G, Alfieri L, Wyser K, et al (2018) Global Changes in Drought Conditions Under Different Levels of Warming. *Geophys Res Lett* 45:3285–3296. doi: 10.1002/2017GL076521
- Neophytou AM, Yiallourou P, Coull BA, et al (2013) Particulate matter concentrations during desert dust outbreaks and daily mortality in Nicosia, Cyprus. *J Expo Sci Environ Epidemiol* 23:275–280. doi: 10.1038/jes.2013.10

- Nissen KM, Leckebusch GC, Pinto JG, Ulbrich U (2014) Mediterranean cyclones and windstorms in a changing climate. *Reg Environ Chang* 14:1873–1890. doi: 10.1007/s10113-012-0400-8
- Notaro M, Yu Y, Kalashnikova O V. (2015) Regime shift in arabian dust activity, triggered by persistent fertile crescent drought. *J Geophys Res* 120:10229–10249. doi: 10.1002/2015JD023855
- Nourmoradi H, Omid Khaniabadi Y, Goudarzi G, et al (2016) Air Quality and Health Risks Associated With Exposure to Particulate Matter: A Cross-Sectional Study in Khorramabad, Iran. *Heal Scope* 5:. doi: 10.17795/jhealthscope-31766
- Ntoumos A, Hadjinicolaou P, Zittis G, Lelieveld J (2020) Updated Assessment of Temperature Extremes over the Middle East–North Africa (MENA) Region from Observational and CMIP5 Data. *Atmosphere (Basel)* 11:813. doi: 10.3390/atmos11080813
- Önol B, Unal YS (2014) Assessment of climate change simulations over climate zones of Turkey. *Reg Environ Chang* 14:1921–1935. doi: 10.1007/s10113-012-0335-0
- Oppenheimer M, Glavovic B, Hinkel J, et al (2019) Sea Level Rise and Implications for Low Lying Islands, Coasts and Communities. In: Pörtner H-O, Roberts DC, Masson-Delmotte V, et al. (eds) IPCC Special Report on the Ocean and Cryosphere in a Changing Climate. in press, pp 126–129
- Oroud IM (2008) The Impacts of Climate Change on Water Resources in Jordan. In: Zereini F, Hötzl H (eds) *Climatic Changes and Water Resources in the Middle East and North Africa*. Springer Berlin Heidelberg, Berlin, Heidelberg, pp 109–123
- Osipov S, Stenchikov G (2018) Simulating the Regional Impact of Dust on the Middle East Climate and the Red Sea. *J Geophys Res Ocean* 123:1032–1047. doi: 10.1002/2017JC013335
- Oswald SM, Hollosi B, Žuvela-Aloise M, et al (2020) Using urban climate modelling and improved land use classifications to support climate change adaptation in urban environments: A case study for the city of Klagenfurt, Austria. *Urban Clim* 31:100582. doi: 10.1016/j.uclim.2020.100582
- Quarda TBMJ, Charron C, Niranjana Kumar K, et al (2014) Evolution of the rainfall regime in the united arab emirates. *J Hydrol* 514:258–270. doi: 10.1016/j.jhydrol.2014.04.032
- Ozturk T, Turp MT, Türkeş M, Kurnaz ML (2018) Future projections of temperature and precipitation climatology for CORDEX-MENA domain using RegCM4.4. *Atmos Res* 206:87–107. doi: 10.1016/j.atmosres.2018.02.009
- Pal JS, Eltahir EAB (2016) Future temperature in southwest Asia projected to exceed a threshold for human adaptability. *Nat Clim Chang* 6:197–200. doi: 10.1038/nclimate2833
- Palaiologou P, Ager AA, Nielsen-Pincus M, et al (2018) Using transboundary wildfire exposure assessments to improve fire management programs: A case study in Greece. *Int J Wildl Fire* 27:501–513. doi: 10.1071/WF17119
- Papadaskalopoulou C, Moriondo M, Lemesios I, et al (2020) Assessment of total climate change impacts on the agricultural sector of Cyprus. *Atmosphere (Basel)* 11:1–17. doi: 10.3390/atmos11060608
- Papadimas CD, Hatzianastassiou N, Matsoukas C, et al (2012) The direct effect of aerosols on solar radiation over the broader Mediterranean basin. *Atmos Chem Phys* 12:7165–7185. doi: 10.5194/acp-12-7165-2012
- Paravantis J, Santamouris M, Cartalis C, et al (2017) Mortality associated with high ambient temperatures, heat-waves, and the urban heat island in Athens, Greece. *Sustain* 9:. doi: 10.3390/su9040606
- Pardo M, Katra I, Schaefer JJ, Rudich Y (2017) Mitochondria-mediated oxidative stress induced by desert dust in rat alveolar macrophages. *GeoHealth* 1:4–16. doi: 10.1002/2016GH000017
- Pardo M, Li C, He Q, et al (2020) Mechanisms of lung toxicity induced by biomass burning aerosols. *Part Fibre Toxicol* 17:4. doi: 10.1186/s12989-020-0337-x
- Pardo M, Porat Z, Rudich A, et al (2016) Repeated exposures to roadside particulate matter extracts suppresses pulmonary defense mechanisms, resulting in lipid and protein oxidative damage. *Environ Pollut* 210:227–237. doi: 10.1016/j.envpol.2015.12.009
- Pardo M, Shafer MM, Rudich A, et al (2015) Single Exposure to near Roadway Particulate Matter Leads to Confined Inflammatory and Defense Responses: Possible Role of Metals. *Environ Sci Technol* 49:8777–8785. doi: 10.1021/acs.est.5b01449

- Partal T, Kahya E (2006) Trend analysis in Turkish precipitation data. *Hydrol Process* 20:2011–2026. doi: 10.1002/hyp.5993
- Pashiardis S, Michaelides S (2008) Implementation of the Standardized Precipitation Index (SPI) and the Reconnaissance Drought Index (RDI) for Regional Drought Assessment: A case study for Cyprus. *Eur Water* 23:57–65
- Paxian A, Hertig E, Seubert S, et al (2015) Present-day and future mediterranean precipitation extremes assessed by different statistical approaches. *Clim Dyn* 44:845–860. doi: 10.1007/s00382-014-2428-6
- Paz S, Carmel Y, Jahshan F, Shoshany M (2011) Post-fire analysis of pre-fire mapping of fire-risk: A recent case study from Mt. Carmel (Israel). *For Ecol Manage* 262:1184–1188. doi: 10.1016/j.foreco.2011.06.011
- Peretz C, Biggeri A, Alpert P, Baccini M (2012) The Effect of Heat Stress on Daily Mortality in Tel Aviv, Israel. In: Fernando HJS, Klaić Z, McCulley JL (eds) *NATO Science for Peace and Security Series C: Environmental Security*. Springer Netherlands, Dordrecht, pp 241–251
- Perkins-Kirkpatrick SE, Lewis SC (2020) Increasing trends in regional heatwaves. *Nat Commun* 11:1–8. doi: 10.1038/s41467-020-16970-7
- Philandras CM, Nastos PT, Kapsomenakis J, et al (2011) Long term precipitation trends and variability within the Mediterranean region. *Nat Hazards Earth Syst Sci* 11:3235–3250. doi: 10.5194/nhess-11-3235-2011
- Philip S, Martin R V., Snider G, et al (2017) Anthropogenic fugitive, combustion and industrial dust is a significant, underrepresented fine particulate matter source in global atmospheric models. *Environ Res Lett* 12:44018. doi: 10.1088/1748-9326/aa65a4
- Pikridas M, Bezantakos S, Močnik G, et al (2019) On-flight intercomparison of three miniature aerosol absorption sensors using unmanned aerial systems (UASs). *Atmos Meas Tech* 12:6425–6447. doi: 10.5194/amt-12-6425-2019
- Pikridas M, Vrekoussis M, Sciare J, et al (2018) Spatial and temporal (short and long-term) variability of submicron, fine and sub-10 m particulate matter (PM₁, PM_{2.5}, PM₁₀) in Cyprus. *Atmos Environ* 191:79–93. doi: 10.1016/j.atmosenv.2018.07.048
- Pozzer A, De Meij A, Yoon J, et al (2015) AOD trends during 2001–2010 from observations and model simulations. *Atmos Chem Phys* 15:5521–5535. doi: 10.5194/acp-15-5521-2015
- Price C, Michaelides S, Pashiardis S, Alpert P (1999) Long term changes in diurnal temperature range in Cyprus. *Atmos Res* 51:85–98. doi: 10.1016/S0169-8095(99)00022-8
- Prudhomme C, Giuntoli I, Robinson EL, et al (2014) Hydrological droughts in the 21st century, hotspots and uncertainties from a global multimodel ensemble experiment. *Proc Natl Acad Sci U S A* 111:3262–3267. doi: 10.1073/pnas.1222473110
- Pugh DT, Abualnaja Y (2015) *Sea-Level Changes*. Springer Earth System Sciences. Springer, Berlin, Heidelberg
- Pyrgou A, Hadjinicolaou P, Santamouris M (2020) Urban-rural moisture contrast: Regulator of the urban heat island and heatwaves' synergy over a mediterranean city. *Environ Res* 182:109102. doi: 10.1016/j.envres.2019.109102
- Pyrgou A, Santamouris M (2018) Increasing probability of heat-related mortality in a mediterranean city Due to urban warming. *Int J Environ Res Public Health* 15:. doi: 10.3390/ijerph15081571
- Qadir M, Sharma BR, Bruggeman A, et al (2007) Non-conventional water resources and opportunities for water augmentation to achieve food security in water scarce countries. *Agric Water Manag* 87:2–22. doi: 10.1016/j.agwat.2006.03.018
- Rajczak J, Schär C (2017) Projections of Future Precipitation Extremes Over Europe: A Multimodel Assessment of Climate Simulations. *J Geophys Res Atmos* 122:10,773–10,800. doi: 10.1002/2017JD027176
- Rajsekhar D, Gorelick SM (2017) Increasing drought in Jordan: Climate change and cascading Syrian land-use impacts on reducing transboundary flow. *Sci Adv* 3:e1700581. doi: 10.1126/sciadv.1700581
- Ramadan HH, Beighley RE, Ramamurthy AS (2013) Temperature and Precipitation Trends in Lebanon's Largest River: The Litani Basin. *J Water Resour Plan Manag* 139:86–95. doi: 10.1061/(asce)wr.1943-5452.0000238
- Ramanathan V, Crutzen PJ, Kiehl JT, Rosenfeld D (2007) Atmosphere: aerosols, climate, and the hydrological cycle. *Science* (80-) 294: 2119–2124

- Rashki A, Eriksson PG, Rautenbach CJ d. W, et al (2013a) Assessment of chemical and mineralogical characteristics of airborne dust in the Sistan region, Iran. *Chemosphere* 90:227–236. doi: 10.1016/j.chemosphere.2012.06.059
- Rashki A, Kaskaoutis DG, Eriksson PG, et al (2014) Spatio-temporal variability of dust aerosols over the Sistan region in Iran based on satellite observations. *Nat Hazards* 71:563–585. doi: 10.1007/s11069-013-0927-0
- Rashki A, Kaskaoutis DG, Goudie AS, Kahn RA (2013b) Dryness of ephemeral lakes and consequences for dust activity: The case of the Hamoun drainage basin, Southeastern Iran. *Sci Total Environ* 463–464:552–564. doi: 10.1016/j.scitotenv.2013.06.045
- Rashki A, Kaskaoutis DG, Mofidi A, et al (2019) Effects of Monsoon, Shamal and Levant winds on dust accumulation over the Arabian Sea during summer – The July 2016 case. *Aeolian Res* 36:27–44. doi: 10.1016/j.aeolia.2018.11.002
- Rashki A, Kaskaoutis DG, Sepehr A (2018) Statistical evaluation of the dust events at selected stations in Southwest Asia: From the Caspian Sea to the Arabian Sea. *Catena* 165:590–603. doi: 10.1016/j.catena.2018.03.011
- Rashki A, Middleton NJ, Goudie AS (2021) Dust storms in Iran – Distribution, causes, frequencies and impacts. *Aeolian Res* 48:. doi: 10.1016/j.aeolia.2020.100655
- Rezazadeh M, Irannejad P, Shao Y (2013) Climatology of the Middle East dust events. *Aeolian Res* 10:103–109. doi: 10.1016/j.aeolia.2013.04.001
- Riahi K, Grübler A, Nakicenovic N (2007) Scenarios of long-term socio-economic and environmental development under climate stabilization. *Technol Forecast Soc Change* 74:887–935. doi: 10.1016/j.techfore.2006.05.026
- Riahi K, van Vuuren DP, Kriegler E, et al (2017) The Shared Socioeconomic Pathways and their energy, land use, and greenhouse gas emissions implications: An overview. *Glob Environ Chang* 42:153–168. doi: 10.1016/j.gloenvcha.2016.05.009
- Rockström J, Karlberg L, Wani SP, et al (2010) Managing water in rainfed agriculture—The need for a paradigm shift. *Agric Water Manag* 97:543–550. doi: 10.1016/j.agwat.2009.09.009
- Romero R, Emanuel K (2013) Medcane risk in a changing climate. *J Geophys Res Atmos* 118:5992–6001. doi: 10.1002/jgrd.50475
- Rosenfeld D, Dai J, Yu X, et al (2007) Inverse relations between amounts of air pollution and orographic precipitation. *Science* (80-) 315:1396–1398. doi: 10.1126/science.1137949
- Rosenfeld D, Rudich Y, Lahav R (2001) Desert dust suppressing precipitation: A possible desertification feedback loop. *Proc Natl Acad Sci U S A* 98:5975–5980. doi: 10.1073/pnas.101122798
- Russo S, Dosio A, Gravensén RG, et al (2014) Magnitude of extreme heat waves in present climate and their projection in a warming world. *J Geophys Res Atmos* 119:12,500–12,512. doi: 10.1002/2014JD022098
- Ruti PM, Somot S, Giorgi F, et al (2016) Med-CORDEX initiative for Mediterranean climate studies. *Bull Am Meteorol Soc* 97:1187–1208. doi: 10.1175/BAMS-D-14-00176.1
- Saaroni H, Ziv B, Edelson J, Alpert P (2003) Long-term variations in summer temperatures over the Eastern Mediterranean. *Geophys Res Lett* 30:1946. doi: 10.1029/2003GL017742
- Sabetghadam S, Alizadeh O, Khoshsima M, Pierleoni A (2021) Aerosol properties, trends and classification of key types over the Middle East from satellite-derived atmospheric optical data. *Atmos Environ* 246:118100. doi: 10.1016/j.atmosenv.2020.118100
- Saeed F, Schleussner C-F, Almazroui M (2021) From Paris to Makkah: heat stress risks for Muslim pilgrims at 1.5 °C and 2 °C. *Environ Res Lett* 16:024037. doi: 10.1088/1748-9326/abd067
- Saeed TM, Al-Dashti H, Spyrou C (2014) Aerosol's optical and physical characteristics and direct radiative forcing during a shamal dust storm, a case study. *Atmos Chem Phys* 14:3751–3769. doi: 10.5194/acp-14-3751-2014
- Salimi M, Al-Ghamdi SG (2020) Climate change impacts on critical urban infrastructure and urban resiliency strategies for the Middle East. *Sustain Cities Soc* 54:101948. doi: 10.1016/j.scs.2019.101948
- Samuels R, Hochman A, Baharad A, et al (2018) Evaluation and projection of extreme precipitation indices in the Eastern Mediterranean based on CMIP5 multi-model ensemble. *Int J Climatol* 38:2280–2297. doi: 10.1002/joc.5334

- Santamouris M (2015) Analyzing the heat island magnitude and characteristics in one hundred Asian and Australian cities and regions. *Sci Total Environ* 512–513:582–598. doi: 10.1016/j.scitotenv.2015.01.060
- Schewe J, Heinke J, Gerten D, et al (2014) Multimodel assessment of water scarcity under climate change. *Proc Natl Acad Sci U S A* 111:3245–3250. doi: 10.1073/pnas.1222460110
- Seager R, Liu H, Henderson N, et al (2014) Causes of increasing aridification of the mediterranean region in response to rising greenhouse gases. *J Clim* 27:4655–4676. doi: 10.1175/JCLI-D-13-00446.1
- Seager R, Osborn TJ, Kushnir Y, et al (2019) Climate variability and change of mediterranean-type climates. *J Clim* 32:2887–2915. doi: 10.1175/JCLI-D-18-0472.1
- Sefelnasr A, Sherif M (2014) Impacts of Seawater Rise on Seawater Intrusion in the Nile Delta Aquifer, Egypt. *Groundwater* 52:264–276. doi: 10.1111/gwat.12058
- Sen B, Topcu S, Türkeş M, et al (2012) Projecting climate change, drought conditions and crop productivity in Turkey. *Clim Res* 52:175–191. doi: 10.3354/cr01074
- Seng DC (2012) Improving the Governance Context and Framework Conditions of Natural Hazard Early Warning Systems. *J Integr Disaster Risk Manag* 2:1–25. doi: 10.5595/idrim.2012.0020
- Shaban A (2009) Indicators and aspects of hydrological drought in Lebanon. *Water Resour Manag* 23:1875–1891. doi: 10.1007/s11269-008-9358-1
- Shaban A (2008) Impact of Climate Change on Water Resources of Lebanon: Indications of Hydrological Droughts. In: Zereini F, Hötzl H (eds) *Climatic Changes and Water Resources in the Middle East and North Africa*. Springer Berlin Heidelberg, Berlin, Heidelberg, pp 125–143
- Shaheen A, Kidwai AA, Ain NU, et al (2017) Estimating Air Particulate Matter 10 Using Landsat Multi-Temporal Data and Analyzing its Annual Temporal Pattern over Gaza Strip, Palestine. *J Asian Sci Res* 7:22–37. doi: 10.18488/journal.2/2017.7.2/2.2.22.37
- Shaheen A, Wu R, Aldabash M (2020) Long-term AOD trend assessment over the Eastern Mediterranean region: A comparative study including a new merged aerosol product. *Atmos Environ* 238:. doi: 10.1016/j.atmosenv.2020.117736
- Shaheen A, Wu R, Lelieveld J, et al (2021) Winter AOD Trend Changes over the Eastern Mediterranean and Middle East Region . *Int J Climatol* n/a: doi: 10.1002/joc.7139
- Shahsavani A, Naddafi K, Jaafarzadeh Haghhighifard N, et al (2012) Characterization of ionic composition of TSP and PM10 during the Middle Eastern Dust (MED) storms in Ahvaz, Iran. *Environ Monit Assess* 184:6683–6692. doi: 10.1007/s10661-011-2451-6
- Shahsavani A, Tobias A, Querol X, et al (2020) Short-term effects of particulate matter during desert and non-desert dust days on mortality in Iran. *Environ Int* 134:. doi: 10.1016/j.envint.2019.105299
- Shaltout M, Tonbol K, Omstedt A (2015) Sea-level change and projected future flooding along the Egyptian Mediterranean coast. *Oceanologia* 57:293–307. doi: 10.1016/j.oceano.2015.06.004
- Shawon MJ, El Chaar L, Lamont LA (2013) Overview of wind energy and its cost in the Middle East. *Sustain Energy Technol Assessments* 2:1–11. doi: 10.1016/j.seta.2013.01.002
- Shohami D, Dayan U, Morin E (2011) Warming and drying of the eastern Mediterranean: Additional evidence from trend analysis. *J Geophys Res Atmos* 116:1–12. doi: 10.1029/2011JD016004
- Shuster-Meiseles T, Shafer MM, Heo J, et al (2016) ROS-generating/ARE-activating capacity of metals in roadway particulate matter deposited in urban environment. *Environ Res* 146:252–262. doi: 10.1016/j.envres.2016.01.009
- Siddig NA, Al-subhi AM, Alsaafani MA (2019) ScienceDirect Tide and mean sea level trend in the west coast of the Arabian Gulf from tide gauges and multi-missions satellite altimeter. *Oceanologia* 61:401–411. doi: 10.1016/j.oceano.2019.05.003
- Sillmann J, Kharin V V., Zhang X, et al (2013) Climate extremes indices in the CMIP5 multimodel ensemble: Part 1. Model evaluation in the present climate. *J Geophys Res Atmos* 118:1716–1733. doi: 10.1002/jgrd.50203
- Sinha A, Kathayat G, Weiss H, et al (2019) Role of climate in the rise and fall of the neo-assyrian empire. *Sci Adv* 5:eaax6656. doi: 10.1126/sciadv.aax6656

- Soleimani Z, Teymouri P, Darvishi Boloorani A, et al (2020) An overview of bioaerosol load and health impacts associated with dust storms: A focus on the Middle East. *Atmos Environ* 223:. doi: 10.1016/j.atmosenv.2019.117187
- Solmon F, Nair VS, Mallet M (2015) Increasing Arabian dust activity and the Indian summer monsoon. *Atmos Chem Phys* 15:8051–8064. doi: 10.5194/acp-15-8051-2015
- Soltani N, Keshavarzi B, Moore F, et al (2015) Ecological and human health hazards of heavy metals and polycyclic aromatic hydrocarbons (PAHs) in road dust of Isfahan metropolis, Iran. *Sci Total Environ* 505:712–723. doi: 10.1016/j.scitotenv.2014.09.097
- Soto-Navarro J, Jordá G, Amores A, et al (2020) Evolution of Mediterranean Sea water properties under climate change scenarios in the Med-CORDEX ensemble
- Sousa PM, Trigo RM, Aizpurua P, et al (2011) Trends and extremes of drought indices throughout the 20th century in the Mediterranean. *Nat Hazards Earth Syst Sci* 11:33–51. doi: 10.5194/nhess-11-33-2011
- Spinoni J, Barbosa P, Bucchignani E, et al (2020) Future Global Meteorological Drought Hot Spots: A Study Based on CORDEX Data. *J Clim* 33:3635–3661. doi: 10.1175/jcli-d-19-0084.1
- Spinoni J, Barbosa P, De Jager A, et al (2019) A new global database of meteorological drought events from 1951 to 2016. *J Hydrol Reg Stud* 22:100593. doi: 10.1016/j.ejrh.2019.100593
- Spinoni J, Vogt J V., Naumann G, et al (2018) Will drought events become more frequent and severe in Europe? *Int J Climatol* 38:1718–1736. doi: 10.1002/joc.5291
- Spyrou C, Varlas G, Pappa A, et al (2020) Implementation of a nowcasting hydrometeorological system for studying flash flood events: The Case of Mandra, Greece. *Remote Sens* 12:. doi: 10.3390/RS12172784
- Stafoggia M, Zauli-Sajani S, Pey J, et al (2016) Desert dust outbreaks in Southern Europe: Contribution to daily PM10 concentrations and short-term associations with mortality and hospital admissions. *Environ Health Perspect* 124:413–419. doi: 10.1289/ehp.1409164
- Tabari H (2020) Climate change impact on flood and extreme precipitation increases with water availability. *Sci Rep* 10:1–10. doi: 10.1038/s41598-020-70816-2
- Tabari H, Willems P (2018) More prolonged droughts by the end of the century in the Middle East. *Environ Res Lett* 13:. doi: 10.1088/1748-9326/aae09c
- Tanarhte M, Hadjinicolaou P, Lelieveld J (2012) Intercomparison of temperature and precipitation data sets based on observations in the Mediterranean and the Middle East. *J Geophys Res Atmos* 117:D12102. doi: 10.1029/2011JD017293
- Tibaldi C, Debeire K, Eyring V, et al (2020) Climate model projections from the Scenario Model Intercomparison Project (ScenarioMIP) of CMIP6. *Earth Syst Dyn Discuss* 12:1–50. doi: 10.5194/esd-2020-68
- Tolika K (2019) Assessing Heat Waves over Greece Using the Excess Heat Factor (EHF). *Climate* 7:9. doi: 10.3390/cli7010009
- Touma D, Ashfaq M, Nayak MA, et al (2015) A multi-model and multi-index evaluation of drought characteristics in the 21st century. *J Hydrol* 526:196–207. doi: 10.1016/j.jhydrol.2014.12.011
- Tramblay Y, Somot S (2018) Future evolution of extreme precipitation in the Mediterranean. *Clim Change* 151:289–302. doi: 10.1007/s10584-018-2300-5
- Tsiouri V, Kakosimos KE, Kumar P (2015) Concentrations, sources and exposure risks associated with particulate matter in the Middle East Area—a review. *Air Qual Atmos Heal* 8:67–80. doi: 10.1007/s11869-014-0277-4
- Turco M, Levin N, Tessler N, Saaroni H (2017a) Recent changes and relations among drought, vegetation and wildfires in the Eastern Mediterranean: The case of Israel. *Glob Planet Change* 151:28–35. doi: https://doi.org/10.1016/j.gloplacha.2016.09.002
- Turco M, Rosa-Cánovas JJ, Bedia J, et al (2018) Exacerbated fires in Mediterranean Europe due to anthropogenic warming projected with non-stationary climate-fire models. *Nat Commun* 9:1–9. doi: 10.1038/s41467-018-06358-z
- Turco M, Von Hardenberg J, AghaKouchak A, et al (2017b) On the key role of droughts in the dynamics of summer fires in Mediterranean Europe. *Sci Rep* 7:81. doi: 10.1038/s41598-017-00116-9
- Tzounis A, Katsoulas N, Bartzanas T, Kittas C (2017) Internet of Things in agriculture, recent advances and future challenges. *Biosyst Eng* 164:31–48. doi: 10.1016/j.biosystemseng.2017.09.007

- Ukhov A, Mostamandi S, Da Silva A, et al (2020) Assessment of natural and anthropogenic aerosol air pollution in the Middle East using MERRA-2, CAMS data assimilation products, and high-resolution WRF-Chem model simulations. *Atmos Chem Phys* 20:9281–9310. doi: 10.5194/acp-20-9281-2020
- Van Donkelaar A, Martin R V., Brauer M, et al (2016) Global Estimates of Fine Particulate Matter using a Combined Geophysical-Statistical Method with Information from Satellites, Models, and Monitors. *Environ Sci Technol* 50:3762–3772. doi: 10.1021/acs.est.5b05833
- Van Vuuren DP, Den Elzen MGJ, Lucas PL, et al (2007) Stabilizing greenhouse gas concentrations at low levels: An assessment of reduction strategies and costs. *Clim Change* 81:119–159. doi: 10.1007/s10584-006-9172-9
- Vara A de la, Gutiérrez C, González-Alemán JJ, Gaertner MÁ (2020) Intercomparison study of the impact of climate change on renewable energy indicators on the mediterranean islands. *Atmosphere (Basel)* 11:. doi: 10.3390/atmos11101036
- Varela R, Rodríguez-Díaz L, deCastro M (2020) Persistent heat waves projected for Middle East and North Africa by the end of the 21st century. *PLoS One* 15:e0242477. doi: 10.1371/journal.pone.0242477
- Varotsos K V, Karali A, Lemesios G, et al (2021) Near future climate change projections with implications for the agricultural sector of three major Mediterranean islands
- Vaughan GO, Al-Mansoori N, Burt JA (2018) The arabian gulf. In: Sheppard C (ed) *World Seas: An Environmental Evaluation Volume II: The Indian Ocean to the Pacific*, 2nd Edn. Elsevier Science, Amsterdam, NL, pp 1–23
- Vinoy V, Rasch PJ, Wang H, et al (2014) Short-term modulation of Indian summer monsoon rainfall by West Asian dust. *Nat Geosci* 7:308–313. doi: 10.1038/ngeo2107
- Vodonos A, Friger M, Katra I, et al (2014) The impact of desert dust exposures on hospitalizations due to exacerbation of chronic obstructive pulmonary disease. *Air Qual Atmos Heal* 7:433–439. doi: 10.1007/s11869-014-0253-z
- Waha K, Krummenauer L, Adams S, et al (2017) Climate change impacts in the Middle East and Northern Africa (MENA) region and their implications for vulnerable population groups. *Reg Environ Chang* 17:1623–1638. doi: 10.1007/s10113-017-1144-2
- Walter A, Finger R, Huber R, Buchmann N (2017) Smart farming is key to developing sustainable agriculture. *Proc Natl Acad Sci U S A* 114:6148–6150. doi: 10.1073/pnas.1707462114
- Wittenberg L, Kutiel H (2016) Dryness in a Mediterranean-type climate - Implications for wildfire burnt area: A case study from Mount Carmel, Israel. *Int J Wildl Fire* 25:579–591. doi: 10.1071/WF15135
- Xoplaki E, Fleitmann D, Luterbacher J, et al (2016) The Medieval Climate Anomaly and Byzantium: A review of the evidence on climatic fluctuations, economic performance and societal change. *Quat Sci Rev* 136:229–252. doi: 10.1016/j.quascirev.2015.10.004
- Xoplaki E, González-Rouco JF, Luterbacher J, Wanner H (2004) Wet season Mediterranean precipitation variability: Influence of large-scale dynamics and trends. *Clim Dyn* 23:63–78. doi: 10.1007/s00382-004-0422-0
- Xoplaki E, Luterbacher J, Burkard R, et al (2000) Connection between the large-scale 500 hPa geopotential height fields and precipitation over Greece during wintertime. *Clim Res* 14:129–146. doi: 10.3354/cr014129
- Xoplaki E, Luterbacher J, Wagner S, et al (2018) Modelling Climate and Societal Resilience in the Eastern Mediterranean in the Last Millennium. *Hum Ecol* 46:363–379. doi: 10.1007/s10745-018-9995-9
- Xu X, Xie L, Yang X, et al (2020) Aerosol optical properties at seven AERONET sites over Middle East and Eastern Mediterranean Sea. *Atmos Environ* 243:117884. doi: 10.1016/j.atmosenv.2020.117884
- Yatagai A, Xie P, Alpert P (2007) Development of a daily gridded precipitation data set for the Middle East. *Adv Geosci* 12:165–170. doi: 10.5194/adgeo-12-165-2008
- Yıldırım Ü, Güler C, Önel B, et al (2021) Modelling of the Discharge Response to Climate Change under RCP8.5 Scenario in the Alata River Basin (Mersin, SE Turkey). *Water* 13:483. doi: 10.3390/w13040483
- Yoon J, Burrows JP, Vountas M, et al (2014) Changes in atmospheric aerosol loading retrieved from space-based measurements during the past decade. *Atmos Chem Phys* 14:6881–6902. doi: 10.5194/acp-14-6881-2014
- Yosef Y, Aguilar E, Alpert P (2019) Changes in extreme temperature and precipitation indices: Using an innovative daily homogenized database in Israel. *Int J Climatol* 39:5022–5045. doi: 10.1002/joc.6125

- Yu Y, Kalashnikova O V., Garay MJ, et al (2018) Identification and Characterization of Dust Source Regions Across North Africa and the Middle East Using MISR Satellite Observations. *Geophys Res Lett* 45:6690–6701. doi: 10.1029/2018GL078324
- Yu Y, Notaro M, Kalashnikova O V., Garay MJ (2016) Climatology of summer Shamal wind in the Middle East. *J Geophys Res* 121:289–305. doi: 10.1002/2015JD024063
- Yu Y, Notaro M, Liu Z, et al (2015) Climatic controls on the interannual to decadal variability in Saudi Arabian dust activity: Toward the development of a seasonal dust prediction model. *J Geophys Res* 120:1739–1758. doi: 10.1002/2014JD022611
- Zachariadis T, Hadjinicolaou P The effect of climate change on electricity needs - A case study from Mediterranean Europe. *Energy* 76:899–910. doi: 10.1016/j.energy.2014.09.001
- Zanis P, Kapsomenakis I, Philandras C, et al (2009) Analysis of an ensemble of present day and future regional climate simulations for Greece. *Int J Climatol* 29:1614–1633. doi: 10.1002/joc.1809
- Zanis P, Katragkou E, Ntogras C, et al (2015) Transient high-resolution regional climate simulation for Greece over the period 1960–2100: Evaluation and future projections. *Clim Res* 64:123–140. doi: 10.3354/cr01304
- Zappa G, Hoskins BJ, Shepherd TG (2015) The dependence of wintertime Mediterranean precipitation on the atmospheric circulation response to climate change. *Env Res Lett* 10:104012. doi: 10.1088/1748-9326/10/10/104012
- Zarasvandi A, Carranza EJM, Moore F, Rastmanesh F (2011) Spatio-temporal occurrences and mineralogical-geochemical characteristics of airborne dusts in Khuzestan Province (southwestern Iran). *J Geochemical Explor* 111:138–151. doi: 10.1016/j.gexplo.2011.04.004
- Zhao L, Oleson K, Bou-Zeid E, et al (2021a) Global multi-model projections of local urban climates. *Nat Clim Chang*. doi: 10.1038/s41558-020-00958-8
- Zhao Y, Norouzi H, Azarderakhsh M, AghaKouchak A (2021b) Global Patterns of Hottest, Coldest and Extreme Diurnal Variability on Earth. *Bull Am Meteorol Soc* 1–23. doi: 10.1175/BAMS-D-20-0325.1
- Zittis G (2018) Observed rainfall trends and precipitation uncertainty in the vicinity of the Mediterranean, Middle East and North Africa. *Theor Appl Climatol* 134:1207–1230. doi: 10.1007/s00704-017-2333-0
- Zittis G, Almazroui M., Alpert P, et al. (2022) Climate change and weather extremes in the Eastern Mediterranean and Middle East. *Rev Geophys*, e2021RG000762. doi: <https://doi.org/https://doi.org/10.1029/2021RG000762>
- Zittis G, Bruggeman A, Camera C, et al (2017) The added value of convection permitting simulations of extreme precipitation events over the eastern Mediterranean. *Atmos Res* 191:20–33. doi: 10.1016/j.atmosres.2017.03.002
- Zittis G, Bruggeman A, Camera C (2020) 21st Century Projections of Extreme Precipitation Indicators for Cyprus. *Atmosphere (Basel)* 11:343. doi: 10.3390/atmos11040343
- Zittis G, Hadjinicolaou P (2017) The effect of radiation parameterization schemes on surface temperature in regional climate simulations over the MENA-CORDEX domain. *Int J Climatol* 37:3847–3862. doi: 10.1002/joc.4959
- Zittis G, Hadjinicolaou P, Almazroui M, et al (2021) Business-as-usual will lead to super and ultra-extreme heatwaves in the Middle East and North Africa. *npj Clim Atmos Sci* 4:20. doi: 10.1038/s41612-021-00178-7
- Zittis G, Hadjinicolaou P, Fnais M, Lelieveld J (2016) Projected changes in heat wave characteristics in the eastern Mediterranean and the Middle East. *Reg Environ Chang* 16:1863–1876. doi: 10.1007/s10113-014-0753-2
- Zittis G, Hadjinicolaou P, Klangidou M, et al (2019) A multi-model, multi-scenario, and multi-domain analysis of regional climate projections for the Mediterranean. *Reg Environ Chang* 19:2621–2635. doi: 10.1007/s10113-019-01565-w
- Zittis G, Hadjinicolaou P, Lelieveld J (2014) Role of soil moisture in the amplification of climate warming in the eastern Mediterranean and the Middle East. *Clim Res* 59:27–37. doi: 10.3354/cr01205
- Ziv B, Saaroni H, Pargament R, et al (2014) Trends in rainfall regime over Israel, 1975–2010, and their relationship to large-scale variability. *Reg Environ Chang* 14:1751–1764. doi: 10.1007/s10113-013-0414-x
- Ziyade A, Hirmas DR, Karimi A, et al (2019) Geogenic and anthropogenic sources of potentially toxic elements in airborne dust in northeastern Iran. *Aeolian Res* 41:. doi: 10.1016/j.aeolia.2019.100540
- Zoumides C, Bruggeman A, Giannakis E, et al (2017) Community-Based Rehabilitation of Mountain Terraces in Cyprus. *L Degrad Dev* 28:95–105. doi: 10.1002/ldr.2586



Executive Summaries

- 1 The Physical Basis of Climate Change
- 2 Energy Systems
- 3 The Built Environment
- 4 Health
- 5 Water Resources
- 6 Agriculture and the Food Chain
- 7 Marine Environment/Resources (web version only)
- 8 Education and Outreach
- 9 Migration
- 10 Tourism (web version only)
- 11 Enabling Technologies
- 12 The Green Economy and Innovation
- 13 Cultural Heritage